Parametrical study of the tire properties to optimise the vibratory behaviour of a forklift truck.

P. Lemerle, P. Mistrot

Juillet 2001

N° ISSN 0397 - 4529

207

Parametrical study of the tire properties to optimise the vibratory behaviour of a forklift truck.

Etude paramétrique des caractéristiques de pneumatiques pour l'optimisation du comportement vibratoire d'un chariot élévateur.

Pierre LEMERLE
Pierre MISTROT

INSTITUT NATIONAL DE RECHERCHE ET DE SECURITE

SIEGE SOCIAL :
30, RUE OLIVIER-NOYER, 75680 PARIS CEDEX 14

CENTRE DE LORRAINE :
AVENUE DE BOURGOGNE, 54501 VANDOEUVRE CEDEX

CONTENT

Abstract

The aim of this study was to analyse by means of numerical simulation the influence of the tire properties on the vibratory behaviour of a forklift truck. It was shown how to build a model with adequate tests to characterize the tires and forklift truck. This model was validated by comparing predicted results with experiments, according to the procedure defined in the European test code prEN 13059 [2].

A parametrical study was carried out in modifying the damping and stiffness properties of the tire model. The corresponding transmitted acceleration at the driving position was calculated, when the forklift truck was running over standardized obstacles.

This paper reports the results and comments of numerous simulations made within the frame of this study. They may help tire manufacturers to consider.

Key-words : NUMERICAL SIMULATION – MODELLING – TIRE – VIBRATION – STIFFNESS – DAMPING – FORKLIFT TRUCK

Résumé

Cette étude a pour but d'analyser, grâce à la simulation numérique, l'influence des caractéristiques physiques des pneumatiques sur le comportement vibratoire d'un chariot élévateur. On montre comment élaborer un modèle de calcul, grâce à une série d'essais permettant de caractériser les pneumatiques et le chariot lui-même. Ce modèle a été validé par comparaison entre calculs et mesures, dans les conditions d'essais définies par le code normalisé européen n° prEN 13059 [2].

L'étude paramétrique a alors consisté à faire varier les caractéristiques de raideur et d'amortissement du modèle numérique de pneumatiques et à prédire par calcul leur influence sur l'accélération transmise au poste de conduite lorsque le chariot franchit un obstacle (selon les conditions du code d'essai).

Les résultats des nombreuses simulations effectuées dans le cadre de cette étude paramétrique permettent de dresser une liste de recommandations qui pourront être utilisées par les constructeurs de pneumatiques pour prendre en compte des critères d'atténuation des vibrations transmises aux conducteurs de chariot lors de la conception.

Mots-clés : SIMULATION NUMERIQUE – MODELISATION – PNEUMATIQUE – VIBRATION – RAIDEUR – AMORTISSEMENT – CHARIOT ELEVATEUR

Introduction

Within the frame of the study called « Modelling of the dynamical behaviour of the forklift truck tires», INRS designed and validated a new numerical model of forklift truck tires [1]. From the quasi-static measurement of the physical parameters characterizing the tires (solid as well as pneumatic), the results have shown that it was possible to predict their dynamical behaviour. This model was implemented in the whole model of forklift truck including the chassis, the forks and the cab. It was able to predict the vibration emission at the driving position.

The interest of such a model lies in the ability of simulating the effects of design modifications on the vibration emission. The aim of this study was to run this model to analyse the influence of each of the physical parameters of the tires (stiffness, damping...) on the dynamical behaviour of the forklift truck and to optimise their performance in reducing vibration at the driving place.

More precisely, the aim was to evaluate the influence of theoretical physical properties (load/deflection law, damping parameters) on the attenuation properties of the tires. The aim was also to write guidelines, which may be useful to manufacture new tire prototypes. This objective is realistic from a technical point of view.

This report is divided in five chapters :

The 1st chapter is concerned with the forklift truck characterization. It is shown how to measure the mechanical properties of the forklift truck (position of the center of mass, mass and inertia). These data were used to set up the whole model of forklift truck equipped with the four tires.

The 2nd chapter is dedicated to the characterization of the tires. The tests carried out to measure the static properties (stiffness and damping) were realized with a specific test bench designed by INRS. Three sets of tires were tested (front and rear tires) : one set of pneumatic tires, one set of solid tires and one set of mixed tires (pneumatic tires with an inner elastomer ring).

In the 3rd chapter, the procedure used to test forklift trucks is detailed. It follows the recommendations of the corresponding European test code [2]. The protocol used to measure the vertical acceleration at the driving position for each configuration of tires is also explained.

The numerical model of the whole forklift truck equipped with the tires is shown in the 4th chapter. The model was used to simulate the tests presented in the previous chapter. A good correlation between calculation and measurements is noted.

In the 5th chapter, the model was used to test the influence of physical parameter changes :

- shape of the load/deflection law (degree of non-linearity of the stiffness),
- slope of the load/deflection law (stiffness),
- damping.

The model was able to predict the influence of these changes on the vertical acceleration at the driving position, according to the method recommended in the European test code.

Conclusion

This study aimed to analyse the effects of the tire properties on the vibratory behaviour of the forklift truck. It has been shown how to set up the model from static tests knowing the mechanical properties of the tires and of the forklift truck. This model was validated under the testing conditions prescribed by the European test code[2].

The parametrical study consisted in changing the tire characteristics of stiffness and damping and in calculating the effect of such changes on the transmitted vibration at the driving position, when the truck was running over obstacles (according to the European test code).

The numerous results obtained allow us to draw guidelines that may be used by tire manufacturers to take the vibration reduction into account in the process of design :

- Concerning the stiffness, the calculation confirmed that the lower the stiffness, the higher the vibration attenuation. For a given stiffness value, the response of the forklift truck strongly depends on its velocity. The calculations and the experiments showed that there is a critical speed at which the vibration is the highest. Decreasing the stiffness leads to decrease the level of these vibration peaks and also to decrease the corresponding critical speed.
- The calculations have shown that the use of different stiffness for front and rear wheels is not efficient to reduce vibration emission.
- Concerning the stiffness non-linearity, the calculations have shown that the vibration attenuation is the best for « softening tires», this meaning tires with a decreasing stiffness law in function of the deflection. The « softening » concept does not seem to be realistic. Moreover this property could have a bad influence on the forklift truck stability. Then, it may be considered that the aim to be reached corresponds to the linear case when the stiffness does not depend on the deflection.

These guidelines do not take stability or handling problems into consideration. These problems are also linked to the tire properties.

- Concerning the damping, the calculations have shown that it is always beneficial to increase it. Nevertheless it is very difficult to quantify the expected gains of attenuation, because the damping model used was too simple and the damping parameters are not directly connected to the material composition.

1. Characterizing the KOMATSU FD20 forklift truck

I-1 Measurement of the weight of the forklift truck KOMATSU FD20

The forklift truck was hung with ropes fixed to a force sensor.
By so doing, the measured weight was 3420 kg.

Figure I- 1: Weighing of the forklift truck

I-2 Position of the center of mass

I-2-1 longitudinal position of the center of mass

The position was determined with a static balance procedure. This was an iterative method : the aim was to find the position where the forklift truck was stable when placed on the edge of a L section. When the equilibrium point was reached, the center of mass was just up on the section (cf. Figure I- 3).

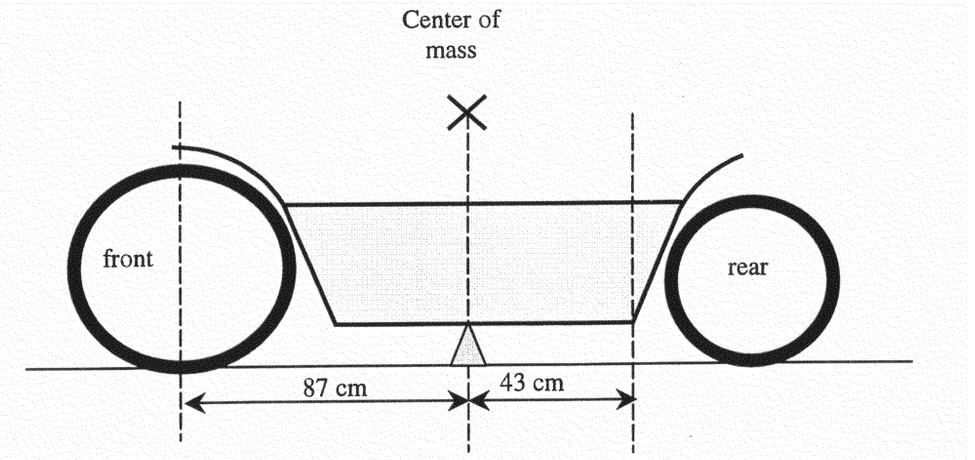

Figure I- 2 : Measurement of the longitudinal position of the center of mass

Figure I- 3 : View of the measurement of the longitudinal position of the center of mass

I-2-2 Verification of the longitudinal position of the center of mass

From the momentum law it was also possible to deduce the longitudinal position of the center of mass: the rear side was hung with ropes (cf. Figure I- 4). When the forklift truck was horizontal the force in the ropes was 1435 kg. From the momentum law the distance between the projection of the center of mass on the floor and the center of the front wheel was deduced. This distance was 85 cm (87=1435*207/3420). So the position of the center of mass was made sure.

I-2-3 Height of the center of mass (measurement by rotating around the pitch axis)

This experiment consists in rotating the forklift truck by pulling ropes fixed on its rear side and measuring the angle of rotation (or equivalently measuring the height of the rear wheel) in function of the static force in the ropes.

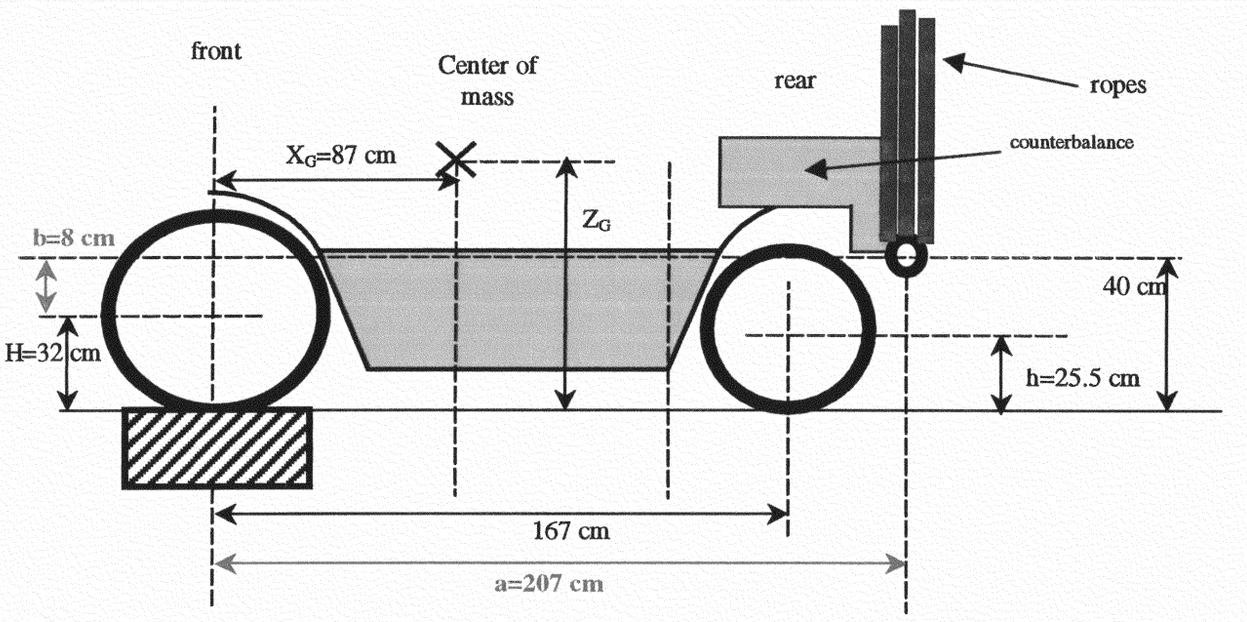

Figure I- 4 : measurement of the height of the center of mass

By applying the theorems of Mechanics, it was possible to get an analytical expression of the tensile force in the ropes in function of the position of the center of mass and of the rotation angle. Reciprocally, with the knowledge of the tensile force and the longitudinal position of the center of mass it was also possible to calculate the height of the center of mass.

The formula linking the height Z_G of the center of mass to the rotation angle of the forklift truck α and the tensile force F is :

$$Z_G = X_G \cot g\alpha - \left(\frac{F \cos\left(Arctg\left(\frac{b}{a}\right) + \alpha \right) \sqrt{a^2 + b^2}}{Mg \sin\alpha} \right) + H \qquad (1)$$

A proof of the formula (1) is given in appendix (1).

Force (kg) F	Height (cm) h	Angle (degrees) α
1421	29	-1,03
1404	35	1,03
1389	40	2,75
1375	45	4,46
1361	50	6,19
1347	55	7,92
1332	60	9,65
1318	65	11,39
1302	70	13,15
1287	75,5	15,09
1272	80	16,70
1257	85	18,50
1244	90	20,32
1228	95	22,16
1216	98	23,27
1196	100	24,02
1180	105	25,92
1160	110	27,84
1136	115	29,80
1118	120	31,79

Table I- 1 : Measured values of the tensile force in function of the rotation angle of the forklift truck

Figure I- 5 : View of the measurement of the height of the center of mass by rotating around the pitch axis

Figure I- 6 shows the evolution of the calculated value Z_G (with the exact formula (1)) for each value of the rotation angle of the forklift truck. The results showed that the calculated value Z_G did not depend of the rotation

angle, for angles larger than 5 degrees. For lower angles, measuring errors involved more discrepancies. Z_G was 64 cm.

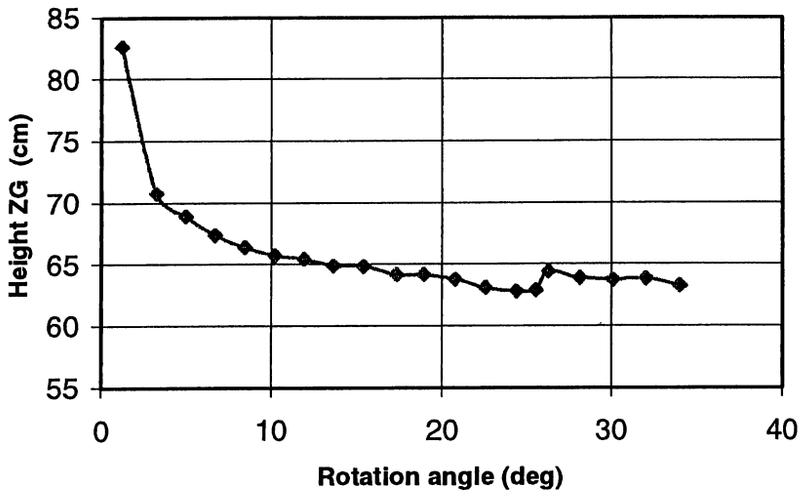

Figure I- 6 : Calculation of the height of the center of mass in function of the rotation angle of the forklift truck

Figure I- 7 shows the evolution of the tensile force F in the ropes (with the exact formula (1)) in function of the rotation angle of the forklift truck and for arbitrary values of Z_G (54 cm, 64 cm et 74 cm). It was observed that the curve obtained with Z_G=64 cm gave the most reliable results, in comparison with the measurements.

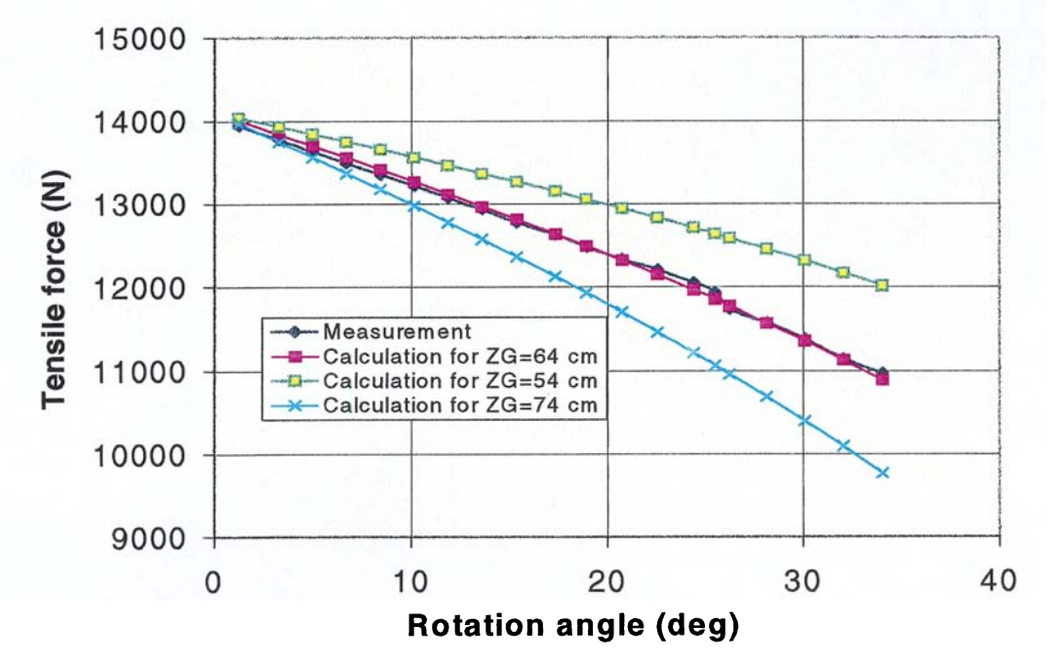

Figure I- 7 : Tensile force in function of the rotation angle of the forklift truck.
(Comparison between the calculation of the force from an arbitrary value of Z_G and its measurement)

I-2-4 Height of the center of mass (measurement by rotating around the roll axis)

The same principle was applied by rotating the forklift truck around the roll axis. In the same manner, the tensile force was measured in function of the rotation angle of the forklift truck.
The forklift truck was disposed on the edge of a L section, longitudinally placed on the floor (cf. Figure I- 8).
The distance between the fixing point of the ropes and the floor was called Z. The wheels of the forklift truck laid on wedges. When the forklift truck was horizontal, Z was 50 cm.

Figure I- 8 : View of the measurement of the height of the center of mass by rotating around the roll axis

Tensile force in the ropes F (kg)	Height of the fixing point of the ropes Z (cm)	Rotation angle α (deg)
1460	51	0,21
1410	57	3,21
1350	62.5	6,00
1290	67.5	8,58
1240	72.5	11,20
1190	76	13,07

Table I- 2 : Measured values of the tensile force in function of the rotation angle of the forklift truck

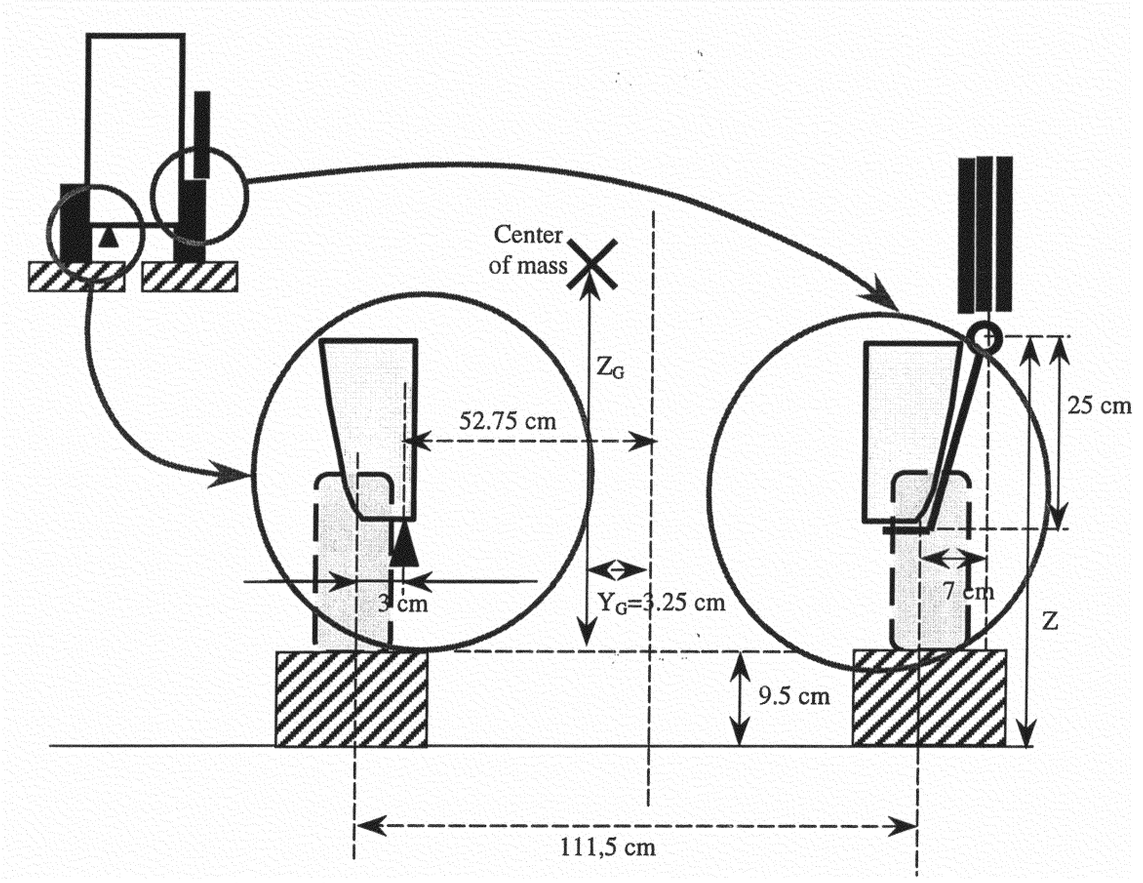

Figure I- 9 : Measurement of the height of the center of mass

Y_G was determined by applying the momentum law when the forklift truck was horizontal (52.75-Y_G=1460*115.5/3420=49.5 cm).
To calculate Z_G, the same method as previously was used, with the analytical formula (1) after replacing X_G with (52.75-Y_G). In this case, a was 25 cm, b was 115.5 cm and H was 15.5 cm.

The evolution of the Z_G value was calculated (with the analytical formula (1)) for each value of the rotation angle of the forklift truck (cf. Figure I- 10). The results showed that the calculated value Z_G did not depend of the rotation angle, for significant values of the angle. It was also verified that the calculated value of Z_G was the same as the value previously calculated : Z_G was 64 cm.

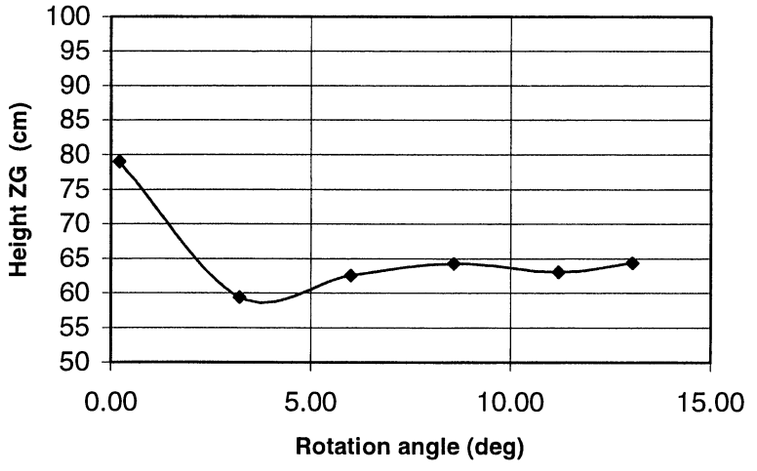

Figure I- 10 : Calculation of the height of the center of mass in function of the rotation angle (roll)

The tensile force in the ropes was also calculated (with the analytical formula (1)) in function of the rotation angle of the forklift truck for arbitrary values of Z_G (54 cm, 64 cm et 74 cm). It was observed that the curve obtained with Z_G=64 cm gave the most reliable results in comparison with the measurements.

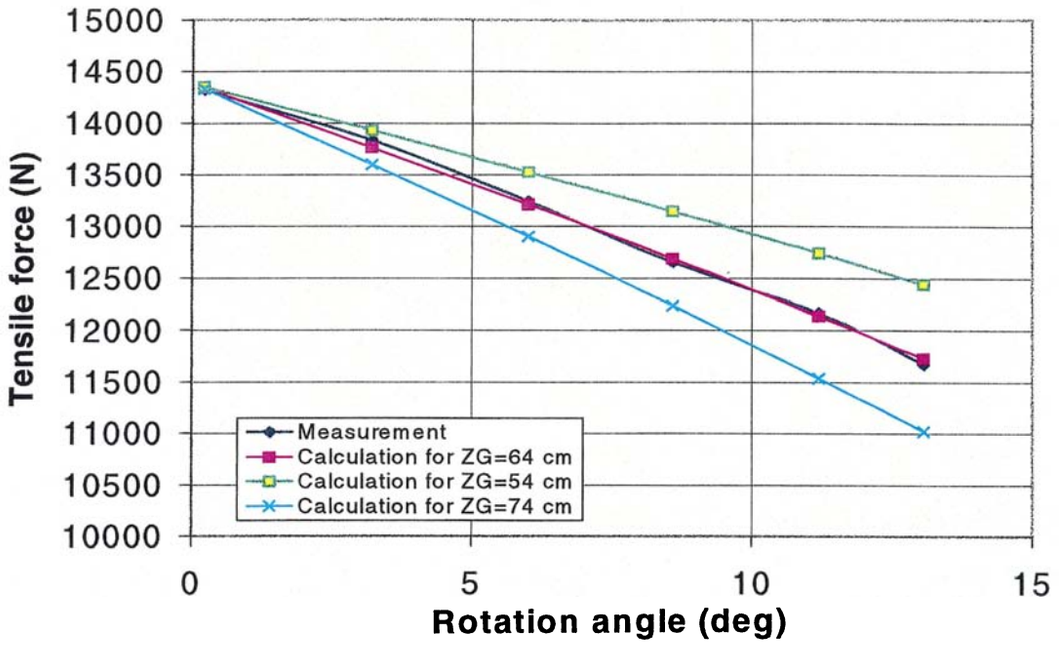

Figure I- 11 : - Tensile force in function of the rotation angle of the forklift truck (roll).
(Comparison between the calculation of the force from an arbitrary value of Z_G and its measurement)

I-3 Inertia measurements :

I-3-1 Ixx Inertia measurements :

The principle of these measurements consisted in hanging the forklift truck on springs in parallel (when the forklift truck was horizontal and laid on the edge of a L section, cf. Figure I- 13) and in measuring the frequency of the free oscillations. The springs had a well-known stiffness (see their characteristics in appendix 2).

Figure I- 12 : Measurement of roll inertia by free oscillations.

With the knowledge of the free oscillation time period, the analytical formula (2) made it possible to calculate the inertia corresponding to the roll axis.

$$I_{xx} = \frac{T^2}{4\pi^2}\left(-MgZ_1 + kY_2^2 + \left(\frac{MgY_1Z_2}{Y_2}\right)\left(\frac{L+Z_2}{L}\right)\right) - M\left(Y_1^2 + Z_1^2\right) \quad (2)$$

The roll inertia in the center of mass was called I_{xx}. See the proof of the formula (2) in appendix 3.

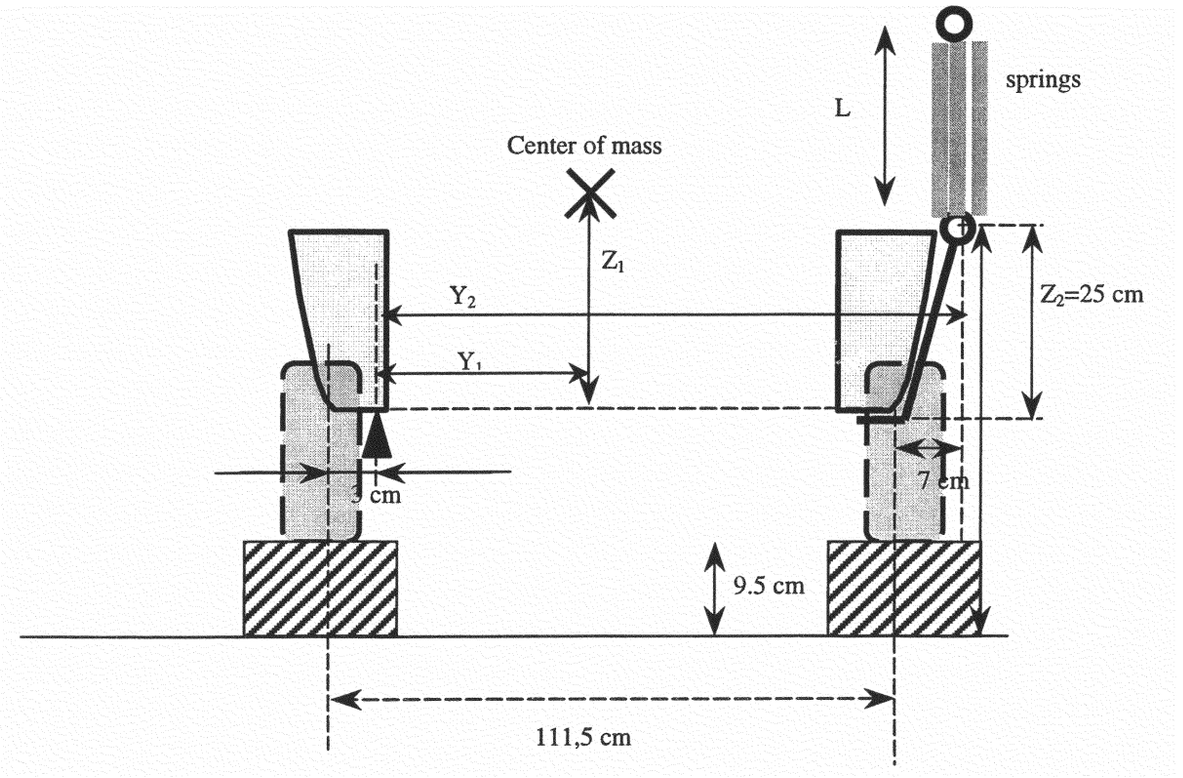

Figure I- 13 : Measurement of the I_{xx} inertia

Y_1=52.75 cm -Y_G –3cm=46.5 cm
Z_1=Z_G –15.5cm=48.5 cm
Y_2=111.5 cm+7 cm-3 cm=115.5 cm
Z_2=25 cm

The same experiment was held with 8 springs in parallel, then with 7 springs.
With the 8 springs the results were : L=60 cm ; k=7500×8=60 000 N/m/s
With the 7 springs the results were : L=62 cm ; k=7500×7=52 500 N/m/s

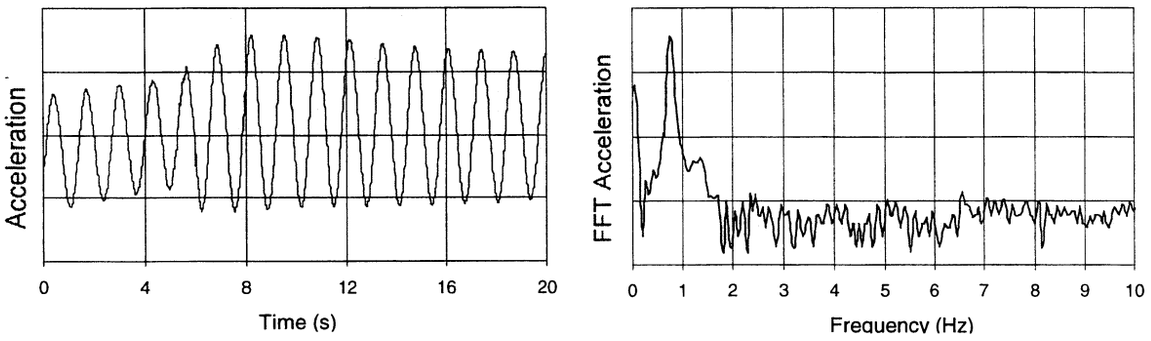

Figure I- 14 : Free oscillations measured with an accelerometer – 8 springs – natural frequency : 0.75 Hz

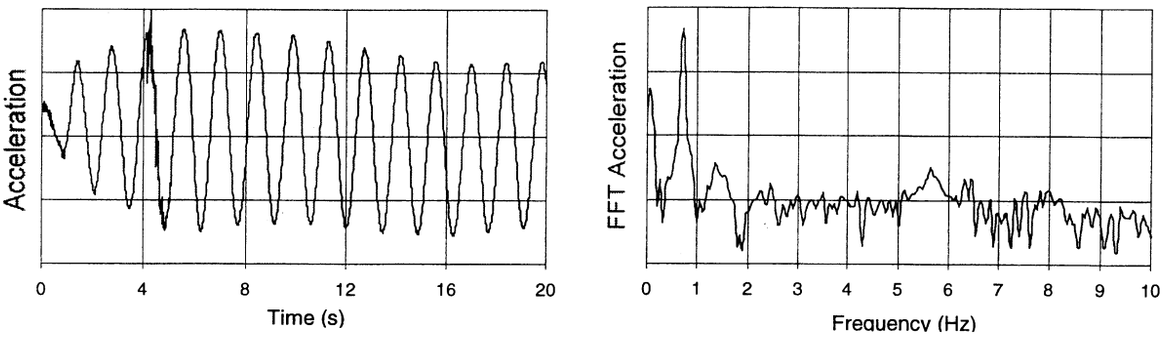

Figure I- 15 : Free oscillations measured with an accelerometer – 7 springs – natural frequency : 0.7 Hz

Ixx inertia was calculated with formula (2):

For the experiment held with the 8 springs Ixx=1480 kg.m^2
For the experiment held with the 7 springs Ixx=1410 kg.m^2
This gave the mean value of 1450 kg.m^2

I-3-2 Iyy Inertia measurements :

The same principle was used for the measurements around the pitch axis (cf. Figure I- 16).

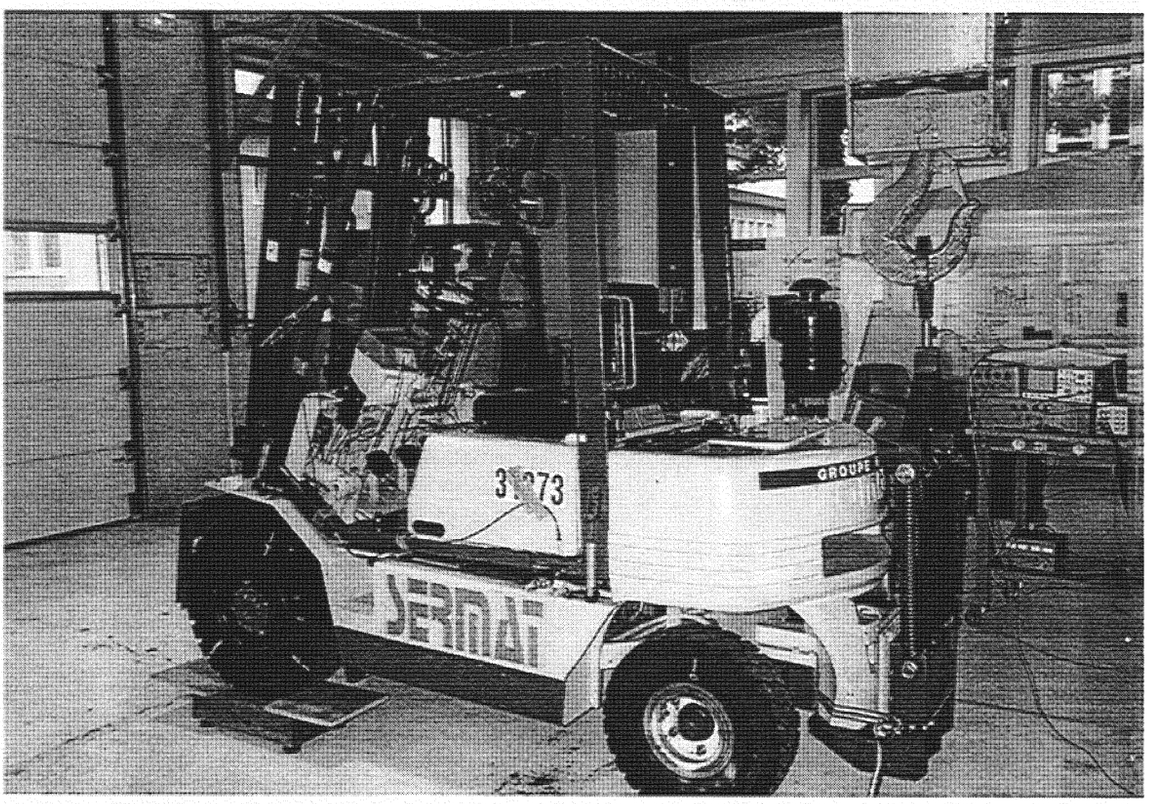

Figure I- 16 : Measurement of the pitch inertia by free oscillations.

The measurement was repeated with different numbers of springs, this meaning with different suspension stiffness. Different locations of the forklift truck support were also tested .

For each tested configuration, the frequency of the free oscillations was measured. The values of the I_{yy} inertia calculated from the natural frequencies are reported in Table I- 3. In theory, all the natural frequencies measured must lead to the same value of I_{yy}.

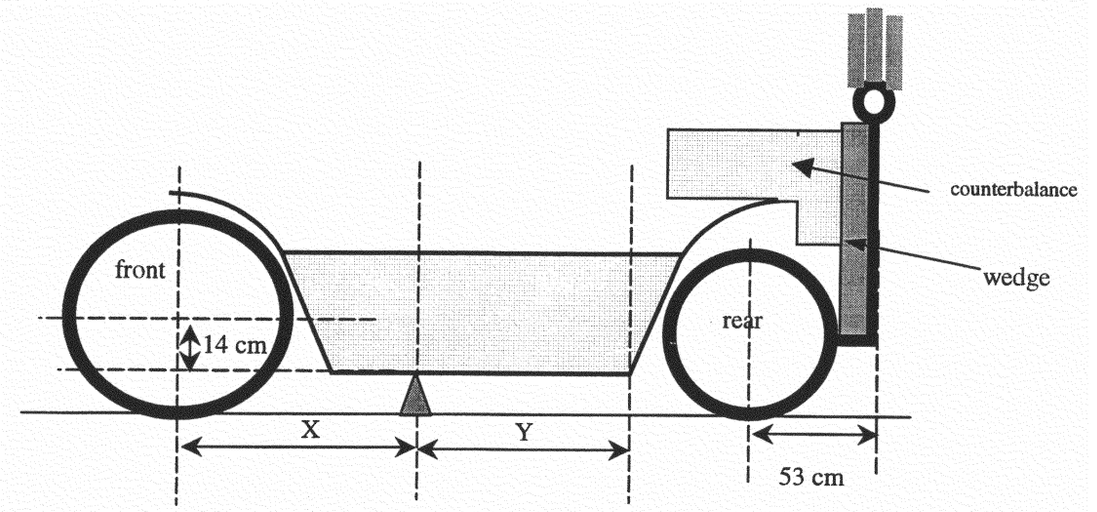

Figure I- 17 : Measurement of the I_{yy} inertia

	X (cm)	L (m)	Number of springs used	Natural frequency (Hz)	Pitch inertia I_{yy} (kg.m^2)
Case 1	54	44	8	0.95	3138
Case 2	54	49	6	0.825	2981
Case 3	0 Oscillations around the front wheel axle	54.5	8	1.025	3823
Case 4	0 Oscillations around the front wheel axle	62.5	6	0.9	3561
Case 5	64	43	6	0.78	3042
Case 6	64	48	4	0.602	3170
Case 7	64	53	3	0.5	3153

Table I- 3 : Different tested configurations of free oscillations

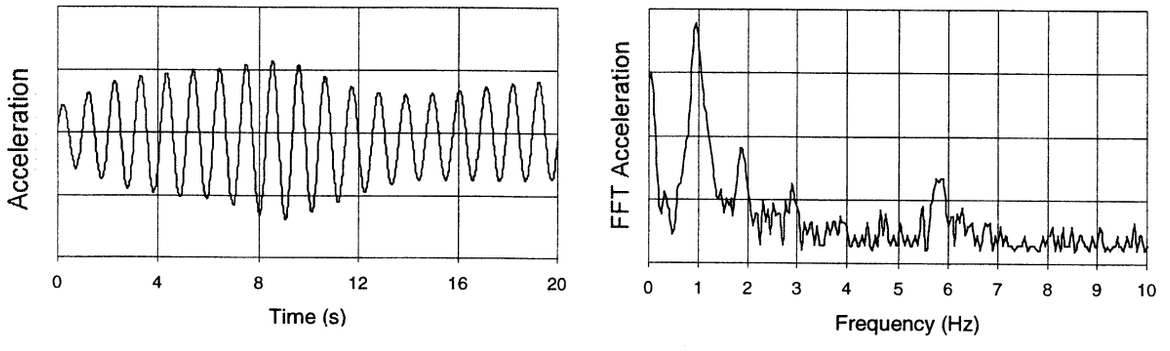

Figure I- 18 : Case 1 ; X=54 cm ; 8 springs ; natural frequency = 0.95 Hz

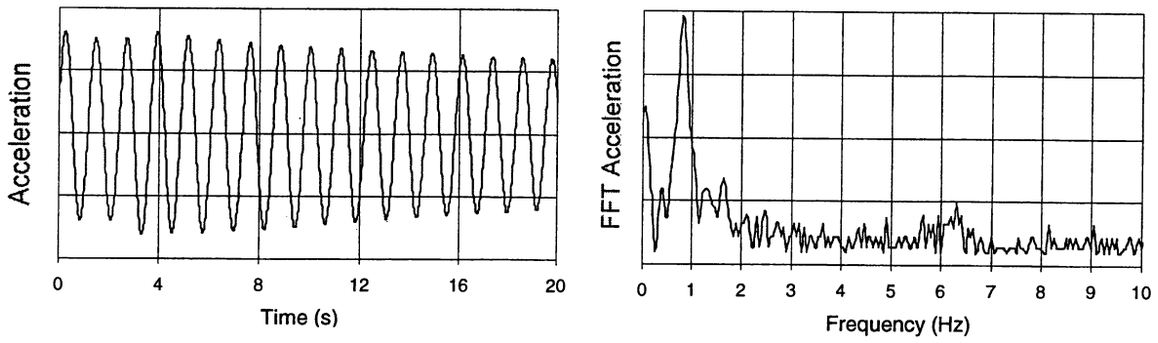

Figure I- 19 : Case 2 ; X=54 cm ; 6 springs ; natural frequency = 0.825 Hz

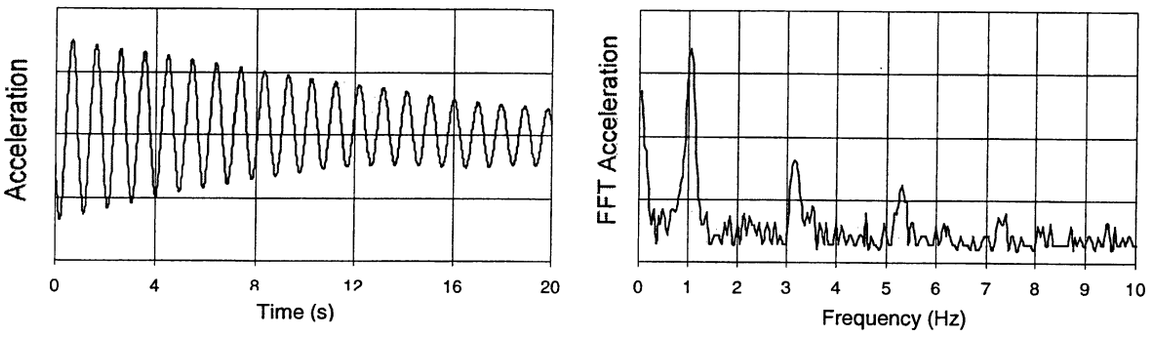

Figure I- 20 : Case 3 ; X=0 cm ; 8 springs ; natural frequency = 1.025 Hz

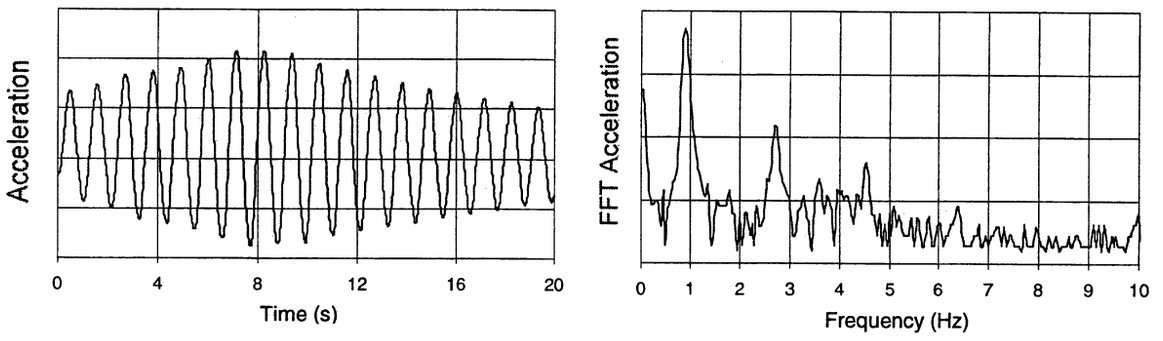

Figure I- 21 : Case 4 ; X=0 cm ; 6 springs ; natural frequency = 0.9 Hz

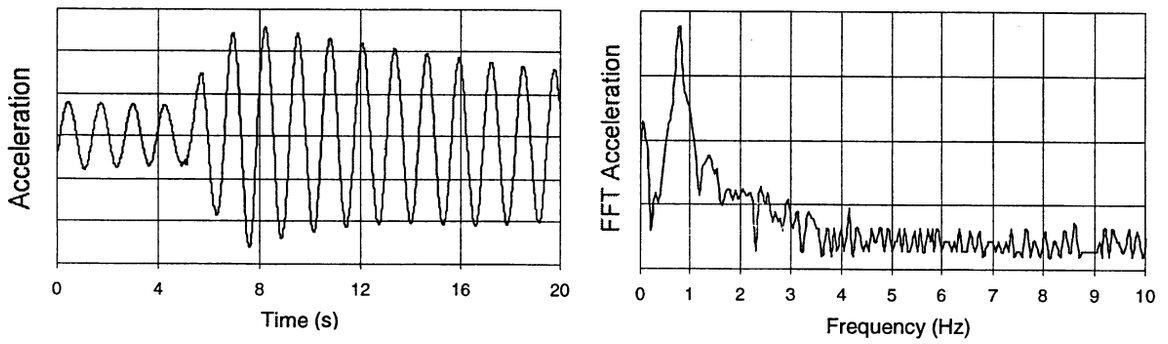

Figure I- 22 : Case 5 ; X=64 cm ; 6 springs ; natural frequency = 0.78 Hz

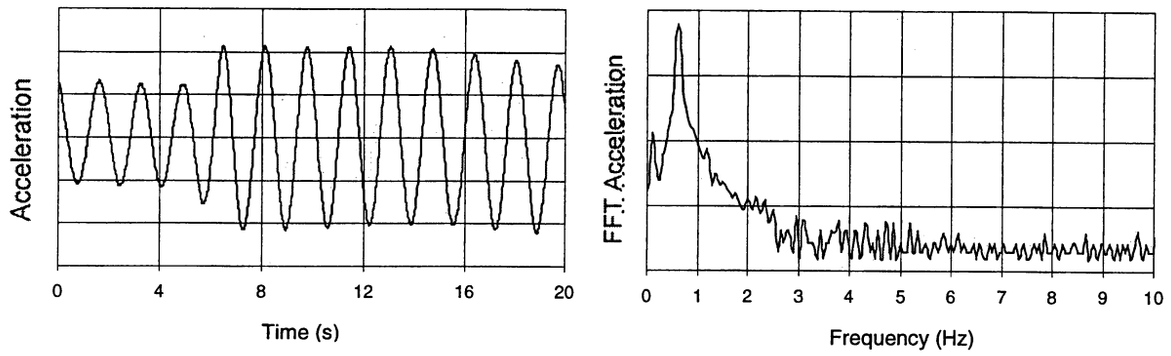

Figure I- 23 : Case 6 ; X=64 cm ; 4 springs ; natural frequency = 0.602 Hz

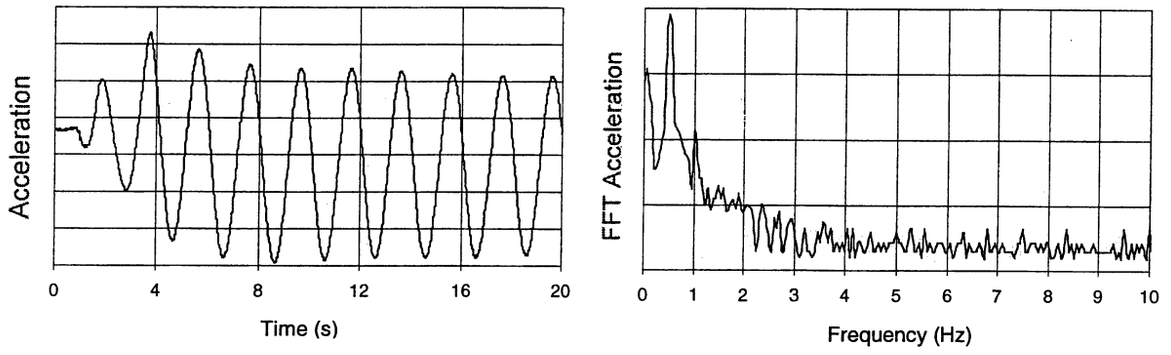

Figure I- 24 : Case 7 ; X=64 cm ; 3 springs ; natural frequency = 0.5 Hz

The cases 3 and 4 are covered with errors because the rotation was around the front wheel axle : for this reason, the inertia of the wheels was not taken into account. Moreover, it was observed that the wheels were slightly moving during the experiment, so that the axis of rotation was not always coincident with the front wheel axle. Then, the mean value of I_{yy} was calculated from the cases 1,2,5,6,7, this giving :

$I_{yy} = 3100 \text{ kg.m}^2$

Taking into account all the symmetries, it was assumed that the axes (xx') and (yy') were "closed" from the principal axes of inertia, or, in other terms, the off-diagonal terms of the matrix of inertia were neglected.

I-4 Forklift truck model

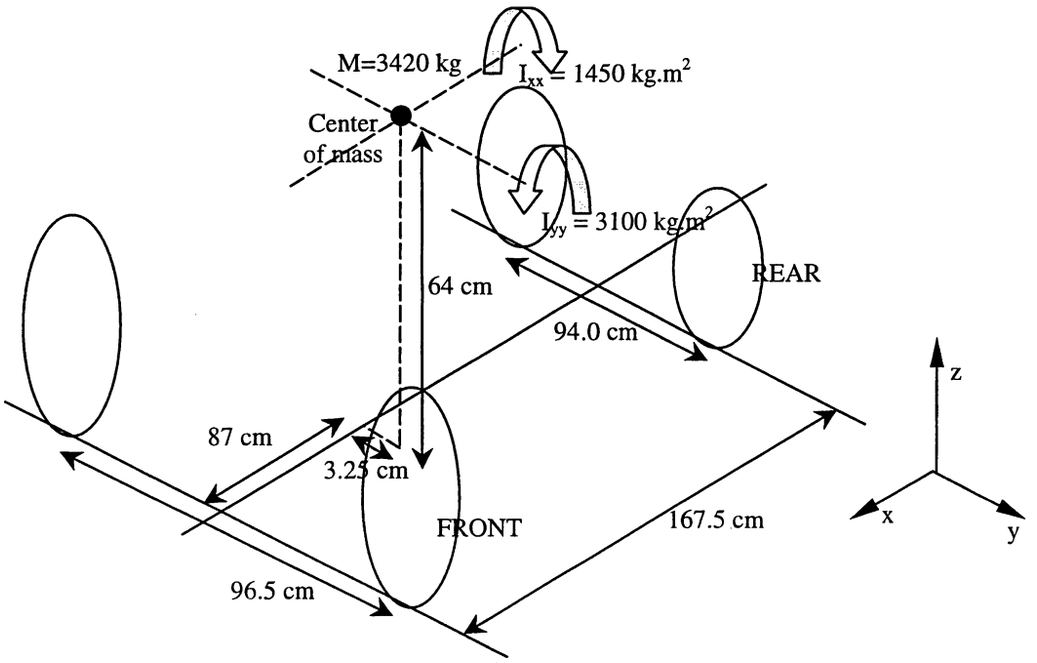

Figure I- 25 : Equivalent mechanical diagram for the KOMATSU FD20

2. Characterizing the tires

The mechanical properties of 3 sets of tires were measured :

- Pneumatic tires (inflated at 10 bars).
  Front wheel tire called G1 (∅=68 cm)
  Rear wheel tire called G2 (∅=54 cm)

- Solid tires.
  Front wheel tire called P1 (∅=68 cm)
  Rear wheel tire called P2 (∅=54 cm)

- Mixed tires composed of pneumatic tires filled with an inner elastomer ring.
  Front wheel tire called H1 (∅=68 cm)
  Rear wheel tire called H2 (∅=54 cm)

According to the modelling method designed by INRS [1], the quasi-static properties characterizing the tires may be measured with two types of tests. One test at constant height (height of the wheel axle) gives the « shape factor » which is the polynomial characterizing the evolution of the contact forces when the tire is running over an obstacle of a given thickness. One other quasi-static test is used to get the load/deflection law of each tire.

II-1 Measurement of the shape factors

This test consists in measuring the changes of the contact force between the tire and the ground and/or the obstacle, in function of the horizontal position of the wheel and for a given constant height of the wheel axle. The shape factor for the upper part gives the evolution of the contact force between the tire and the obstacle and the shape factor of the lower part is related to the changes of the contact force between the tire and the ground. The shear of the tire on the edge of the obstacle is characterized by a parameter called « shock advance ». This parameter was also deduced from this quasi-static test

$$F_{tire/ground} = p_l\left(\frac{L^{ground}}{L_0^{ground}}\right) \bullet F(z) \tag{3}$$

$$F_{tire/obstacle} = p_h\left(\frac{L^{obst}}{L_0^{obst}}\right) \bullet F(z + h_{obst}) \tag{4}$$

With :
$F_{tire/ground}$ = contact force between the tire and the ground.
$F_{tire/obstacle}$ = contact force between the tire and the obstacle.
P_l : shape factor for the lower part, polynomial of 5th order.
P_h : shape factor for the upper part, polynomial of 5th order.
L^{ground} : theoretical tire print on the ground (see appendix 4).
L_0^{ground} : theoretical tire print on an infinite plane surface (see appendix 4).
L^{obst} : theoretical tire print on the obstacle (see appendix 4).
L_0^{obst} : theoretical tire print on an infinite plane surface at the obstacle height (see appendix 4).
F : load/deflection law on an infinite plane surface.

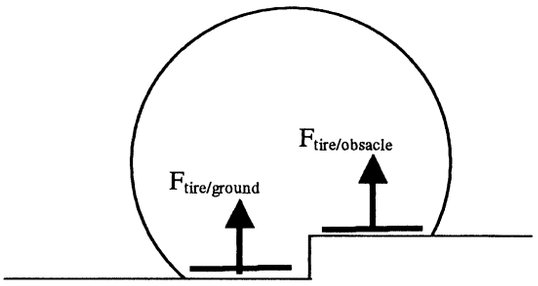

Figure II- 1: Contact forces between the tire and the ground and/or the obstacle

Figure II- 2 shows the test bench used for the measurement of the shape factor: a PVC obstacle (same height as the obstacle used for the vibratory tests carried out with the forklift truck : 1cm) was glued on a thinner PVC strip. The wheel is squeezed on the PVC strip by a hydraulic actuator. The PVC strip is placed on a support covered with TEFLON. The height of the wheel axle is kept constant by the actuator. The wheel is motorized. It can slowly rotate. With the rotation of the wheel, the PVC strip can slide on the support and force the relative displacement between the obstacle and the wheel.

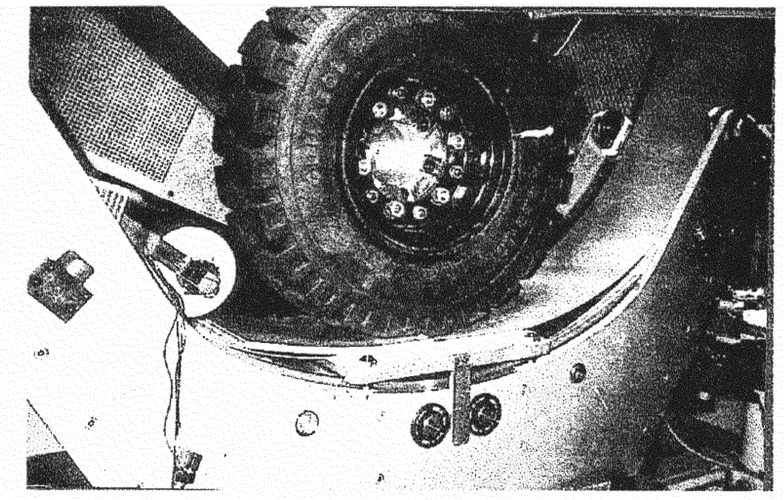

Figure II- 2 : Measurement of the shape factor

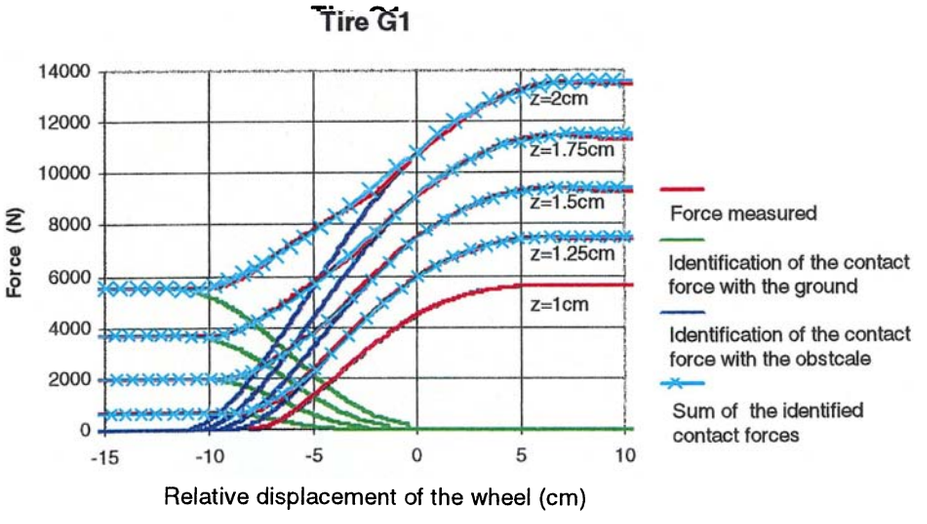

Figure II- 3 : Shape factor of the pneumatic tire (∅=68 cm)

Polynomial interpolating the shape factor (upper part)	
Coefficient $\left(L^{obst} / L_0^{obst}\right)^5$	-3.739172
Coefficient $\left(L^{obst} / L_0^{obst}\right)^4$	14.265972
Coefficient $\left(L^{obst} / L_0^{obst}\right)^3$	-19.527659
Coefficient $\left(L^{obst} / L_0^{obst}\right)^2$	10.159708
Coefficient $\left(L^{obst} / L_0^{obst}\right)$	-0.158293
Constant	-0.001062
Polynomial interpolating the shape factor (lower part)	
Coefficient $\left(L^{ground} / L_0^{ground}\right)^5$	12.504640
Coefficient $\left(L^{ground} / L_0^{ground}\right)^4$	-28.061820
Coefficient $\left(L^{ground} / L_0^{ground}\right)^3$	17.352577
Coefficient $\left(L^{ground} / L_0^{ground}\right)^2$	-0.920485
Coefficient $\left(L^{ground} / L_0^{ground}\right)$	0.100238
Constant	0.020459
Shock advance (m)	
Δ	0.070000

Table II- 1 : Shape factor parameters of the pneumatic tire (∅=68 cm)

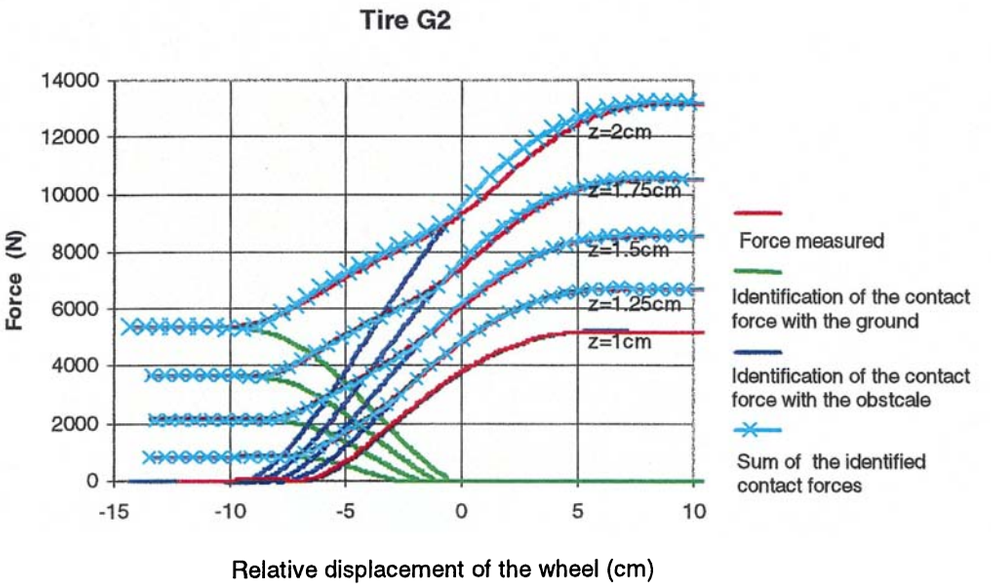

Figure II- 4 : Shape factor of the pneumatic tire (∅=54 cm)

Polynomial interpolating the shape factor (upper part)	
Coefficient $\left(L^{obst} / L_0^{obst}\right)^5$	-2.798085
Coefficient $\left(L^{obst} / L_0^{obst}\right)^4$	10.893064
Coefficient $\left(L^{obst} / L_0^{obst}\right)^3$	-15.842308
Coefficient $\left(L^{obst} / L_0^{obst}\right)^2$	9.030262
Coefficient $\left(L^{obst} / L_0^{obst}\right)$	-0.281056
Constant	-0.003185
Polynomial interpolating the shape factor (lower part)	
Coefficient $\left(L^{ground} / L_0^{ground}\right)^5$	6.368179
Coefficient $\left(L^{ground} / L_0^{ground}\right)^4$	-10.706915
Coefficient $\left(L^{ground} / L_0^{ground}\right)^3$	-0.226016
Coefficient $\left(L^{ground} / L_0^{ground}\right)^2$	6.528285
Coefficient $\left(L^{ground} / L_0^{ground}\right)$	-0.923795
Constant	-0.042564
Shock advance (m)	
Δ	0.050000

Table II- 2 : Shape factor parameters of the pneumatic tire (∅=54 cm)

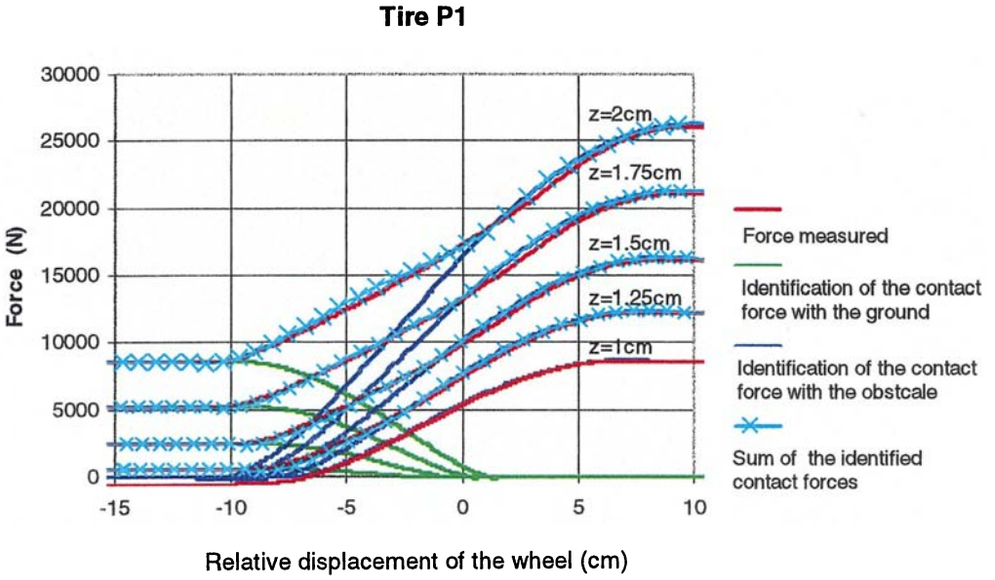

Figure II- 5 : Shape factor of the solid tire (∅=68 cm)

Polynomial interpolating the shape factor (upper part)	
Coefficient $\left(L^{obst} / L_0^{obst}\right)^5$	-0.991967
Coefficient $\left(L^{obst} / L_0^{obst}\right)^4$	4.617628
Coefficient $\left(L^{obst} / L_0^{obst}\right)^3$	-8.840850
Coefficient $\left(L^{obst} / L_0^{obst}\right)^2$	6.517820
Coefficient $\left(L^{obst} / L_0^{obst}\right)$	-0.300187
Constant	-0.003721
Polynomial interpolating the shape factor (lower part)	
Coefficient $\left(L^{ground} / L_0^{ground}\right)^5$	0.988859
Coefficient $\left(L^{ground} / L_0^{ground}\right)^4$	3.579162
Coefficient $\left(L^{ground} / L_0^{ground}\right)^3$	-13.137664
Coefficient $\left(L^{ground} / L_0^{ground}\right)^2$	10.727185
Coefficient $\left(L^{ground} / L_0^{ground}\right)$	-1.156796
Constant	-0.001228
Shock advance (m)	
Δ	0.050000

Table II- 3 : Shape factor parameters of the solid tire (∅=68 cm)

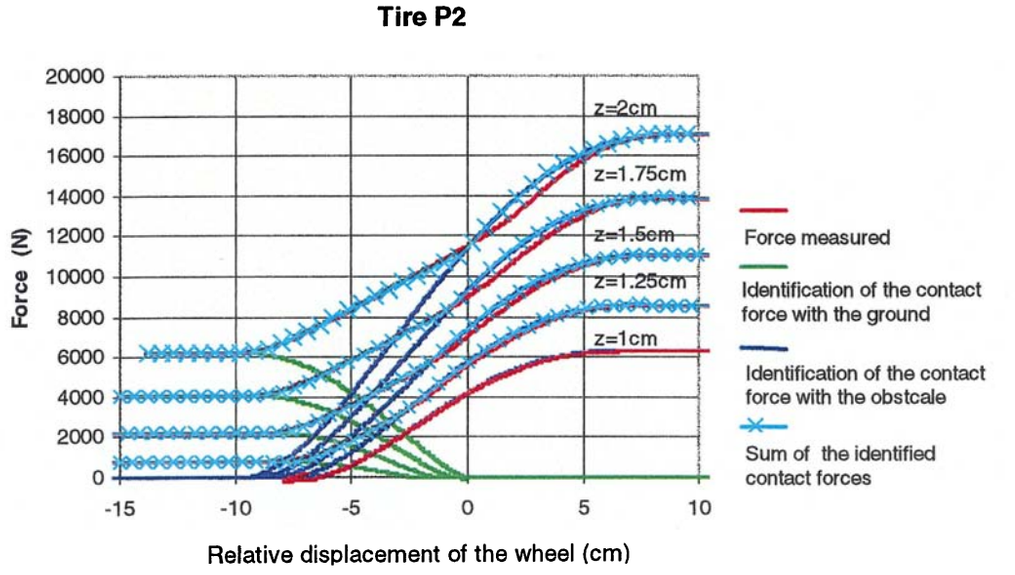

Figure II- 6 : Shape factor of the solid tire (∅=54 cm)

Polynomial interpolating the shape factor (upper part)	
Coefficient $\left(L^{obst} / L_0^{obst}\right)^5$	-0.238756
Coefficient $\left(L^{obst} / L_0^{obst}\right)^4$	3.524886
Coefficient $\left(L^{obst} / L_0^{obst}\right)^3$	-8.613286
Coefficient $\left(L^{obst} / L_0^{obst}\right)^2$	6.510233
Coefficient $\left(L^{obst} / L_0^{obst}\right)$	-0.183172
Constant	-0.000091
Polynomial interpolating the shape factor (lower part)	
Coefficient $\left(L^{ground} / L_0^{ground}\right)^5$	-1.446549
Coefficient $\left(L^{ground} / L_0^{ground}\right)^4$	9.090475
Coefficient $\left(L^{ground} / L_0^{ground}\right)^3$	-18.260364
Coefficient $\left(L^{ground} / L_0^{ground}\right)^2$	13.736148
Coefficient $\left(L^{ground} / L_0^{ground}\right)$	-2.117782
Constant	-0.007583
Shock advance (m)	
Δ	0.045000

Table II- 4 : Shape factor parameters of the solid tire (∅=54 cm)

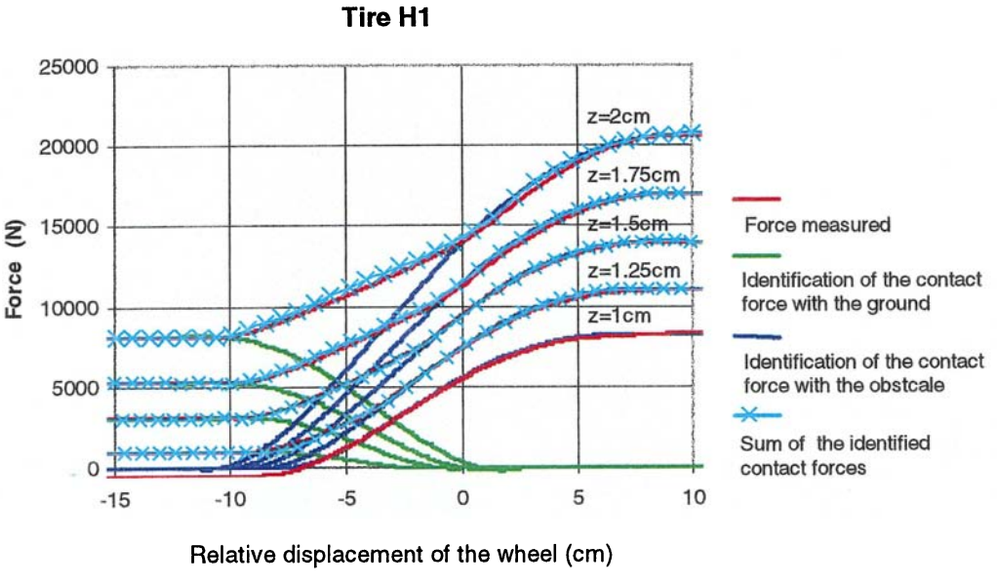

Figure II- 7 : Shape factor of the mixed tire (∅=68 cm)

Polynomial interpolating the shape factor (upper part)	
Coefficient $\left(L^{obst} / L_0^{obst}\right)^5$	-0.588420
Coefficient $\left(L^{obst} / L_0^{obst}\right)^4$	4.717954
Coefficient $\left(L^{obst} / L_0^{obst}\right)^3$	-10.064918
Coefficient $\left(L^{obst} / L_0^{obst}\right)^2$	7.231672
Coefficient $\left(L^{obst} / L_0^{obst}\right)$	-0.296328
Constant	-0.000439
Polynomial interpolating the shape factor (lower part)	
Coefficient $\left(L^{ground} / L_0^{ground}\right)^5$	3.915364
Coefficient $\left(L^{ground} / L_0^{ground}\right)^4$	-5.162269
Coefficient $\left(L^{ground} / L_0^{ground}\right)^3$	-4.054526
Coefficient $\left(L^{ground} / L_0^{ground}\right)^2$	7.093846
Coefficient $\left(L^{ground} / L_0^{ground}\right)$	-0.792396
Constant	0.000099
Shock advance (m)	
Δ	0.055000

Table II- 5 : Shape factor parameters of the mixed tire (∅=68 cm)

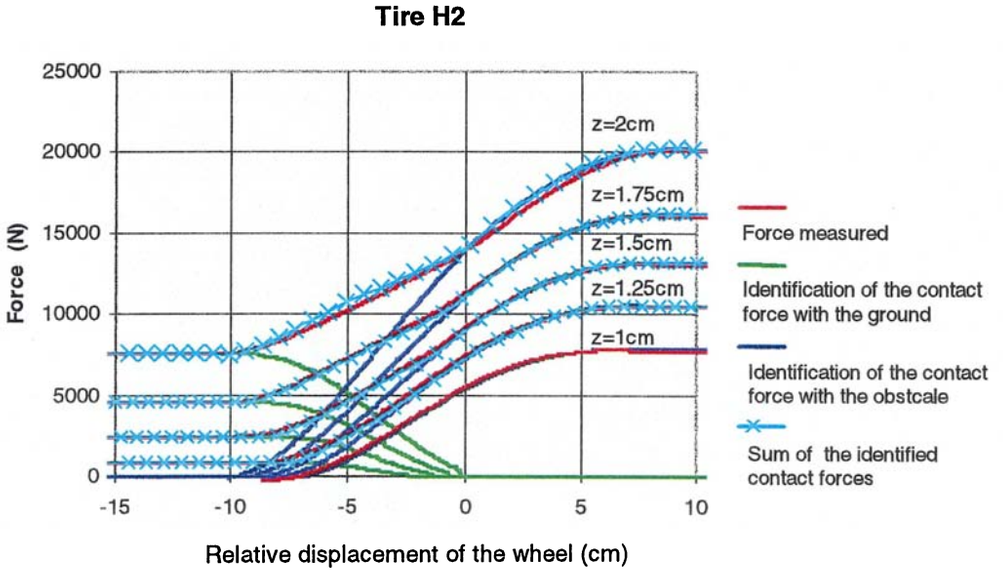

Figure II- 8 : Shape factor of the mixed tire (∅=54 cm)

Polynomial interpolating the shape factor (upper part)	
Coefficient $\left(L^{obst} / L_0^{obst}\right)^5$	-1.628748
Coefficient $\left(L^{obst} / L_0^{obst}\right)^4$	6.749230
Coefficient $\left(L^{obst} / L_0^{obst}\right)^3$	-10.740428
Coefficient $\left(L^{obst} / L_0^{obst}\right)^2$	6.591950
Coefficient $\left(L^{obst} / L_0^{obst}\right)$	0.031157
Constant	-0.003541
Polynomial interpolating the shape factor (lower part)	
Coefficient $\left(L^{ground} / L_0^{ground}\right)^5$	7.507269
Coefficient $\left(L^{ground} / L_0^{ground}\right)^4$	-15.656030
Coefficient $\left(L^{ground} / L_0^{ground}\right)^3$	6.376905
Coefficient $\left(L^{ground} / L_0^{ground}\right)^2$	3.268253
Coefficient $\left(L^{ground} / L_0^{ground}\right)$	-0.501015
Constant	-0.017393
Shock advance (m)	
Δ	0.045000

Table II- 6 : Shape factor parameters of the mixed tire (∅=54 cm)

II- 2 Measurement of the load/deflection law

Cyclic tests were carried out with the hydraulic actuator to obtain the load/deflection curve. The load/deflection curves were fitted with a 3rd order polynomial of z (deflection expressed in cm).

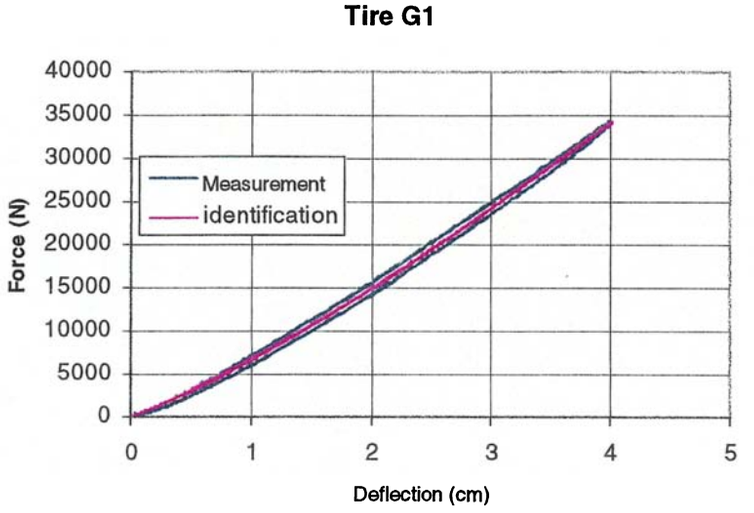

Figure II- 9 : Load/deflection law for the pneumatic tire (∅=68 cm)

Stiffness law of the tire G1 : $F(z) = -86\ z^3 + 1024\ z^2 + 5788\ z$

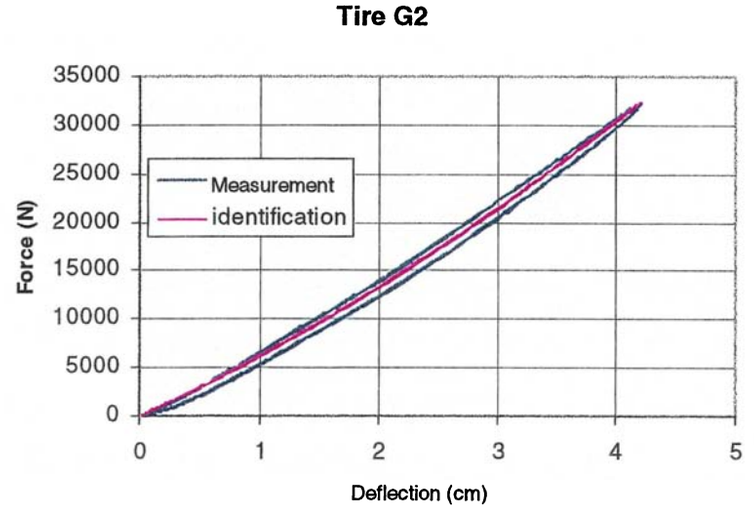

Figure II- 10 : Load/deflection law for the pneumatic tire (∅=54 cm)

Stiffness law of the tire G2 : $F(z) = 474\ z^2 + 5719\ z$

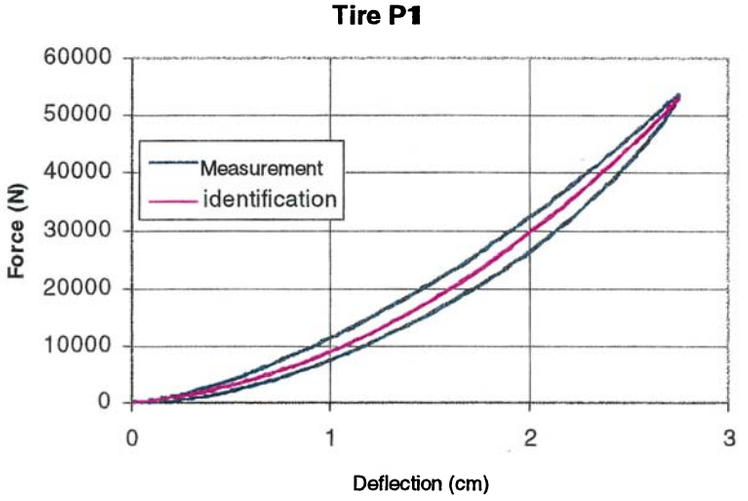

Figure II- 11 : Load/deflection law for the solid tire (∅=68 cm)

Stiffness law of the tire P1 : $F(z) = 176\ z^3 + 5188\ z^2 + 3655\ z$

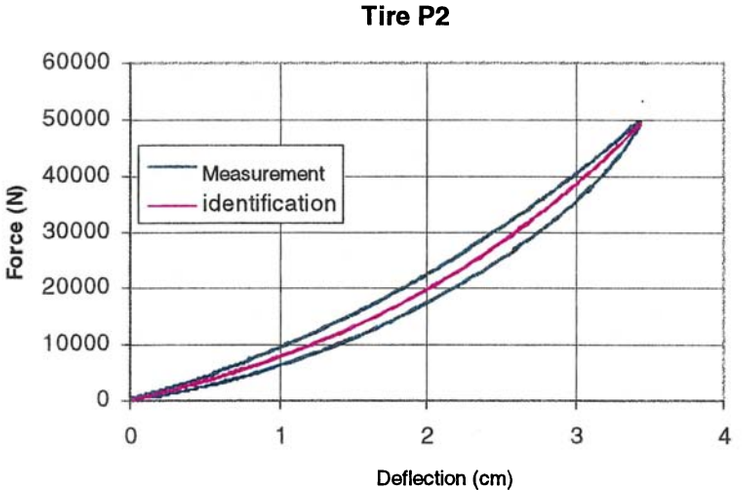

Figure II- 12 : Load/deflection law for the solid tire (∅=54 cm)

Stiffness law of the tire P2 : $F(z) = 398\ z^3 + 865\ z^2 + 6600\ z$

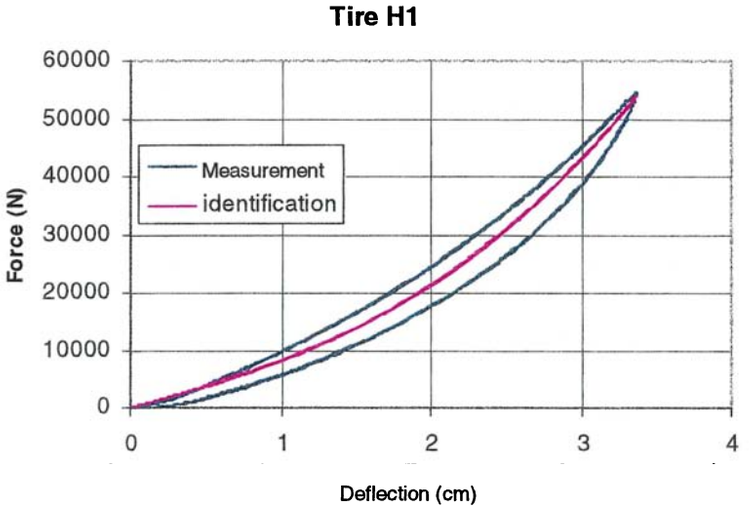

Figure II- 13 : Load/deflection law for the mixed tire (∅=68 cm)

Stiffness law of the tire H1 : $F(z) = 630\ z^3 + 503\ z^2 + 7144\ z$

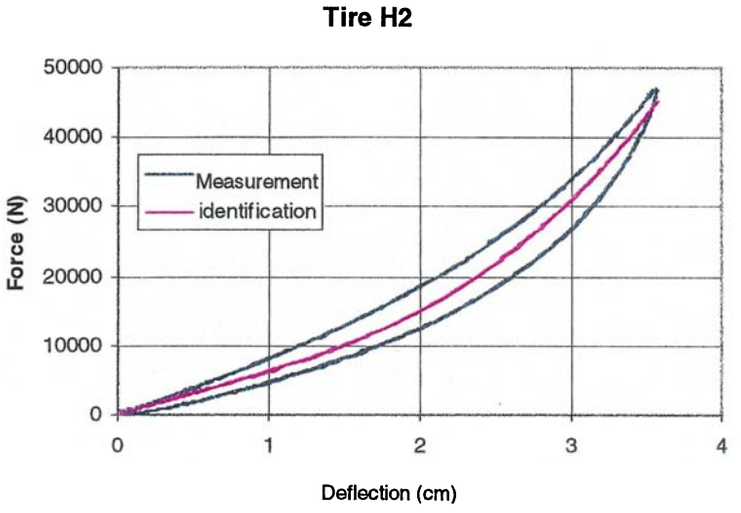

Figure II- 14 : Load/deflection law for the mixed tire (∅=54 cm)

Stiffness law of the tire H2 : $F(z) = 810\ z^3 - 1231\ z^2 + 6775\ z$

II-3 Measurement of the damping coefficient

The damping was assumed linear and of viscous type. This is an important simplification because the damping depends strongly on the magnitude of the oscillations and on their frequency. Nevertheless previous calculations run with tires of different sizes (see ref. [1]) have shown that the viscous model is good enough to predict the vibratory behaviour of the forklift truck. To measure the viscous damping constant, the tire, loaded with 2 tonnes, was lifted up and released to generate free oscillations. The logarithmic decrement method was then used to identify the damping constant from the time histories of the free oscillating deflection.
The logarithmic decrement method consists in measuring two different extrema X_i and X_{i+1} and the two corresponding times t_i and t_{i+1} of the time history. The following formula gives then the damping :

$$\varepsilon = \frac{C}{2\omega_0 M} = \frac{1}{2\pi}\ln\left(\frac{X_i}{X_{i+1}}\right) \qquad (5)$$

Where ε is the critical damping, which is a function of the natural pulsation of the structure ω_0. $\omega_0 = \sqrt{\frac{K}{M}}$ in the linear case.

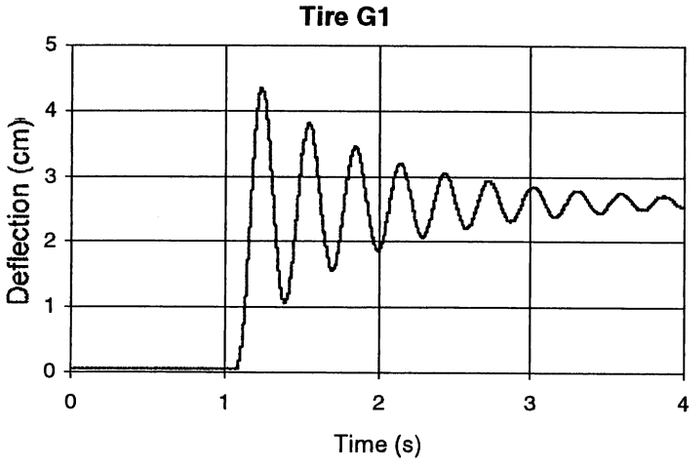

Figure II- 15 : Free oscillation of the pneumatic tire (∅=68 cm)

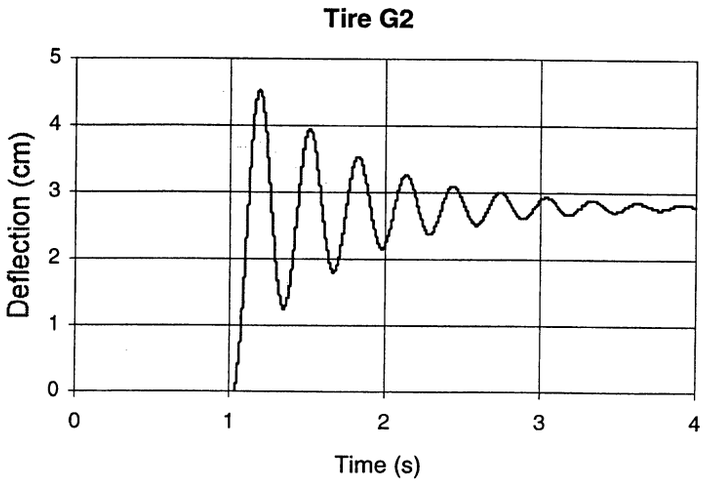

Figure II- 16 : Free oscillation of the pneumatic tire (∅=54 cm)

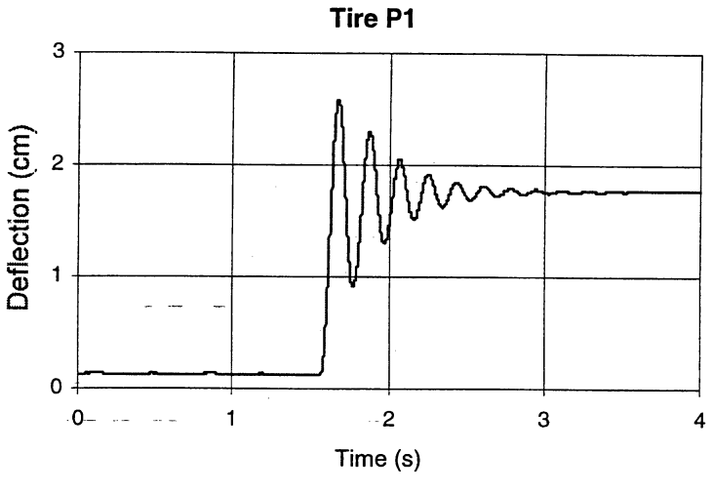

Figure II- 17 : Free oscillation of the solid tire (∅=68 cm)

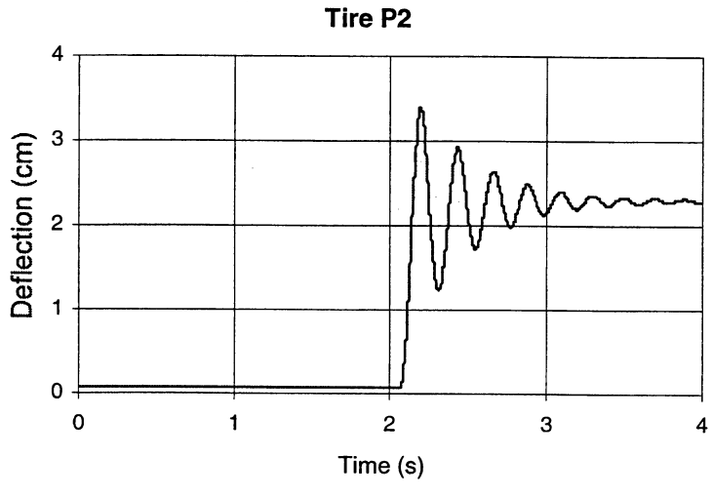

Figure II- 18 : Free oscillation of the solid tire (∅=54 cm)

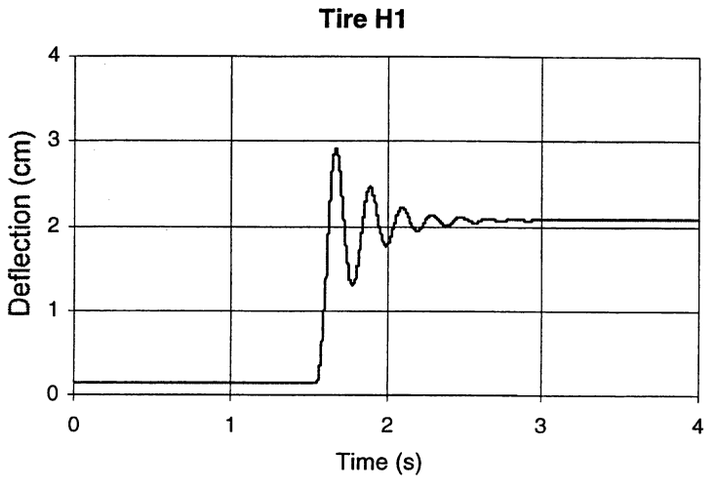

Figure II- 19 : Free oscillation of the mixed tire (∅=68 cm)

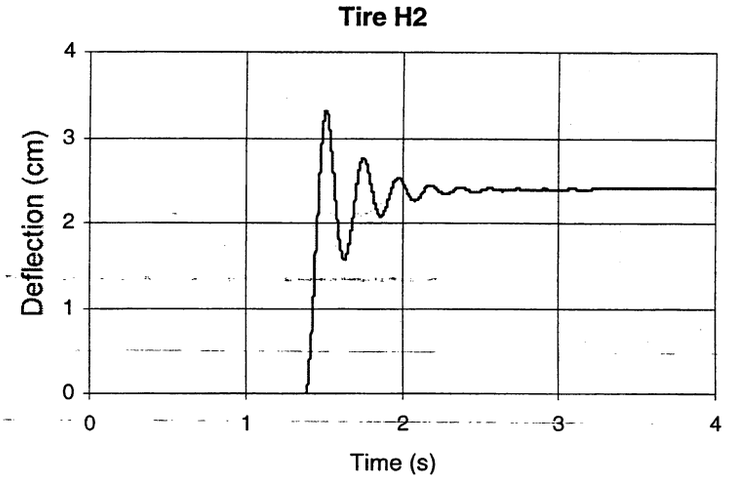

Figure II- 20 : Free oscillation of the mixed tire (∅=54 cm)

	Natural frequency (Hz)	Critical damping	Viscous damping constant (N/m/s)
pneumatic ∅= 68 cm	3.3	0.06	4844
pneumatic ∅= 54 cm	3.16	0.07	5748
solid ∅= 68 cm	5.07	0.09	12113
solid ∅= 54 cm	4.3	0.10	10413
mixed ∅= 68 cm	4.68	0.14	17063
mixed ∅= 54 cm	4.29	0.16	17467

Table II- 7 : Viscous damping constants

To measure the viscous damping constant under dynamical conditions, the tires were tested with the laboratory tire test bench (see the description of the test bench in appendix 5) : the arm supporting the wheel was loaded with 1 tonne. A 1×15 cm PVC obstacle was stuck inside the rolling ring. The tires were due to run over the obstacle and their speed was controlled. At each turn of the ring, after running over the obstacle, the system could freely oscillate. The vertical acceleration of the wheel was measured. The viscous damping constant was deduced from these measurements using the logarithmic decrement method.
Three different velocities were tested : 5 km/h, 10 km/h and 12 or 14 km/h depending on the tire. For each of these tests, 2 values were calculated, one coming from the maximum acceleration values and the other from the minimum acceleration values. Indeed it was observed that for solid and mixed tires the curve decrease was not symmetrical[1] (see Figure II- 27 to Figure II- 38). For the pneumatic tires this tendency was less clear.

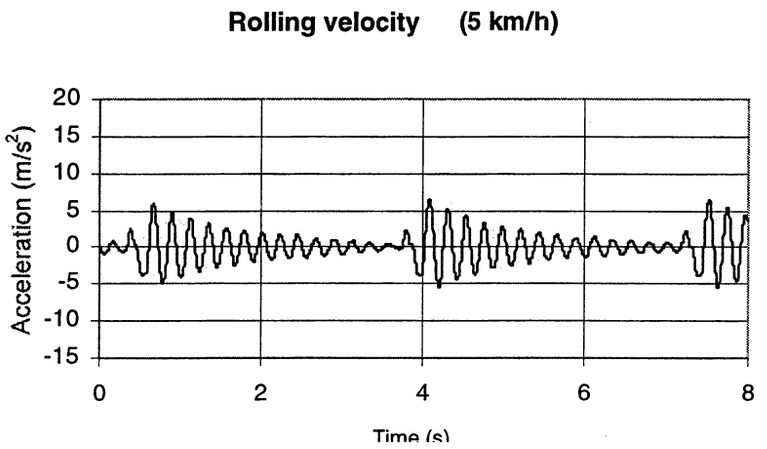

Figure II- 21 : Run over an obstacle
Pneumatic tire (∅=54 cm)

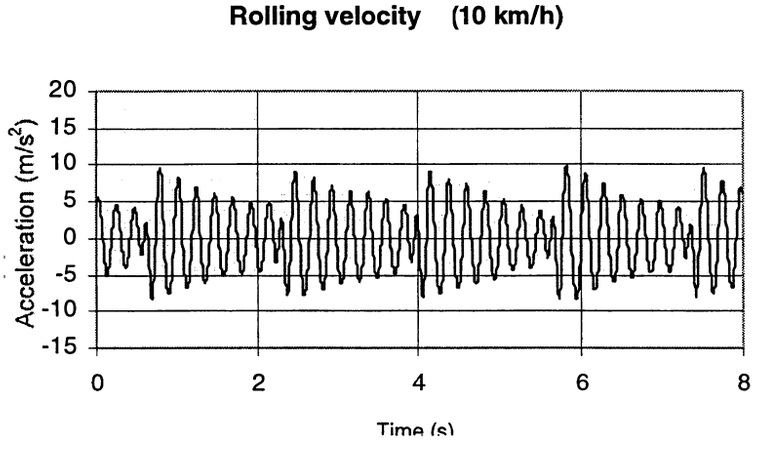

Figure II- 22 : Run over an obstacle
Pneumatic tire (∅=54 cm)

[1] Caution must be care of acceleration peaks of -9.81m.s^{-2}. They do not have to be used because when the aceleration is -9,81m.s^{-2}, that means that the tire has left the ground and it falls down to the ground.

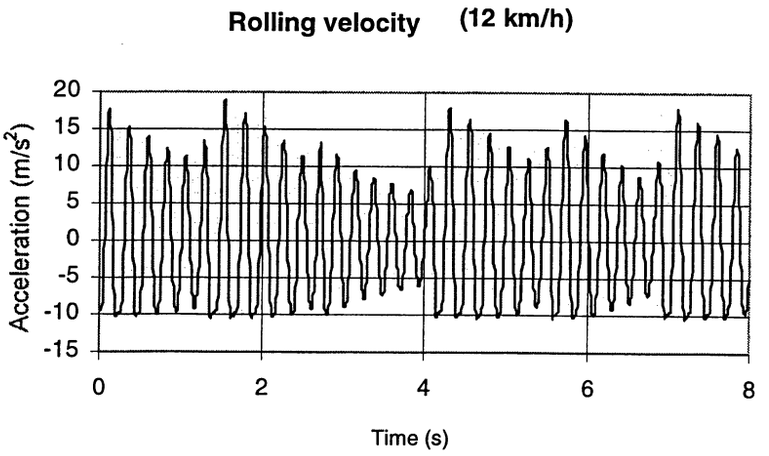

Figure II- 23 : Run over an obstacle
Pneumatic tire (∅=54 cm)

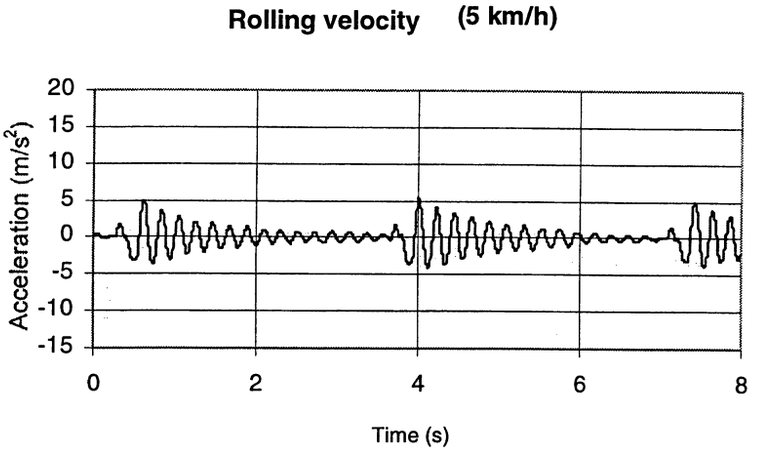

Figure II- 24: Run over an obstacle
Pneumatic tire (∅= 68 cm)

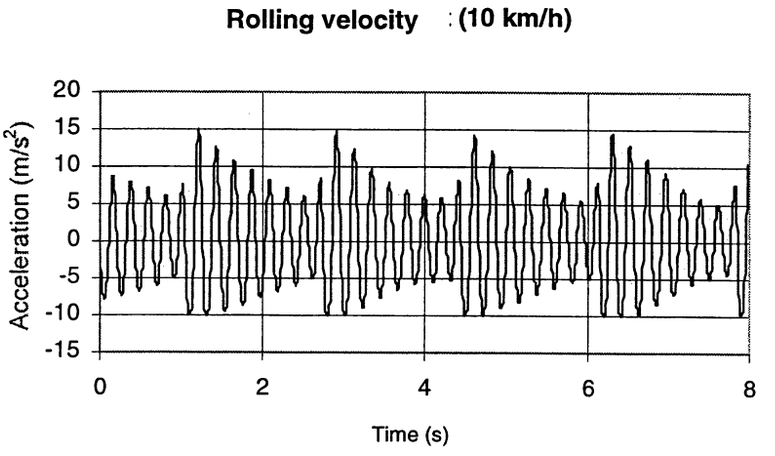

Figure II- 25 : Run over an obstacle
Pneumatic tire (∅= 68 cm)

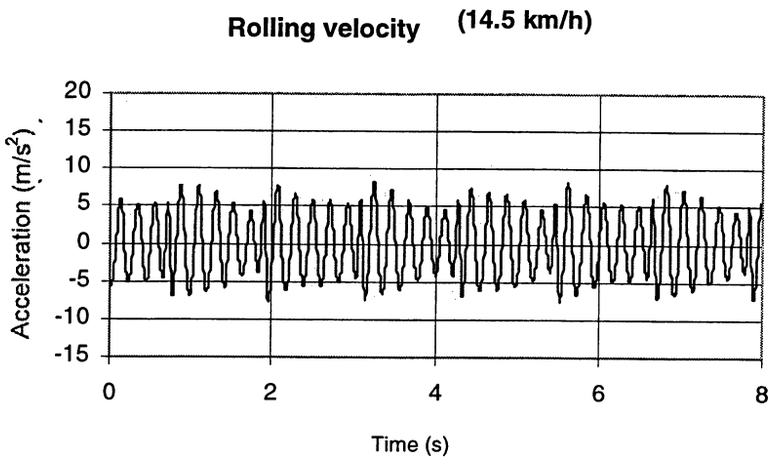

Figure II- 26 : Run over an obstacle
Pneumatic tire (∅= 68 cm)

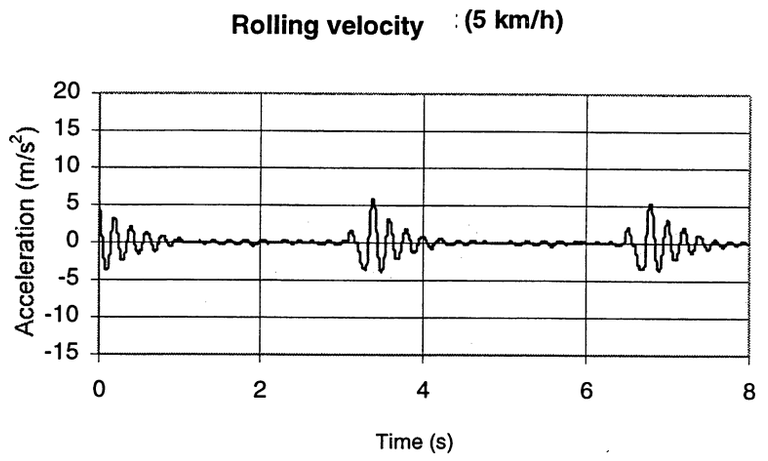

Figure II- 27 : Run over an obstacle
Mixed tire (∅= 54 cm)

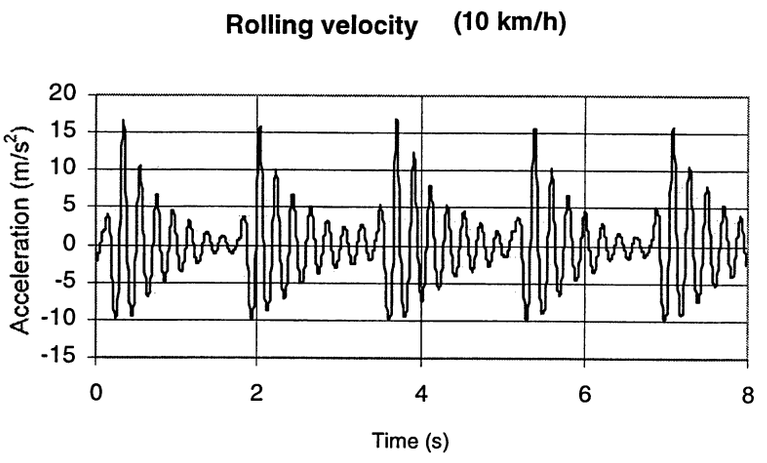

Figure II- 28 : Run over an obstacle
Mixed tire (∅= 54 cm)

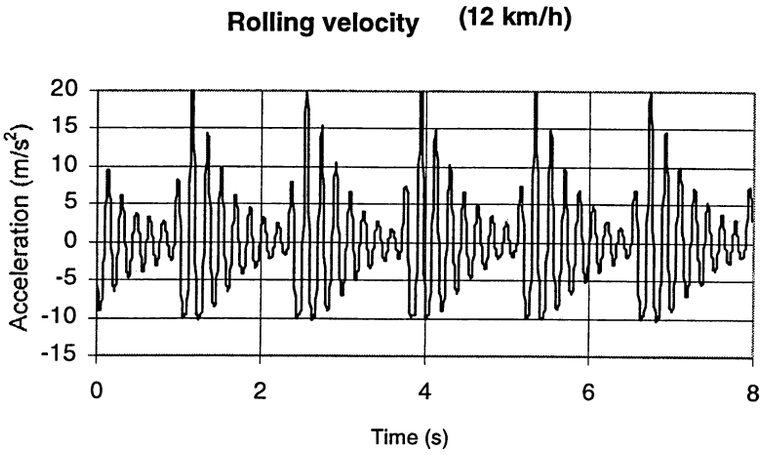

Figure II- 29 : Run over an obstacle
Mixed tire (∅= 54 cm)

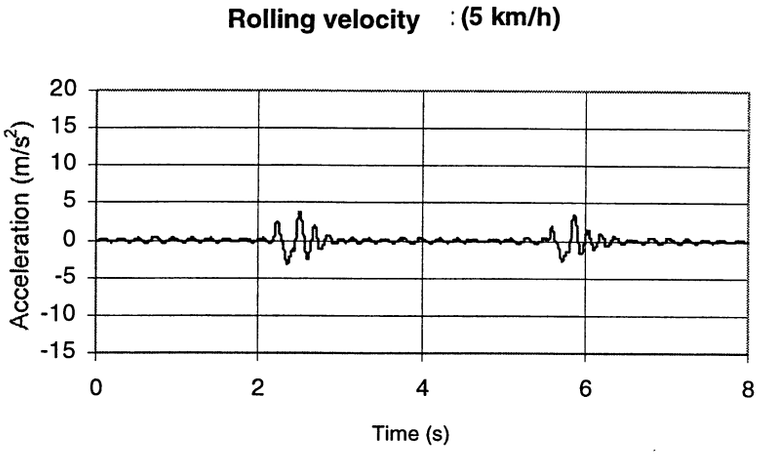

Figure II- 30 : Run over an obstacle
Mixed tire (∅= 68 cm)

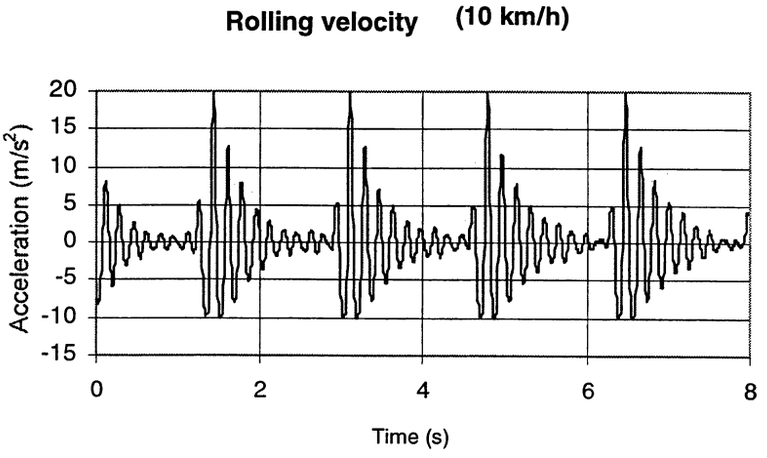

Figure II- 31 : Run over an obstacle
Mixed tire (∅= 68 cm)

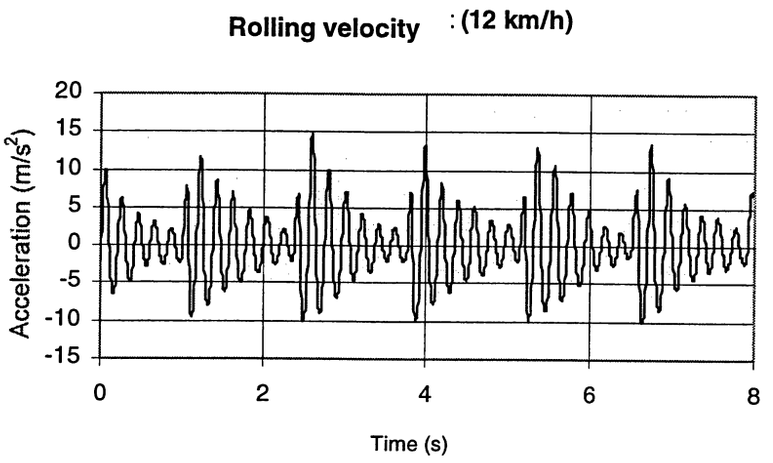

Figure II- 32 : Run over an obstacle
Mixed tire (∅= 68 cm)

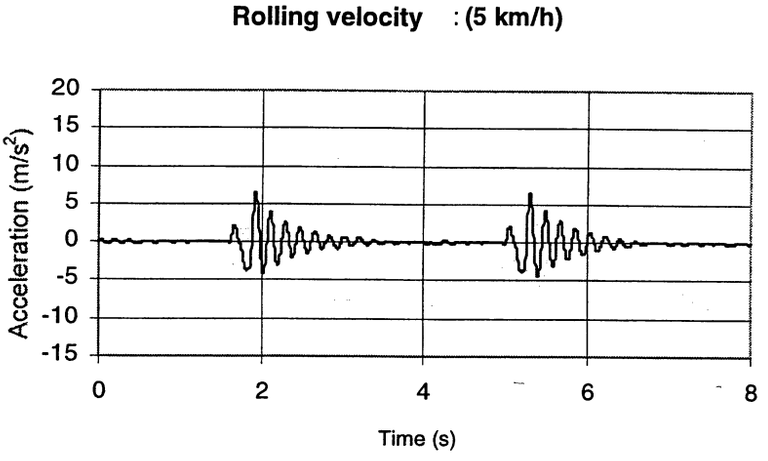

Figure II- 33 : Run over an obstacle
Solid tire (∅= 54 cm)

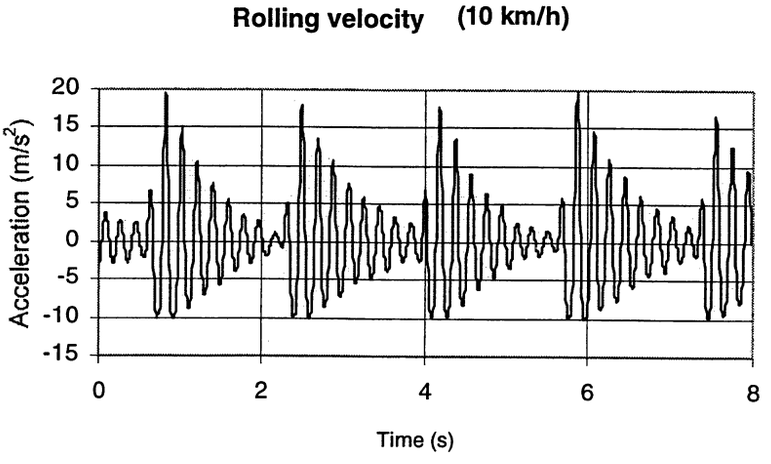

Figure II- 34 : Run over an obstacle
Solid tire (∅= 54 cm)

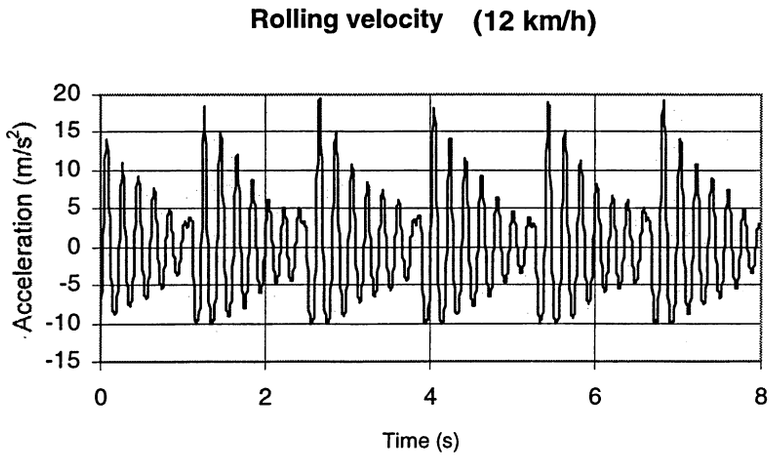

Figure II- 35 : Run over an obstacle
Solid tire (∅= 54 cm)

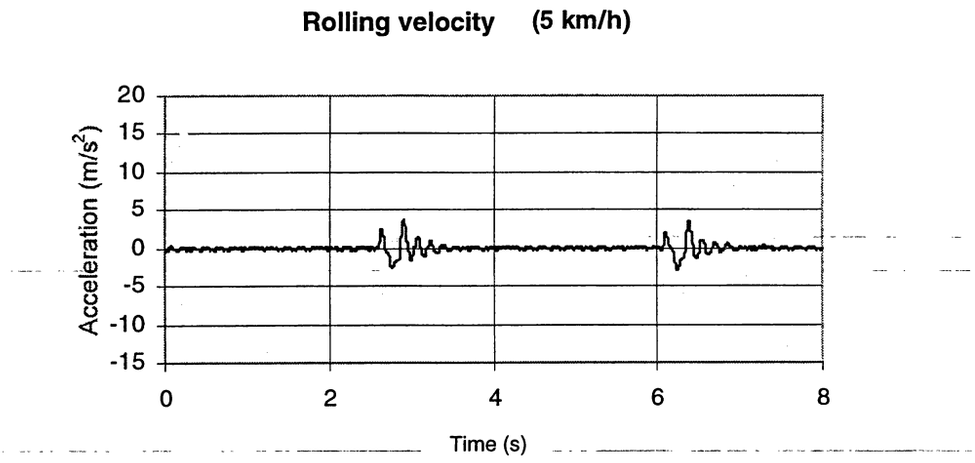

Figure II- 36 : Run over an obstacle
Solid tire (∅= 68 cm)

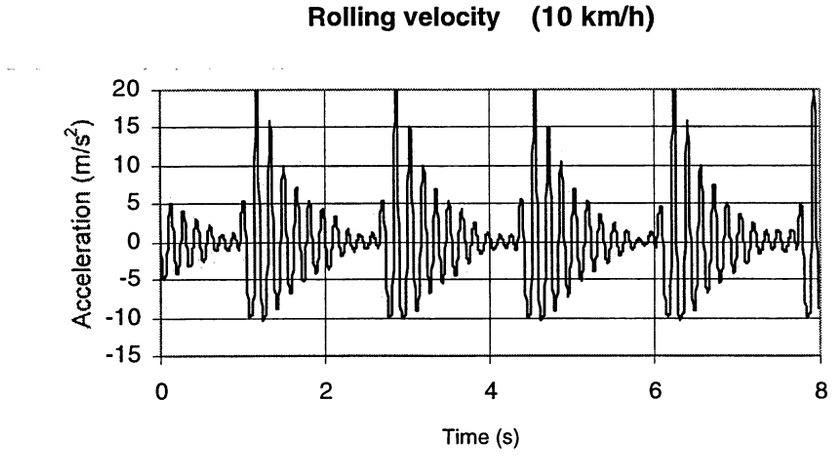

Figure II- 37 : Run over an obstacle
Solid tire (∅= 68 cm)

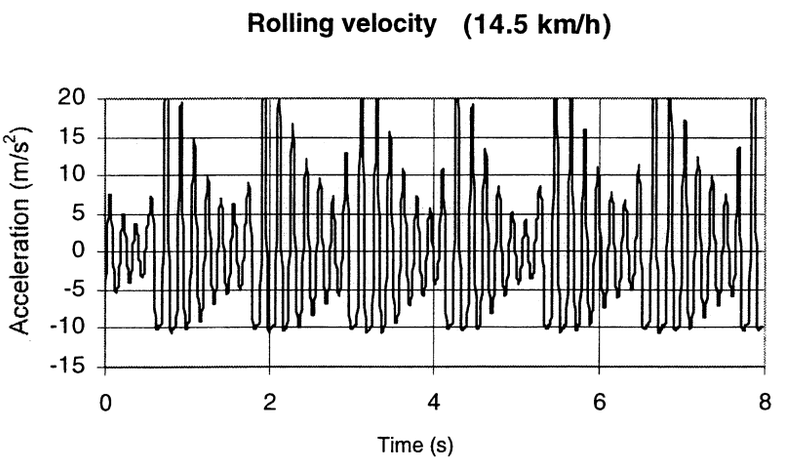

Figure II- 38 : Run over an obstacle
Solid tire (∅= 68 cm)

	Damping constant (N/m/s) v =5 km/h		Damping constant (N/m/s) v =10 km/h		Damping constant (N/m/s)	
	Oscillations MIN	Oscillations MAX	Oscillations MIN	Oscillations MAX	Oscillations MIN	Oscillations MAX
pneumatic ∅= 68 cm	1600	1700	1300	1400	v =12 km/h	
					1000	1150
pneumatic ∅= 54 cm	1400	1400	1100	1350	v =12 km/h	
					1100	1350
solid ∅= 68 cm	6400	7750	3150	4500	v =14.5 km/h	
					2500	3500
solid ∅= 54 cm	4000	4450	2750	3150	v =12 km/h	
					2200	2600
mixed ∅= 68 cm	4800	5800	4200	5400	v =12 km/h	
					3800	4600
mixed ∅= 54 cm	4900	5400	3000	3900	v =12 km/h	
					2950	3700

Table II- 8 : Damping constant in dynamical conditions for different rolling velocities

It was observed that damping values strongly depend on the rolling velocity for the solid and mixed tires. Then the damping was modelled as a 3rd order polynomial of the rolling velocity :

$$C = p_1.v^3 + p_2.v^2 + p_3.v + p_4 \qquad (6)$$

where v is the speed expressed in km/h and C the viscous damping constant (N/m/s).

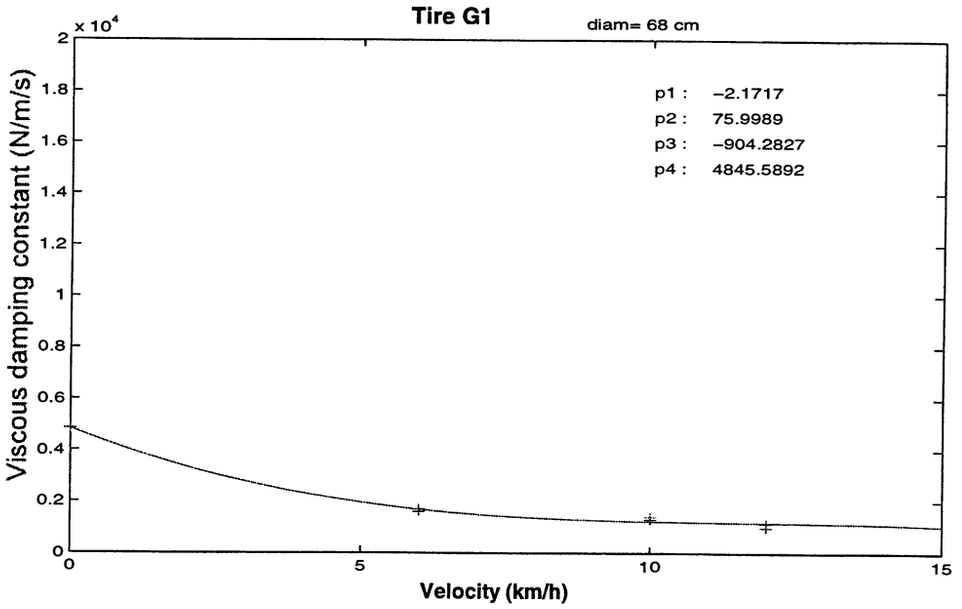

Figure II- 39 : Evolution of the viscous damping constant in function of the tire rolling velocity
Pneumatic tire (∅= 68 cm)

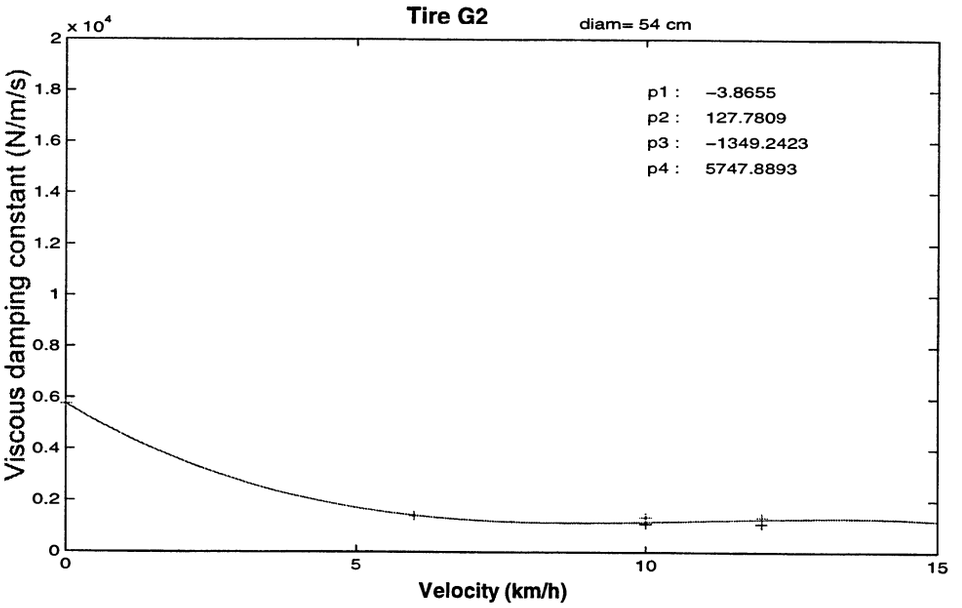

Figure II- 40 : Evolution of the viscous damping constant in function of the tire rolling velocity
Pneumatic tire (∅= 54 cm)

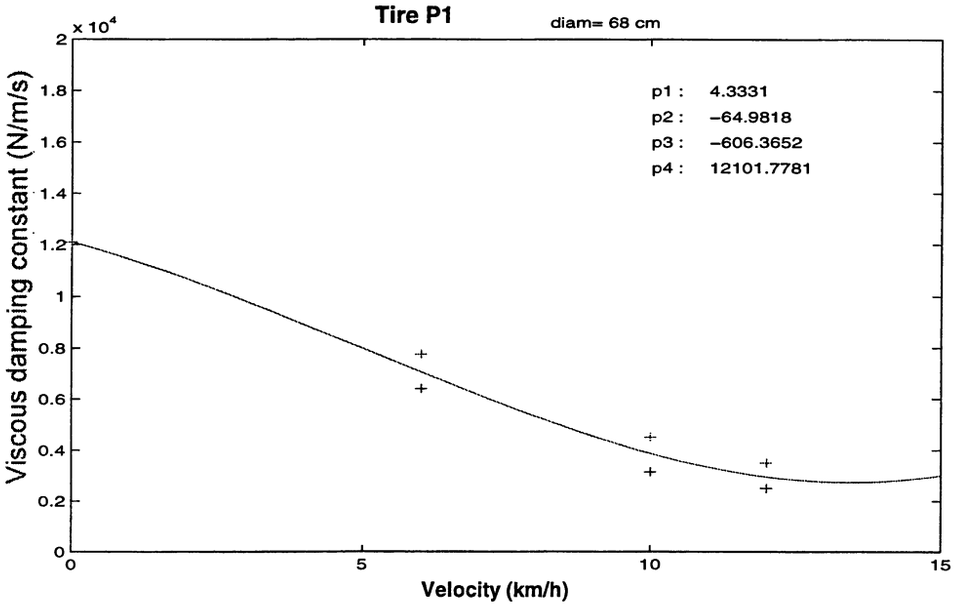

Figure II- 41 : Evolution of the viscous damping constant in function of the tire rolling velocity
Solid tire (∅= 68 cm)

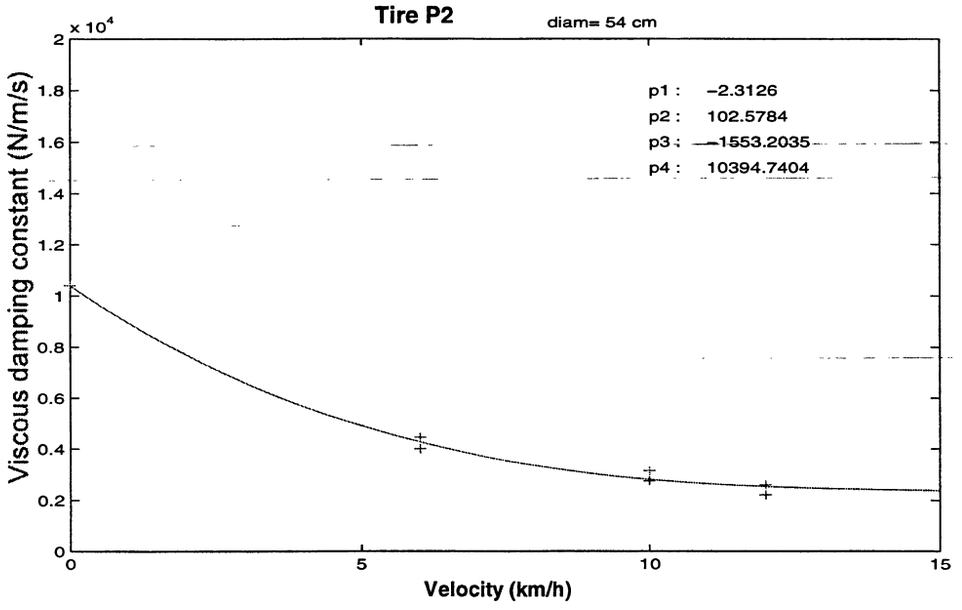

Figure II- 42 : Evolution of the viscous damping constant in function of the tire rolling velocity
Solid tire (∅= 54 cm)

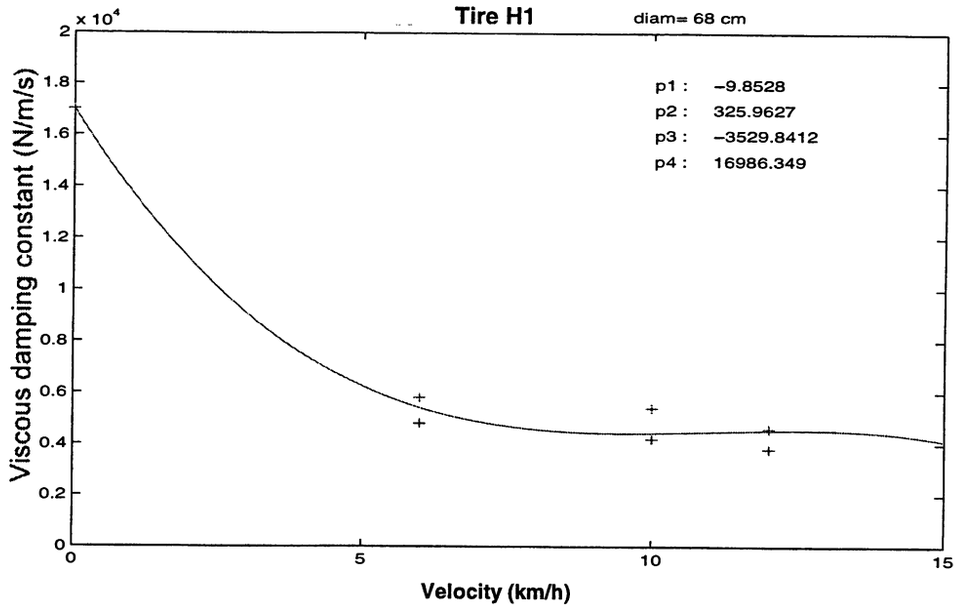

Figure II- 43 : Evolution of the viscous damping constant in function of the tire rolling velocity
Mixed tire (∅= 68 cm)

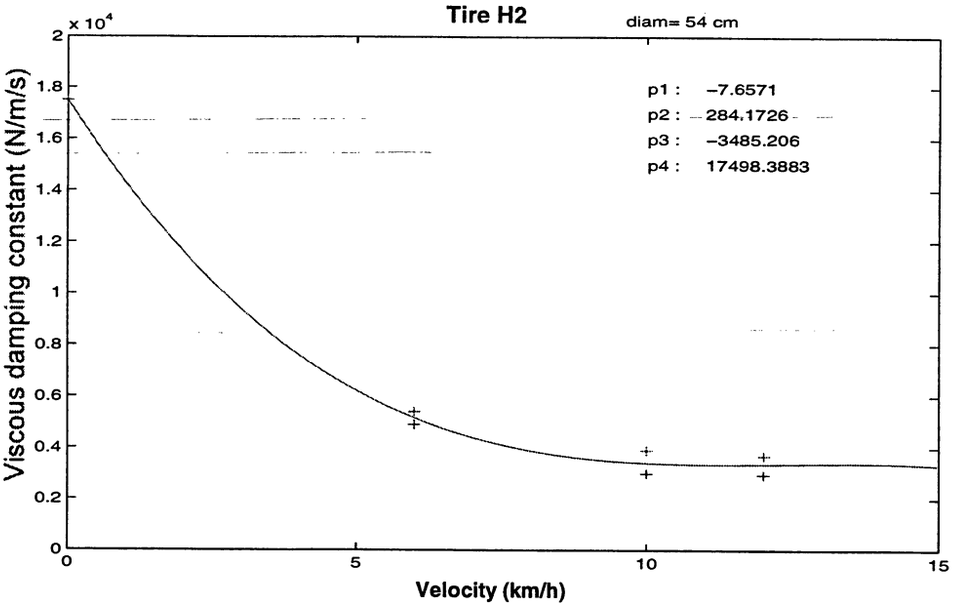

Figure II- 44 : Evolution of the viscous damping constant in function of the tire rolling velocity
Mixed tire (∅= 54 cm)

3. Measurement of the vibration emission of the KOMATSU FD20

III-1 Test protocol

The KOMATSU FD20 forklift truck was tested according to the procedure described in the European test code [2]. The principle of this test code consists in moving the forklift truck along a flat test-track on which two 1×15 cm obstacles were disposed and in measuring the vertical acceleration at the driving position. The space between the two obstacles was 10 m.
Unlike the recommendation of the test code [2], the speed of the forklift truck was not fixed at 10 km/h : several values of velocity were tested, between 2 and 15 km/h with an increment of 1 km/h. Each test was carried out at a constant velocity.

Figure III- 1 : View of the equipped KOMATSU FD20 and the test-track

The acceleration was measured below the suspension seat. By so doing the seat attenuation was not taken into account (the accelerometer was placed in the middle of the seat base on the engine cover; coordinates of the accelerometer position in the center of mass axes : x = -13 cm; y = 32 cm; z = 3 cm) (see Figure III- 2).

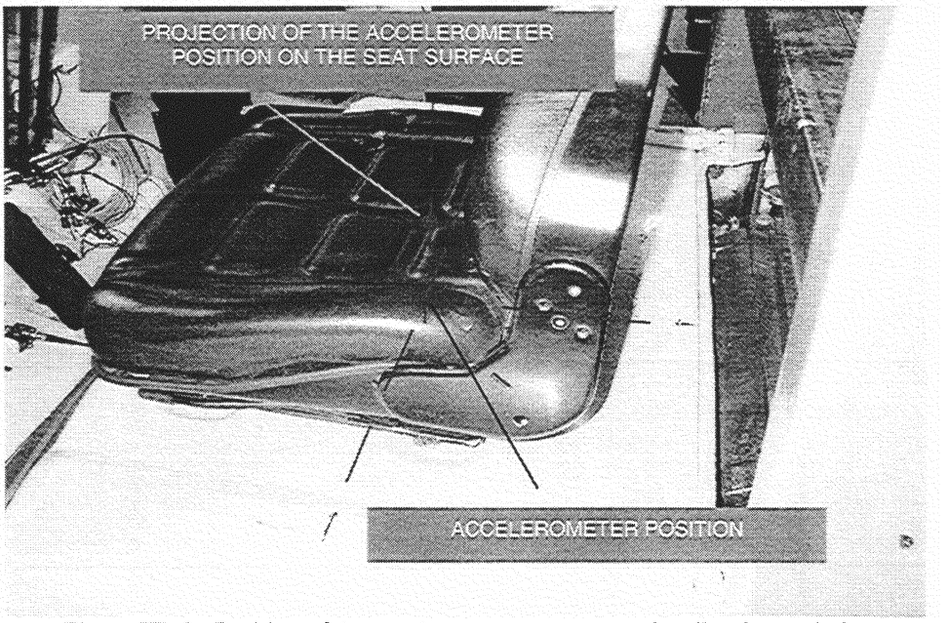

Figure III- 2 : Position of the accelerometer to measure the vibration emission

Figure III- 3 : Position of the control accelerometers

To check that the accelerometer was working correctly, two other accelerometers were placed on each side of the forklift truck (see Figure III- 3).

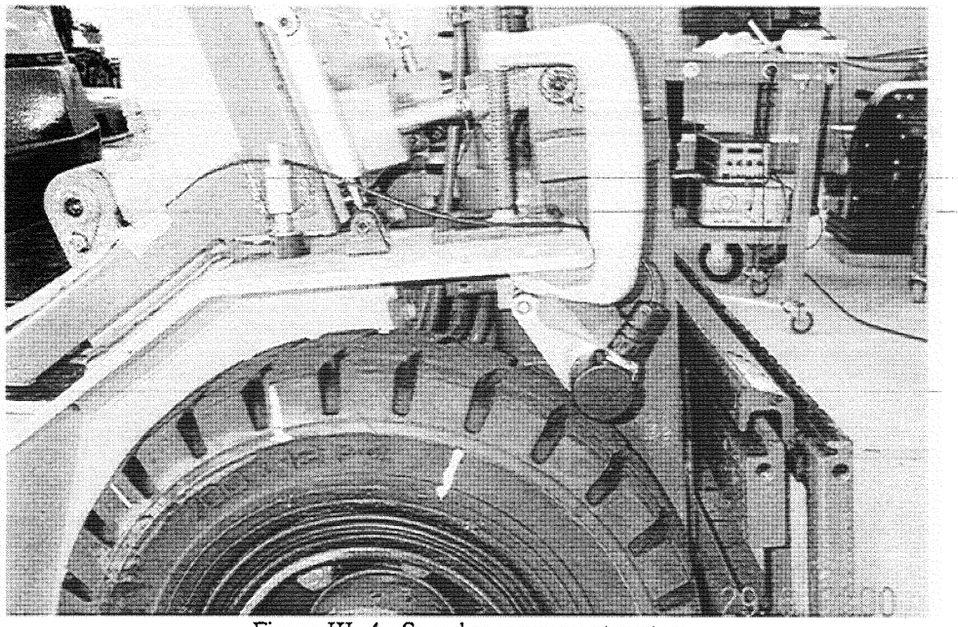

Figure III- 4 : Speed measurement system

An optical encoder sensor was used in contact with the front right wheel to measure the velocity in real-time. The driver could use this information displayed on a multimeter to adjust the forklift truck velocity to the specified value and to keep it constant as much as possible. The velocity and the 3 accelerations were acquired simultaneously. These 4 channels were transmitted in real-time to the laboratory, by means of a telemetry system (see Figure III- 1). They were also acquired with the LMS system.

The same experiment was repeated the three types of tires : forklift truck successively equipped with solid, pneumatic and mixed tires. The aim was to compare the vibration emission for each type of tires tested.

III-2 Results

III-2-1 Time histories of the acceleration for the forklift truck equipped with pneumatic tires

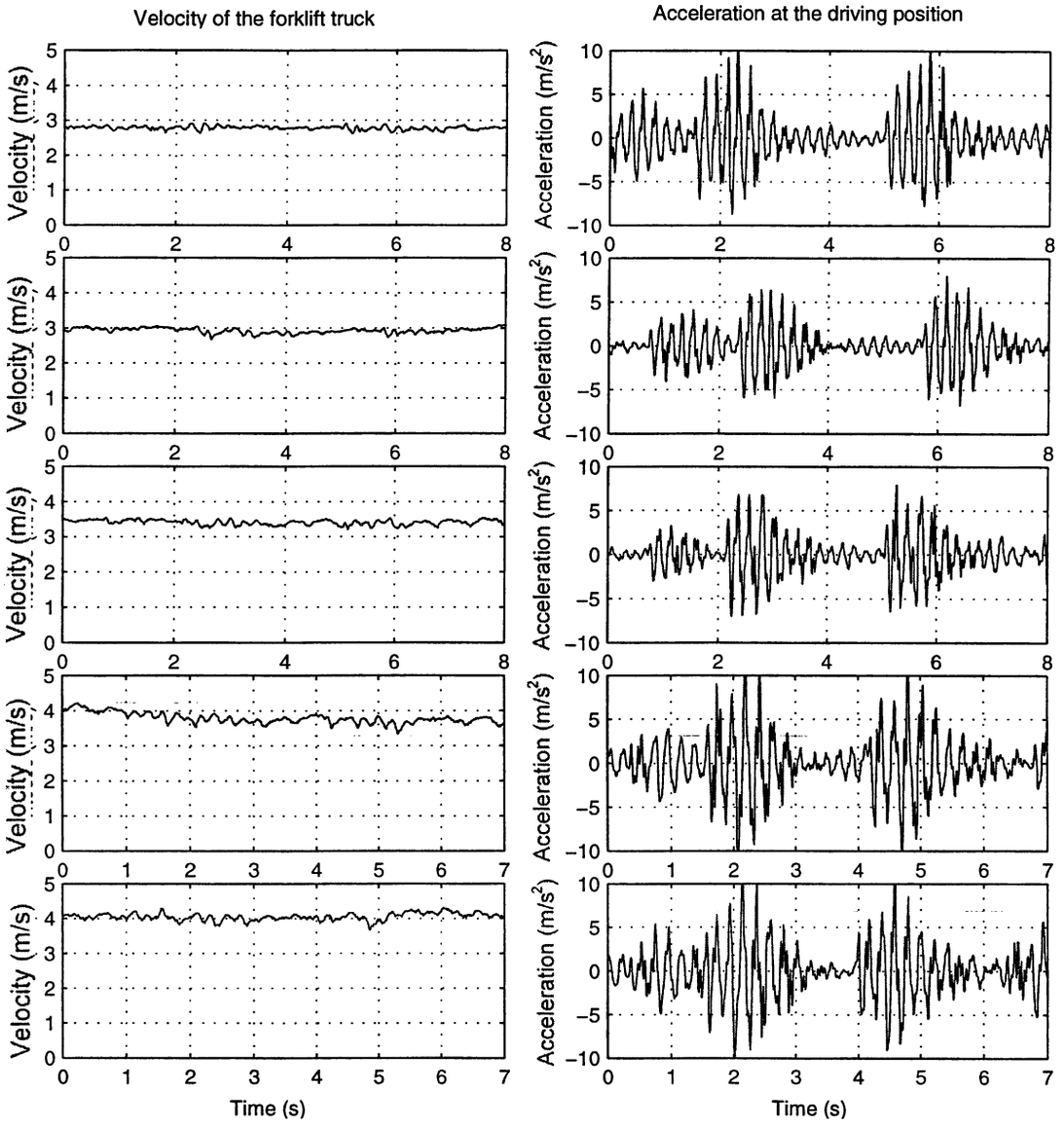

Figure III- 5 : Acceleration measured for the forklift truck equipped with pneumatic tires

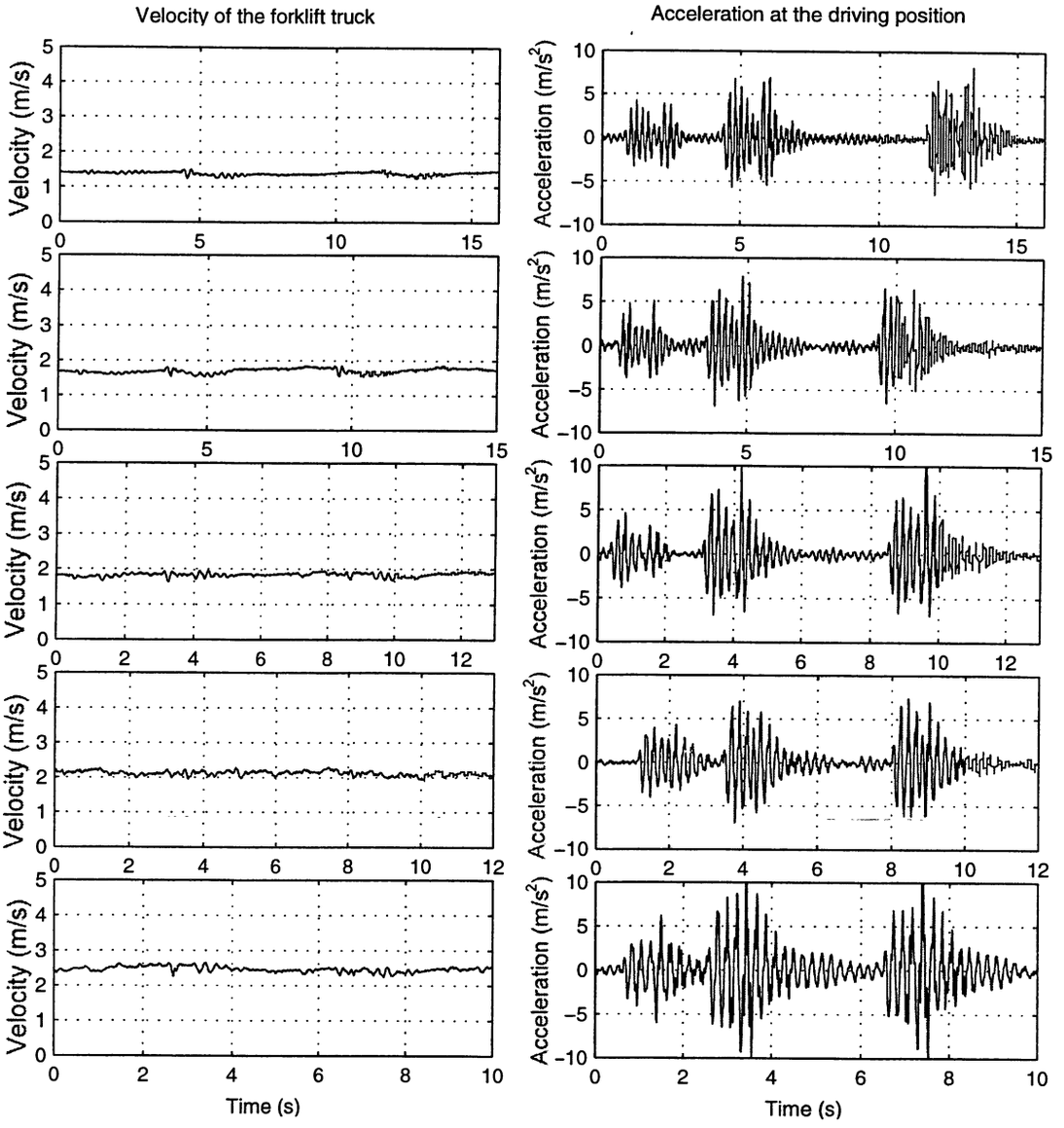

Figure III- 6 : Acceleration measured for the forklift truck equipped with pneumatic tires

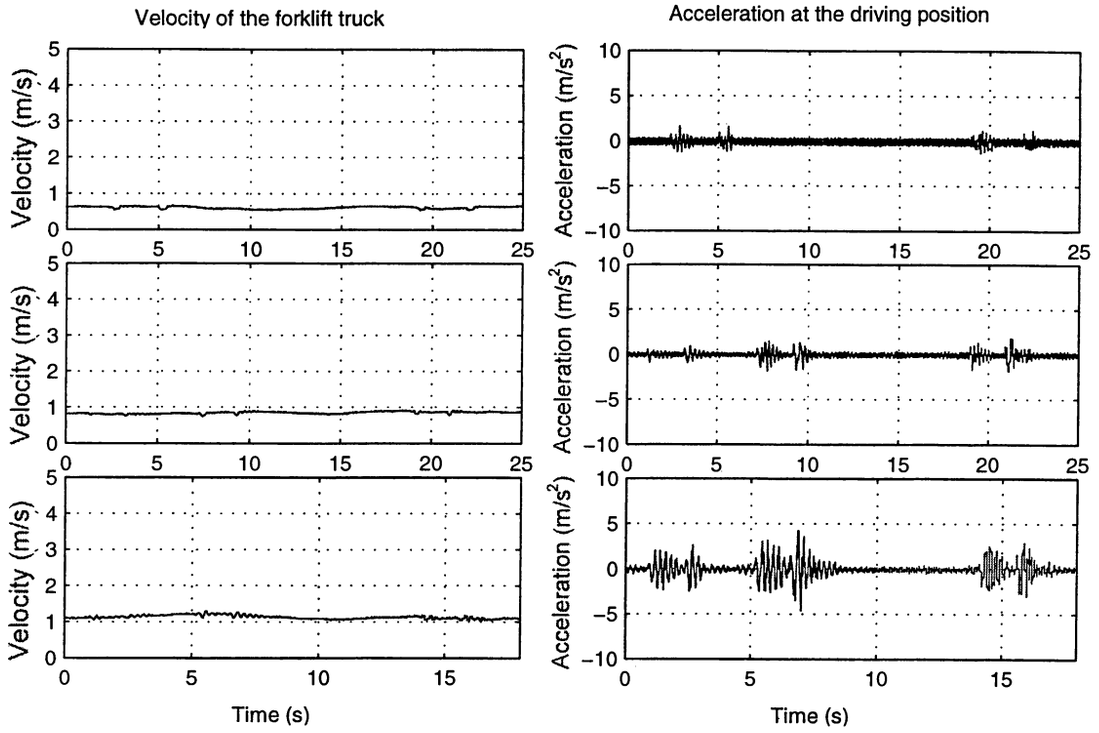

Figure III- 7 : Acceleration measured for the forklift truck equipped with pneumatic tires

III-2-2 Time histories of the acceleration for the forklift truck equipped with solid tires

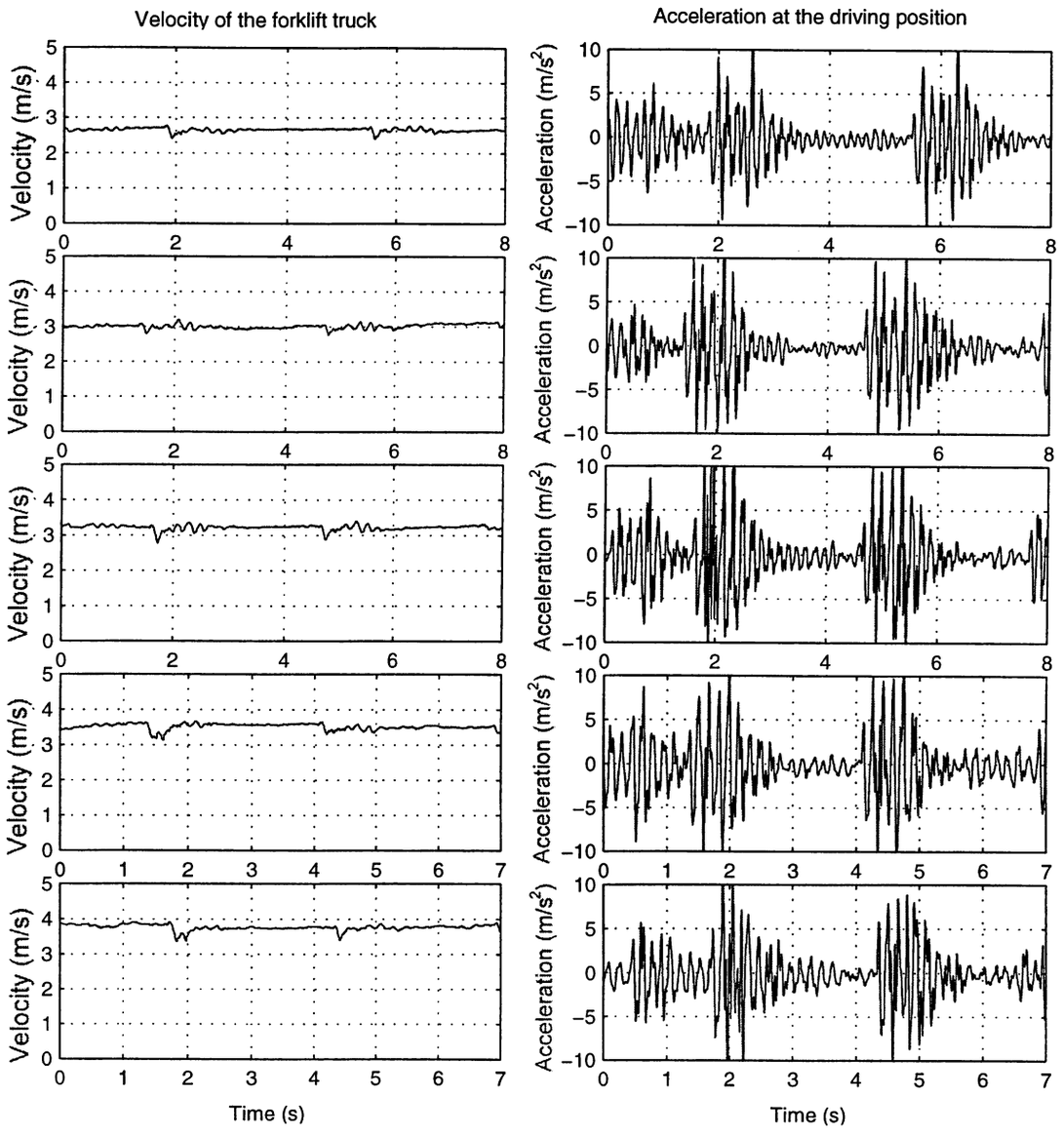

Figure III- 8 : Acceleration measured for the forklift truck equipped with solid tires

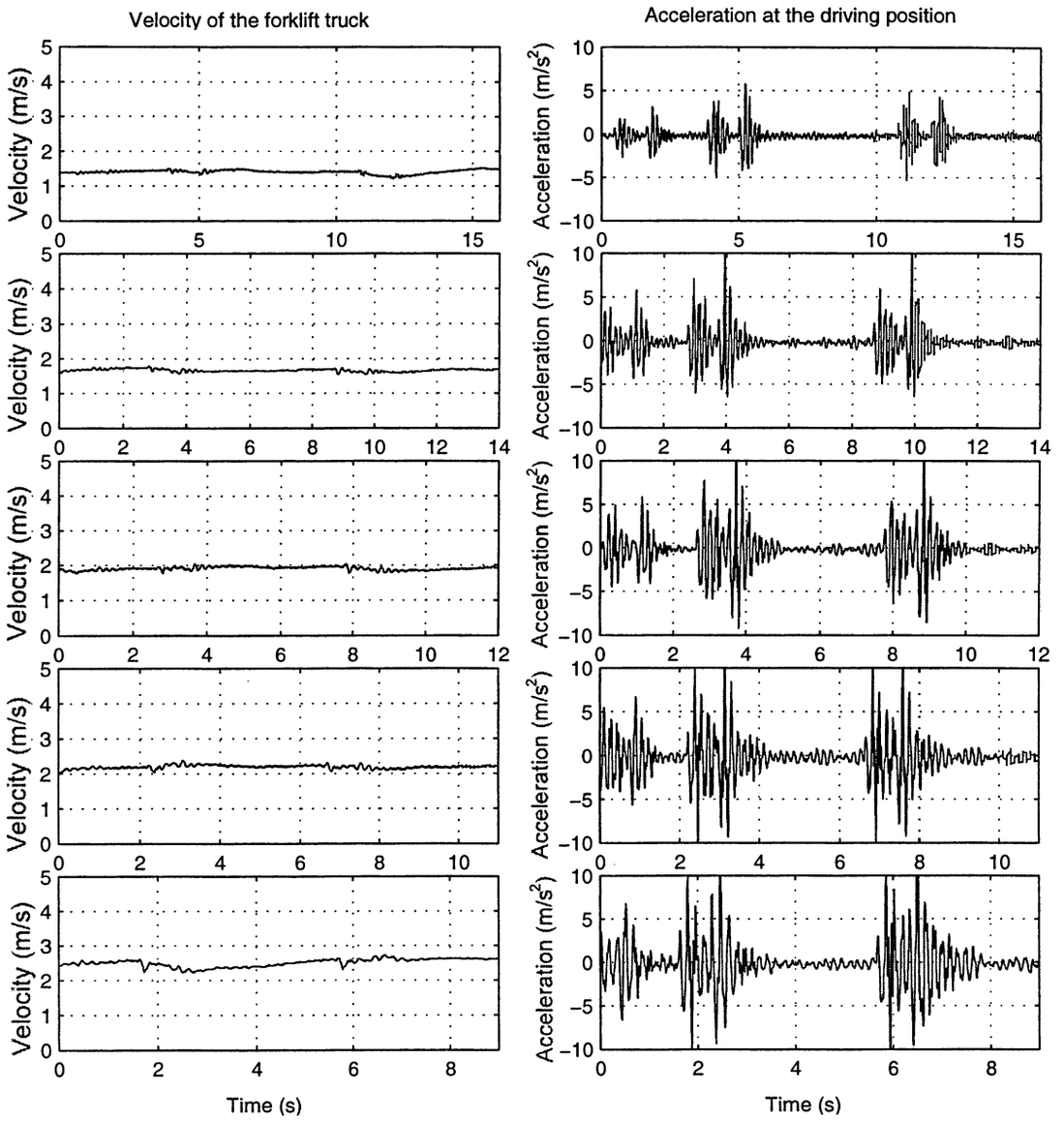

Figure III- 9 : Acceleration measured for the forklift truck equipped with solid tires

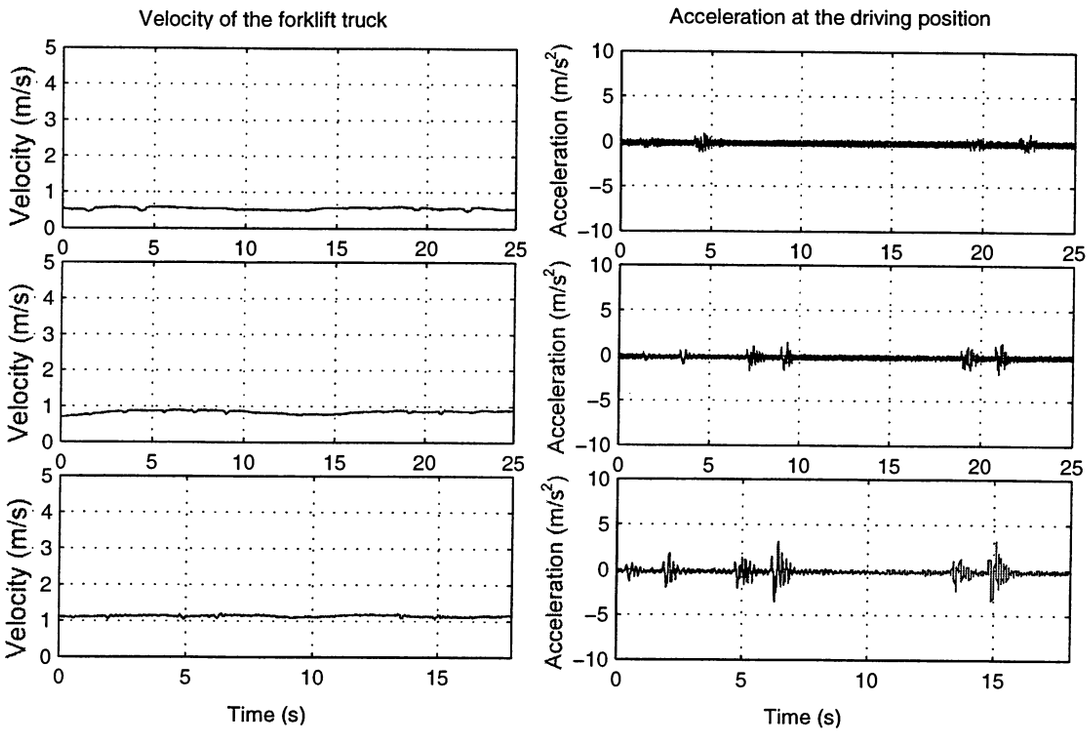

Figure III- 10 : Acceleration measured for the forklift truck equipped with solid tires

III-2-3 Time histories of the acceleration for the forklift truck equipped with mixed tires

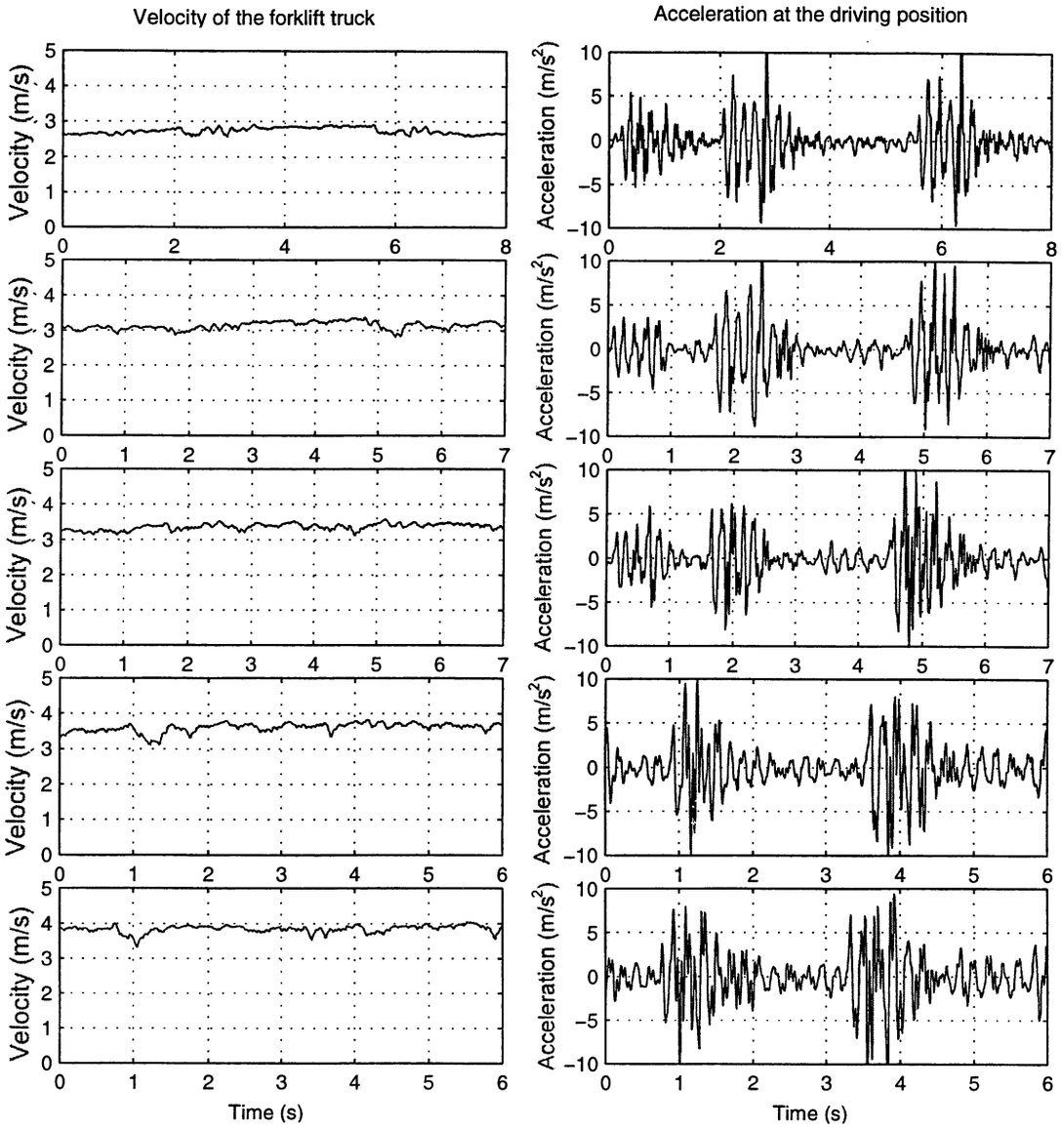

Figure III- 11 : Acceleration measured for the forklift truck equipped with mixed tires

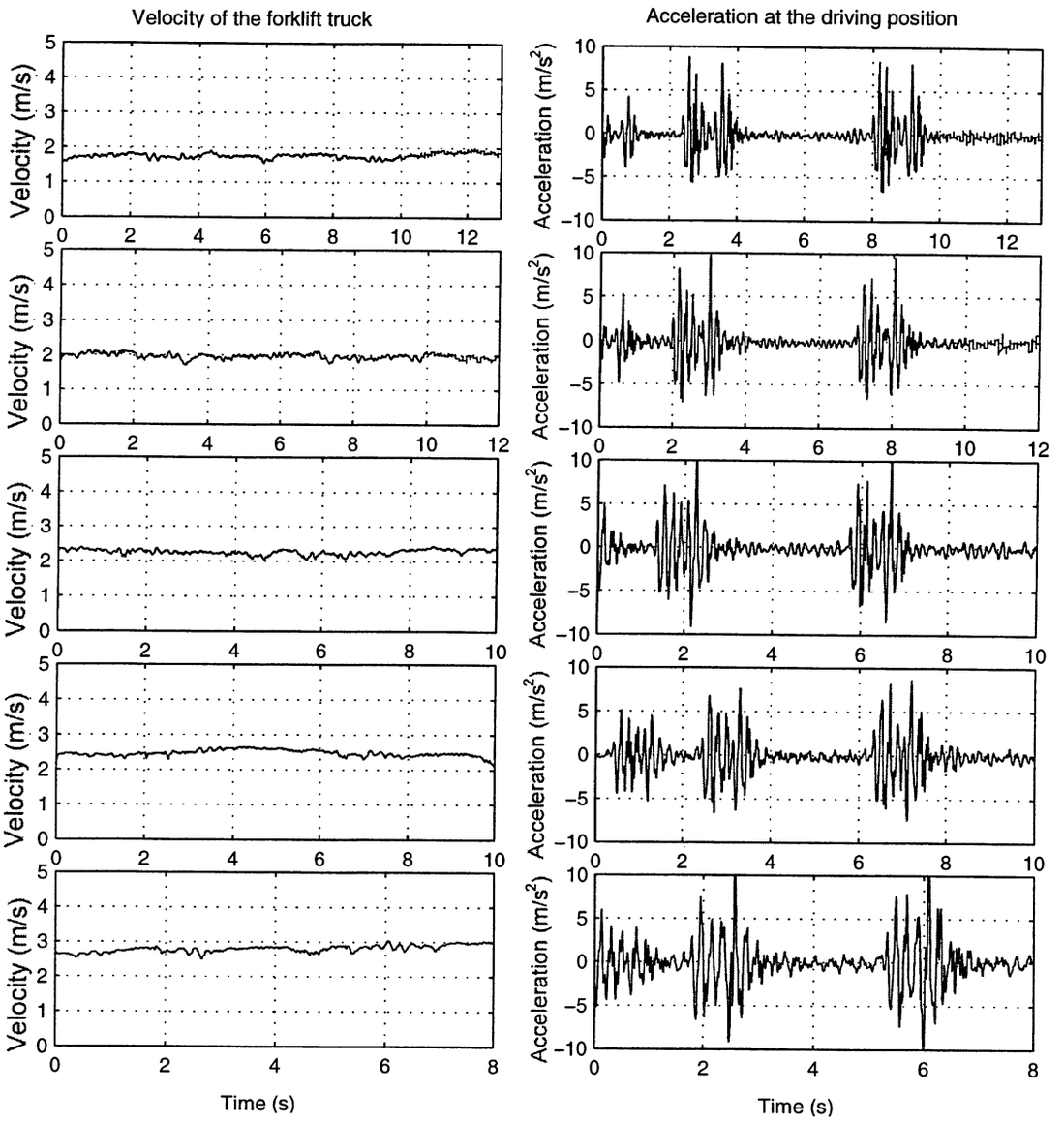

Figure III- 12 : Acceleration measured for the forklift truck equipped with mixed tires

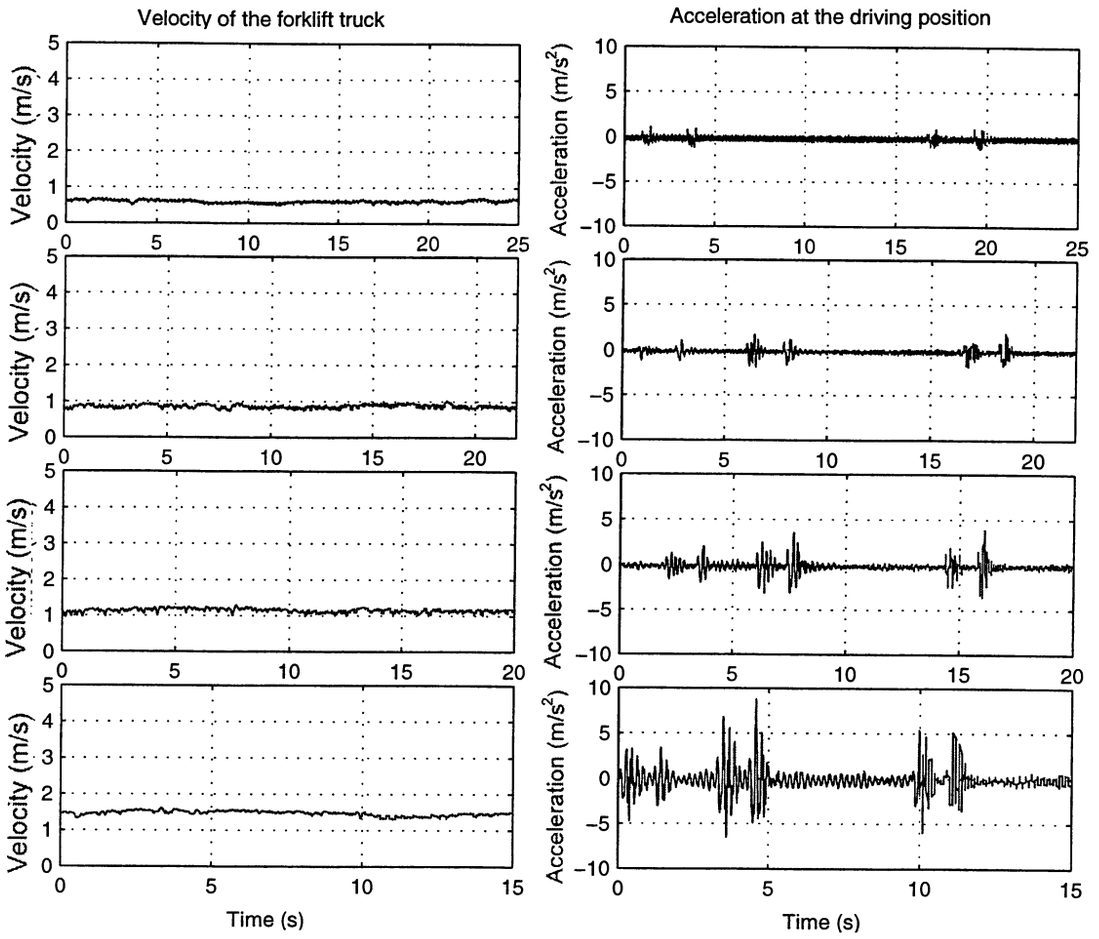

Figure III- 13 : Acceleration measured for the forklift truck equipped with mixed tires

Remark :

For the tests at higher speeds (> 3m/s), three wave trains were observed. These wave trains correspond respectively to the starting point (marked with a few mm thick plank), to the first obstacle of the test code (1×15 cm) and to the second obstacle (1×15 cm). For the lower speeds each of these wave trains is divided into two wave trains : the first wave train is due to the front wheels running over the obstacle and the second wave train is due to the rear wheels.

III-3-Analysis of the results

To quantify the measured acceleration responses, a criterion equivalent to a dose was calculated from each time history[1]. This criterion was expressed as the maximum of a mobile RMS value calculated over a period of 1 s, according to the formula (7). It comes from the ISO standard 2631-1 [3]. It was assumed to be representative of the human perception of shocks. It takes into account both peak values and shock duration. This criterion was calculated for each obstacle crossing, so that two values were deduced from one run.

$$\gamma_{RMS} = \max_{t}\left(\sqrt{\int_{t}^{t+1}\left(\frac{d^2z}{dt^2}\right)^2 dt}\right) \qquad (7)$$

Figure III- 14 shows with an example of measured acceleration the meaning of the criterion (7).

[1] The signals were firstly filtered with a numerical low-pass filter whose cut frequency was 10 Hz.

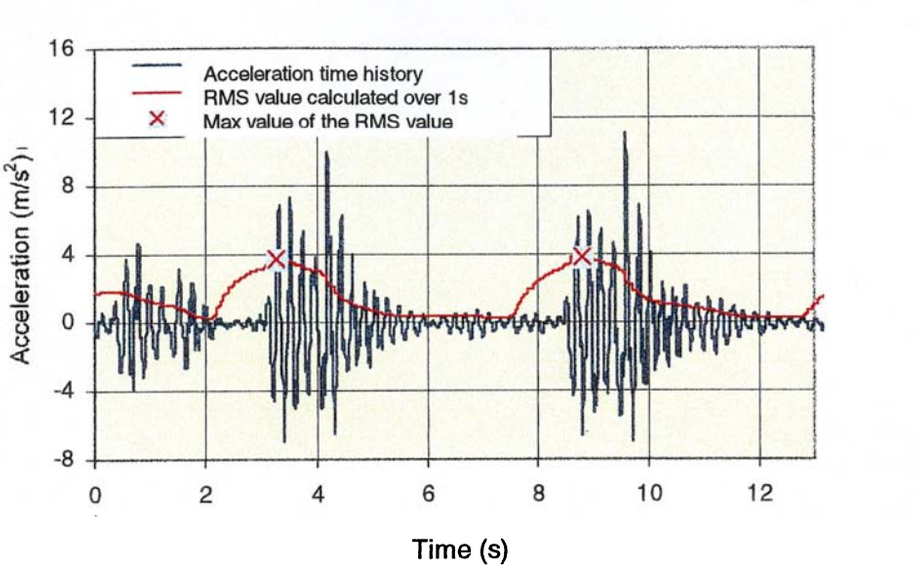

Figure III- 14 : Definition of the γ_{RMS} criterion. Illustration with an example of measured acceleration.

For each type of tires used, the γ_{RMS} values were calculated and drawn in function of the mean value of the speed calculated over the same time window as for γ_{RMS}. In Figure III- 15 the evolution of γ_{RMS} is given in function of the forklift truck velocity and for each type of tires.

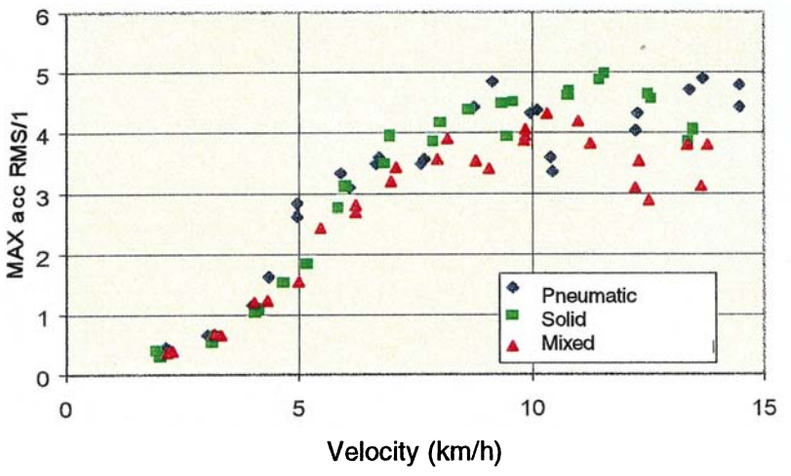

Figure III- 15 : Comparison of the vibration emissions in function of the forklift truck velocity, for the 3 types of tires

The same tendencies as previously with the KOMATSU FG15 [1] may be observed, e.g. the phenomenon of interference between the shock on the front axle and the shock on the rear. Depending on the speed, the second shock can attenuate or amplify the vibration generated by the first shock. So a "critical speed" value still exists. For this value, which is around 12 km/h, (in the case of the FG15 it was around 8.5 km/h, see [1]), the ratio between calculated γ_{RMS} values for solid and mixed tires is around 1.7. Considering the overall range of speeds, the best behaviour was achieved with mixed tires

4. Modelling the forklift truck – Description and validation

IV-1 Description of the KOMATSU FD20 model

The whole model of forklift truck with tires was implemented with SDS [4] (the program code is given in appendix 6).
The forklift truck (chassis, engine, cab, forks ...) was modelled as a mass with inertia. The tires were also modelled as masses on which were applied contact forces with the ground and the obstacles. These contact forces were analytically calculated using the INRS model [1].
The tires were linked to the chassis with spherical joints.
The velocity was imposed on the 2 front wheels (see Figure IV- 1).

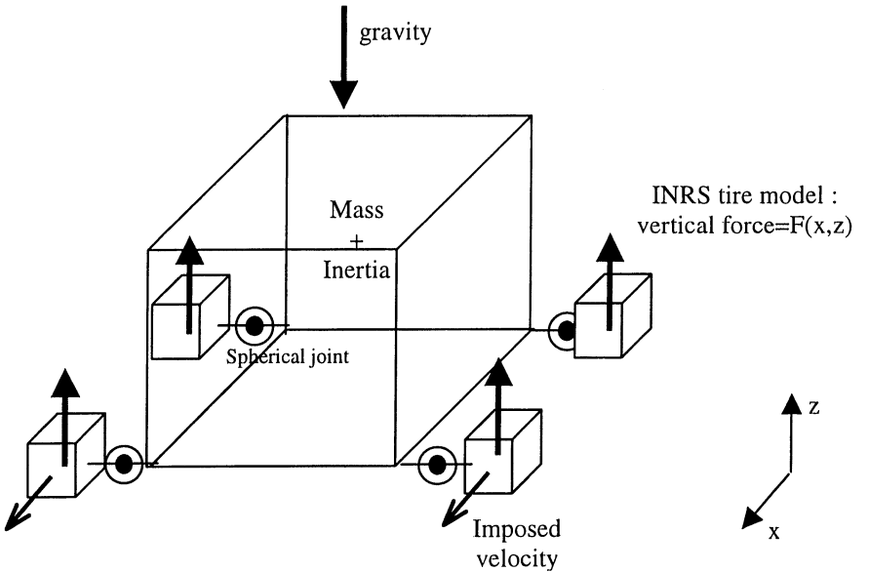

Figure IV- 1 : Diagram of the KOMATSU FD20 model

Remark : the SDS model was "skinned" to give it a realistic look. The shapes representing the chassis, the forks or the tires have only an esthetic function and they do not have any influence on the calculation. For example, the mass and the inertia were entered as numerical values (previously measured data) and they did not result from a geometrical calculation based on the geometries.

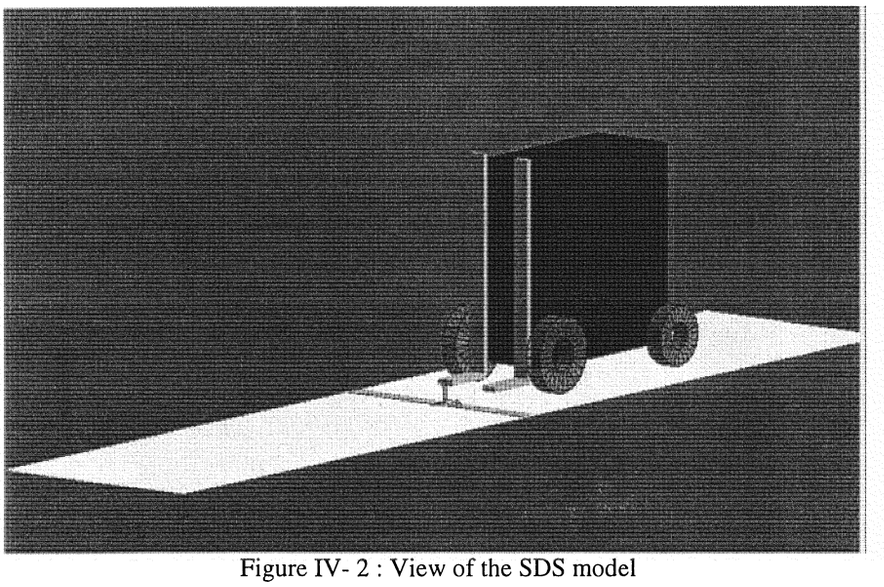

Figure IV- 2 : View of the SDS model

IV-2 Results

The model allowed us to simulate the tests carried out within the frame of the European test code [2] and to compare the calculations with the measurements. For each type of tires, 14 runs at different speeds between 2 and 15 km/h by steps of 1 km/h were computed. In the following figures, the calculated γ_{RMS} values are compared to the measured ones.

IV-2-1 Comparison between calculated and measured γRMS

It can be seen that there is a close agreement between calculations and measurements : the model made it possible to predict the evolution of the γ_{RMS} criterion in function of the forklift truck speed. In previous studies [1], it has been explained that the observed extrema (minima and maxima of the γ_{RMS} criterion) come from an interference phenomenon between the free response of the forklift truck after the shock on the front axle and the shock on the rear axle. Depending on the speed, the second shock may occur in phase or in phase opposition with the free response of the forklift truck, involving attenuation or amplification. The good correlation between the calculated and measured extrema shows that the natural frequency of the forklift truck was well estimated.

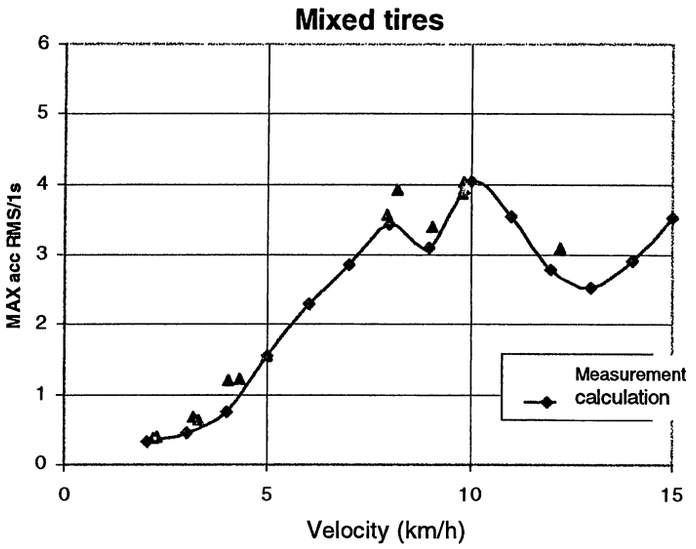

Figure IV- 3 : Comparison between calculated and measured vibration emission of the KOMATSU FD20 equipped with mixed tires.

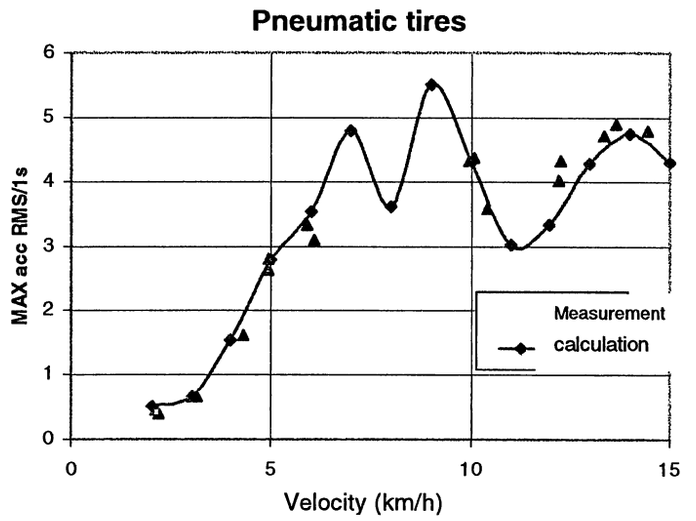

Figure IV- 4 : Comparison between calculated and measured vibration emission of the KOMATSU FD20 equipped with pneumatic tires.

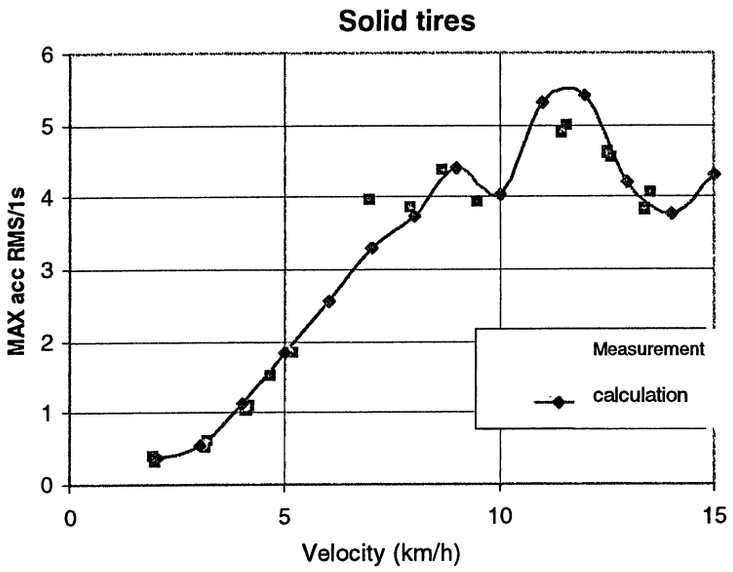

Figure IV- 5 : Comparison between calculated and measured vibration emission of the KOMATSU FD20 equipped with solid tires.

IV-2-2 Comparison of calculated and measured time histories for the KOMATSU FD20 equipped with pneumatic tires

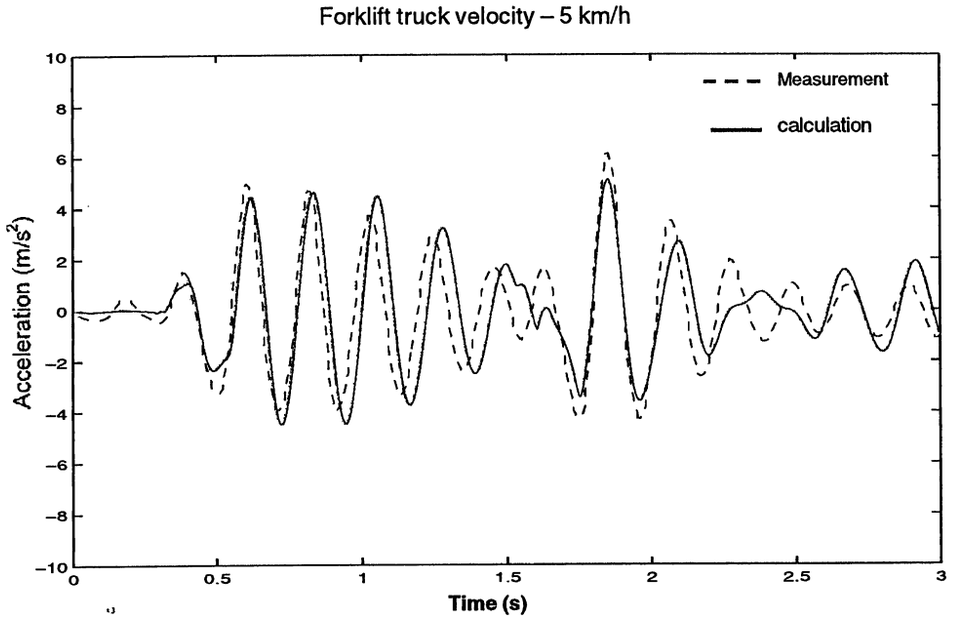

Figure IV- 6 : Comparison of calculated and measured acceleration at driving position. Pneumatic tires – speed : 5 km/h

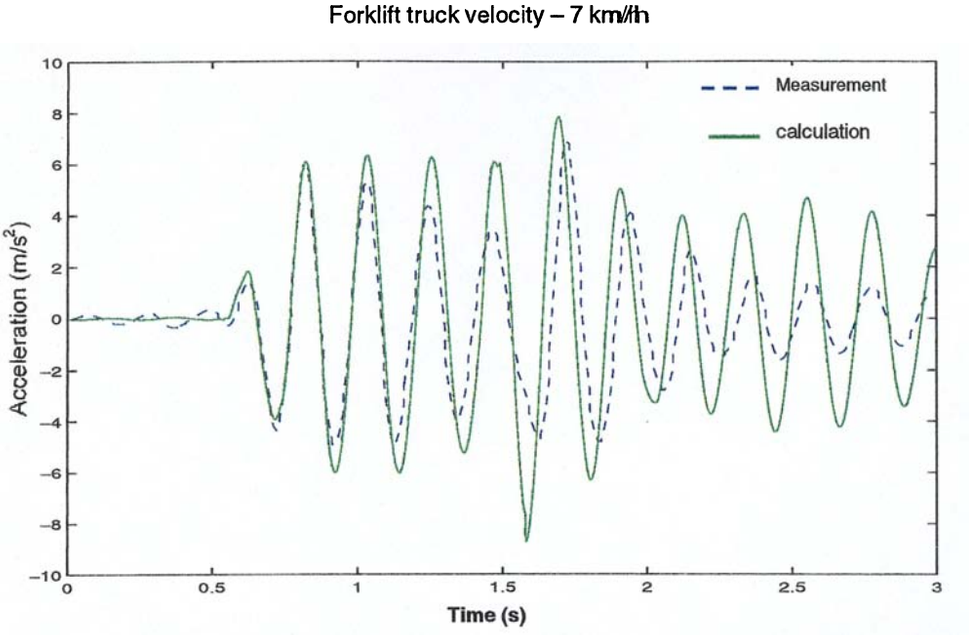

Figure IV- 7 : Comparison of calculated and measured acceleration at driving position.
Pneumatic tires – speed : 7km/h

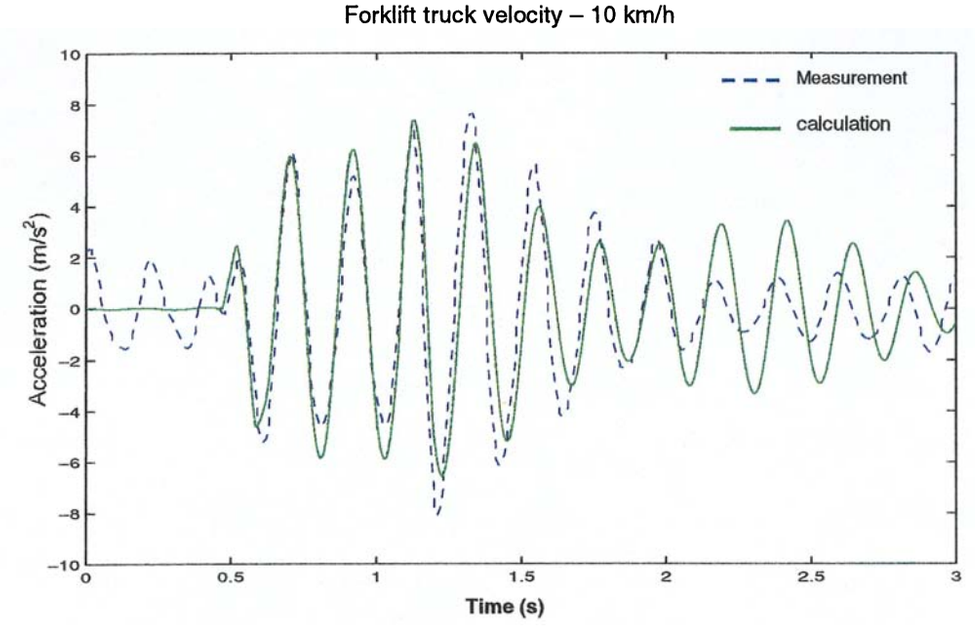

Figure IV- 8 : Comparison of calculated and measured acceleration at driving position.
Pneumatic tires – speed : 10 km/h

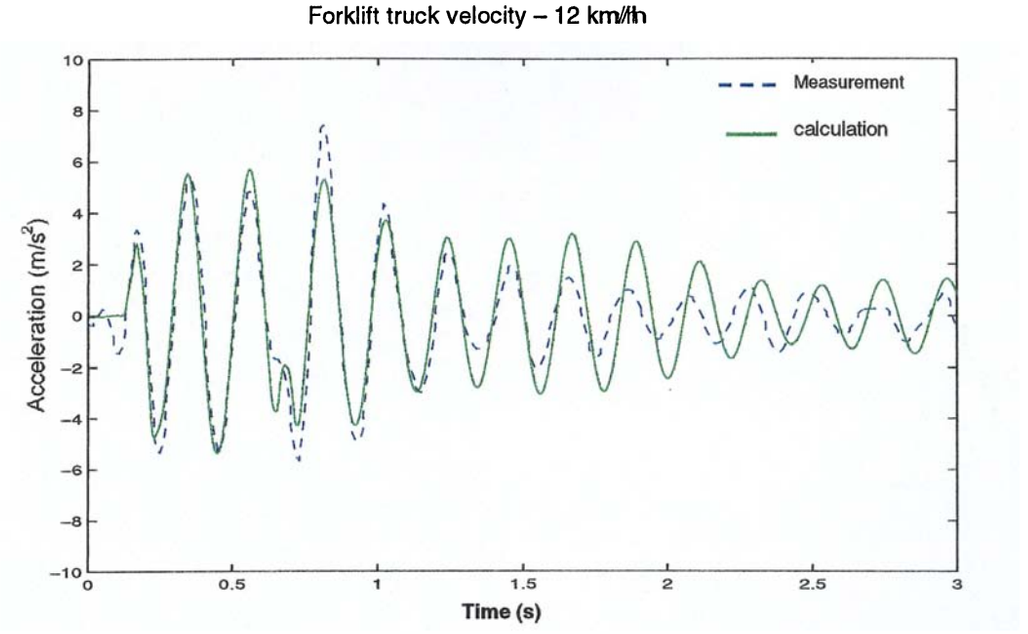

Figure IV- 9 : Comparison of calculated and measured acceleration at driving position.
Pneumatic tires – speed : 12 km/h

5. Parametrical study of the influence of tires on the vibration emission at the driving position

This study was realized with the Komatsu FD20 numerical model. The forklift truck equipped with pneumatic tires was considered to be the reference configuration. The reason is that pneumatic tires had almost linear stiffness (around 6000 N/cm) as well for front wheel tires as for rear wheel tires. The aim of this study was to calculate the vibration emission at the driving position [2], and to evaluate the effects of physical parameters of tires on the transmission of vibration.

The evaluation criterion was the maximum of the mobile RMS value calculated over a 1 s period (see chapter III). This criterion is called « MAX acc RMS/1s » or «γ_{RMS}» in the following figures. Like in the previous chapter, the calculations were made for various speeds between 2 and 15 km/h by steps of 1 km/h.

Firstly our interest was focused on the tire stiffness. The shape factors were always considered as constant and not depending on the stiffness. Indeed, the quasi-static measurements carried out with the three types of tires (cf. fig. II- 3 to II- 8) showed that the shape factors were very similar, though their stiffnesses were extremely different. So, we only dealt with the load/deflection curve.
Four different cases were considered :
Linear case. In this case the load/deflection curve was fully described with one parameter : the stiffness, e.g. the slope of the load/deflection line.
A non-linearity was added by changing the convexity of the load/deflection curve. A first step was to modify the convexity without changing the static equilibrium conditions, this meaning without changing the deflection value of the tires under the forklift truck weight (see §**V-1-3-1**).
A second step was to modify, the convexity without changing the tire stiffness around the static equilibrium (the slope was kept constant for the force value corresponding to the weight of the truck, §**V-1-3-2**).

The effect of the tire damping was also evaluated. The damping model used was basic and not really realistic. So, the aim was not to predict gains of attenuation but to analyse the tendencies.

V-1 Influence of the tire stiffness

V-1-1 Same linear stiffness for front wheels and rear wheels

Six values were successively used : 5000,5500,6000,6500,7000,7500 N/cm.

The results are shown in Figure V- 1.

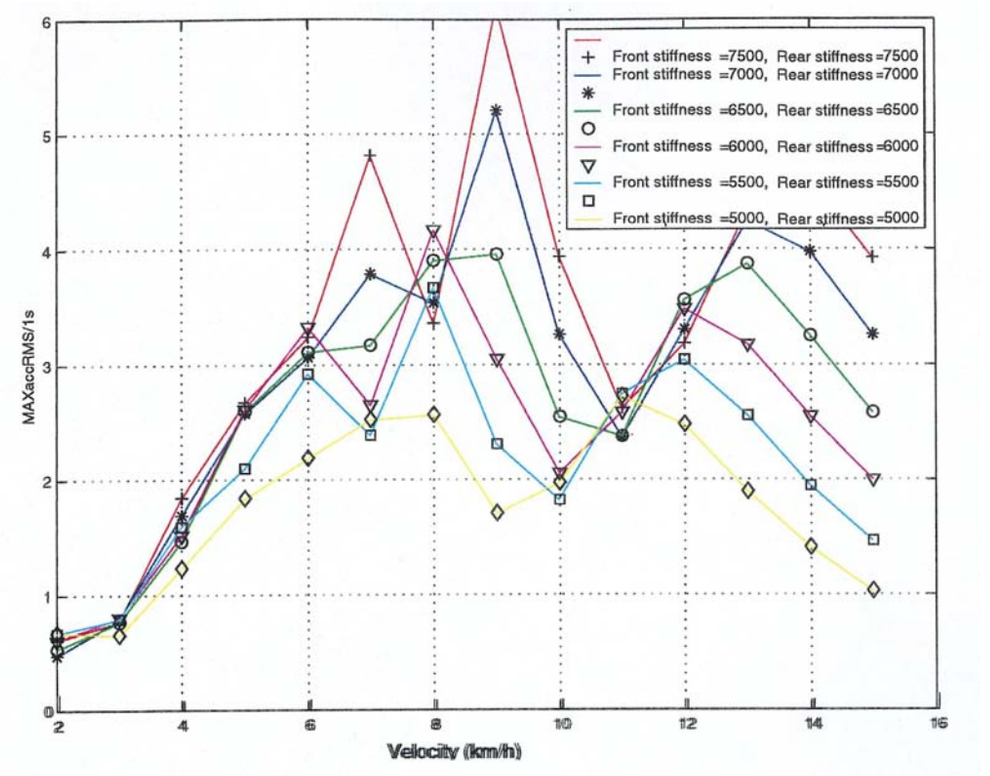

Figure V- 1 : Influence of the tire stiffness on the forklift truck vibration emission.

Linear stiffness – same values for front wheels and rear wheels

The increase of stiffness leads to higher vibration emission, especially within the range of speed where the vibratory behaviour of the forklift truck is governed by interference phenomena between the front and rear axle (speeds higher than 5 km/h). This interference phenomenon, detailed in reference [1], is linked to the natural frequency of the forklift truck. It can be seen that, the higher the stiffness, the higher the natural frequency and consequently the curve is shifted towards the higher speeds.

To get a global comparison of the different sets of tires, the mean value of the criterion was calculated over the 14 velocity values. Figure V- 2 shows the evolution of this mean value versus the various configurations tested.

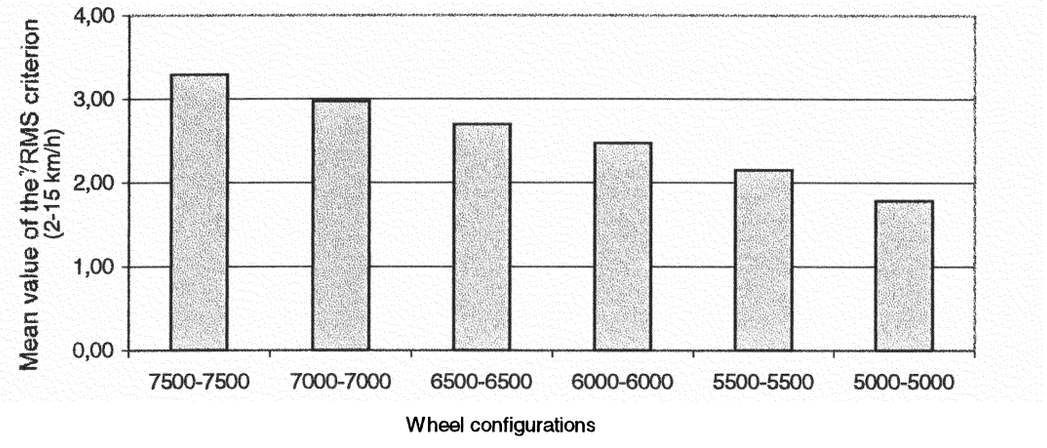

Figure V- 2 : Evolution of the mean value of the γ_{RMS} criterion versus the tire stiffness configurations

Linear stiffness – same values for front wheels and rear wheels

V-1-2 Different linear stiffness for front wheels and rear wheels

Six combination of stiffness between front and rear tires were successively tested. They were respectively : (7500-5000), (7000-5500), (6500-6000), (6000-6500), (5500-7000), (5000-7500) N/cm.
The results are shown in Figure V- 3.

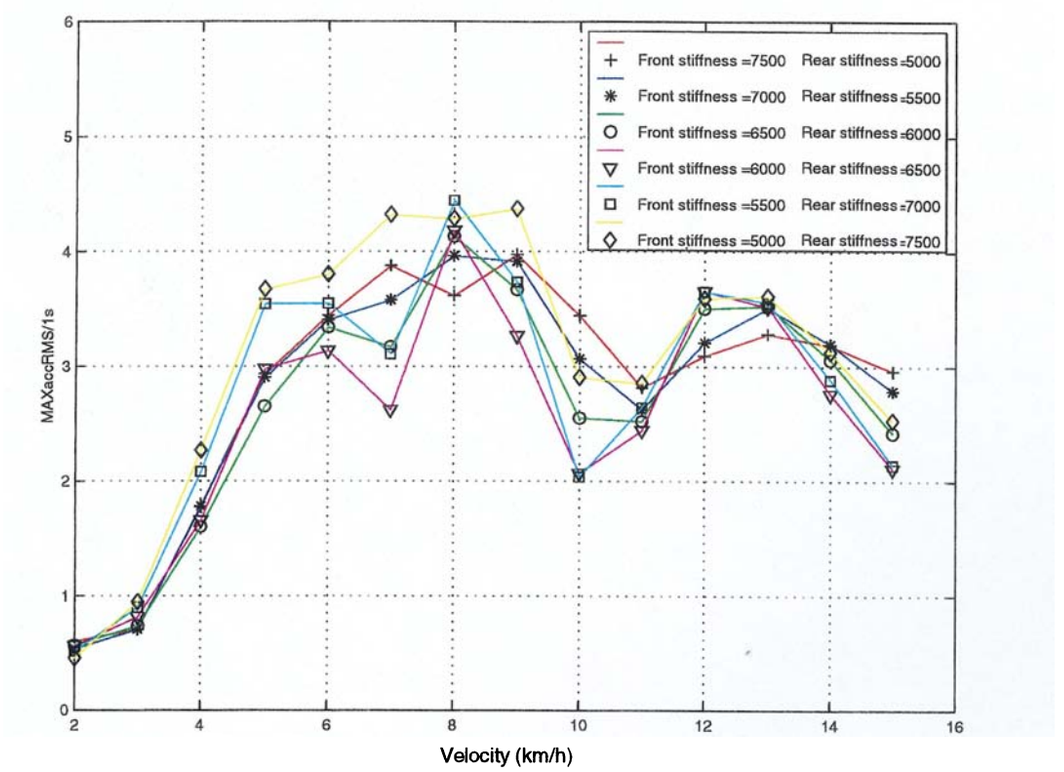

Figure V- 3 : Influence of the tire stiffness on the forklift truck vibration emission.
Linear stiffness – different values for front wheels and rear wheels.

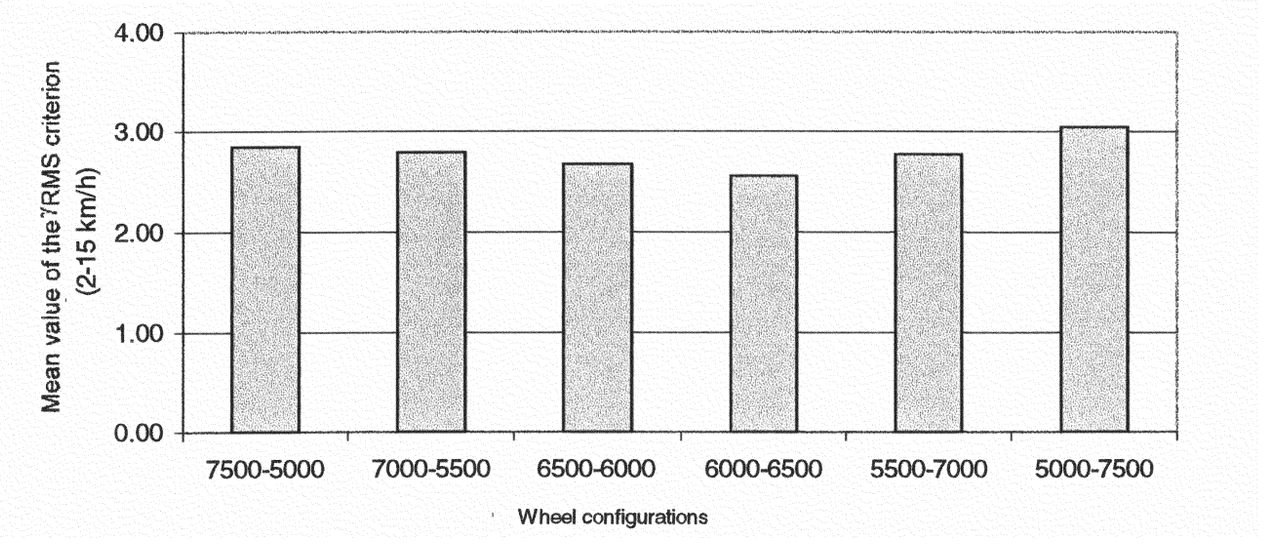

Figure V- 4 : Evolution of the mean value of the γ_{RMS} criterion versus the tire stiffness configurations.
Linear stiffness – different values for front wheels and rear wheels.

The differences are not so high as previously. Then, the use of tires with different stiffness for front wheels and rear wheels is not efficient in terms of vibration reduction.

V-1-3 Same non- linear stiffness for front wheels and rear wheels

V-1-3-1 Static deflection unchanged

The principle of these calculations consisted in changing the stiffness of the tires by increasing the curvature of the load/deflection curve without changing the equilibrium point (static equilibrium defined by the Force $F_0 = 8500$ N and the deflection $z_0 = 1.5$ cm).
The chosen load/deflection curves were defined by the coefficients:
$p_1 = -444\ z^2 + 6333\ z$, $p_2 = -111\ z^2 + 5833\ z$, (decreasing stiffness or « softening » system),
$p_3 = 555\ z^2 + 4833\ z$, $p_4 = 888\ z^2 + 4333\ z$, (increasing stiffness or « hardening » system).

Figure V- 5 shows the shape of these polynomials.

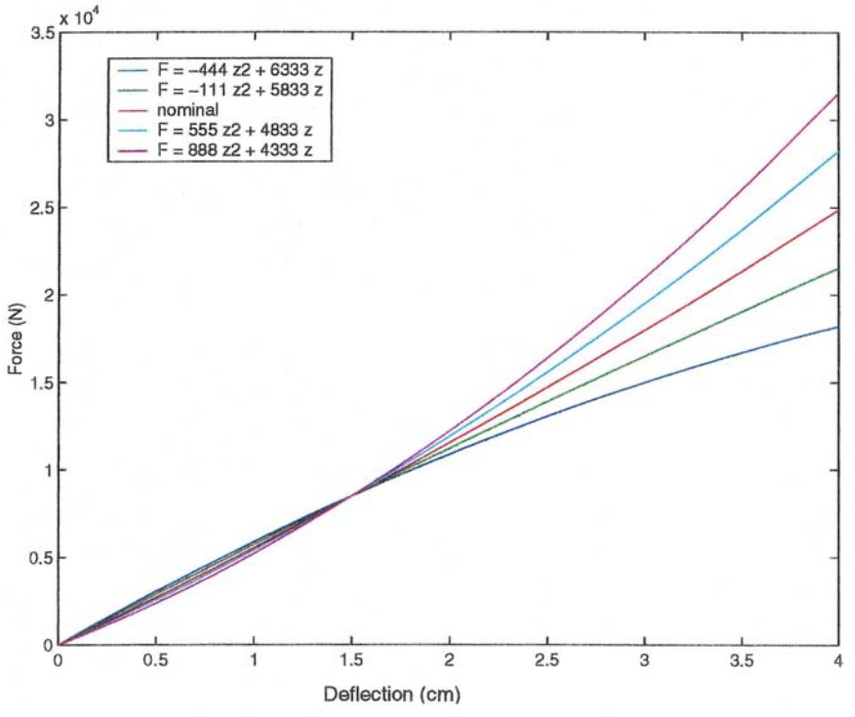

Figure V- 5 : Load/deflection curves with the same equilibrium point (1.5 cm, 8500 N).

The results are shown in Figure V- 6. The values corresponding to the nominal case of 6000 N/cm (for all the tires) are also presented as a reference.

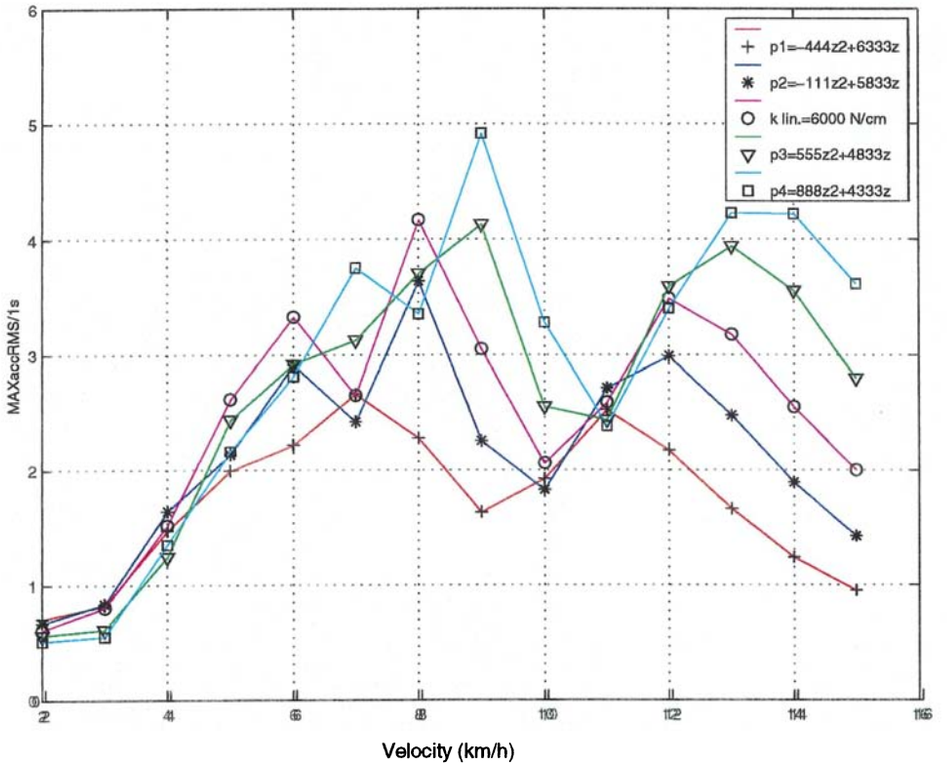

Figure V- 6 : Influence of the tire stiffness on the forklift truck vibration emission.

Non-linear stiffness – same equilibrium point.

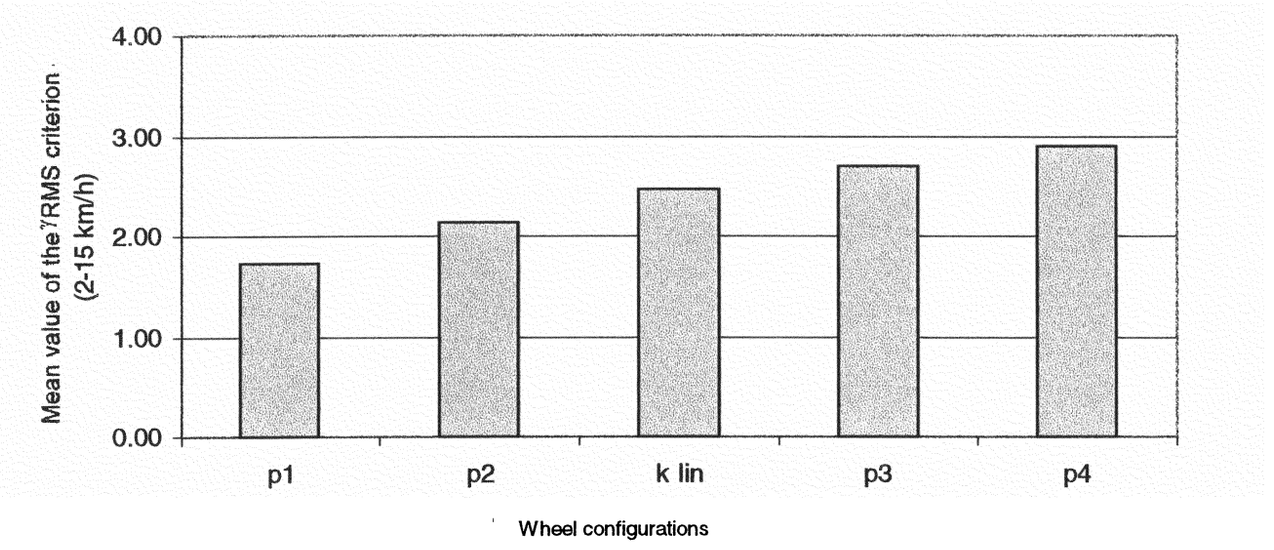

Figure V- 7 : Evolution of the mean value of the γ_{RMS} criterion versus the tire stiffness configurations.

Non-linear stiffness – same equilibrium point.

The lowest acceleration responses were obtained with the polynomial p_1 and p_2 corresponding to decreasing stiffness. Like the linear case, the lower the stiffness, the lower the acceleration response and consequently the curve is horizontally shifted towards the lower speeds.

Remark:
It was also verified that the stiffness law tested for each tire did not involve non-physical behaviour like, for example, very large deflection. For each configuration and for each run, the maximal dynamical deflection of each wheel was computed. We called wheel deflection the difference between the height of the wheel center and the wheel radius. Between 2 km/h and 15 km/h, the maximum deflection values ranged between 1.6 and 3.2 cm for the front tires and between 1.7 and 3.2 cm for the rear tires ; the minimum values ranged between –0.4 and 1.2 cm for the front tires and between –1.2 and 1cm for the rear tires. All these values seem to be reasonable.

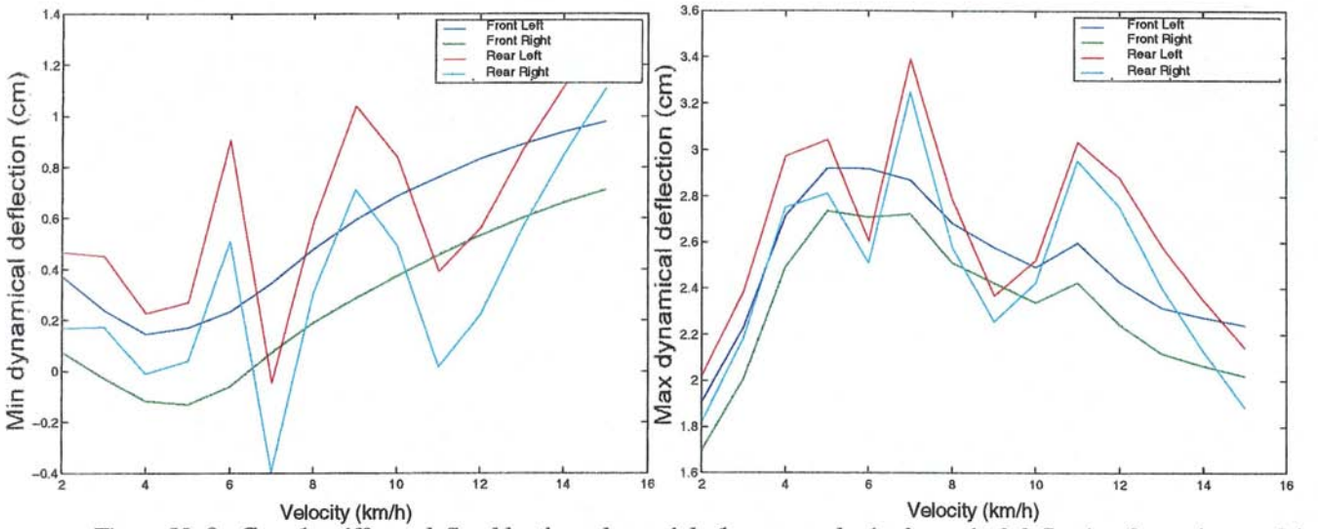

Figure V- 8 : Case 1- stiffness defined by the polynomial p1 : max and min dynamical deflection for each run of the forklift truck

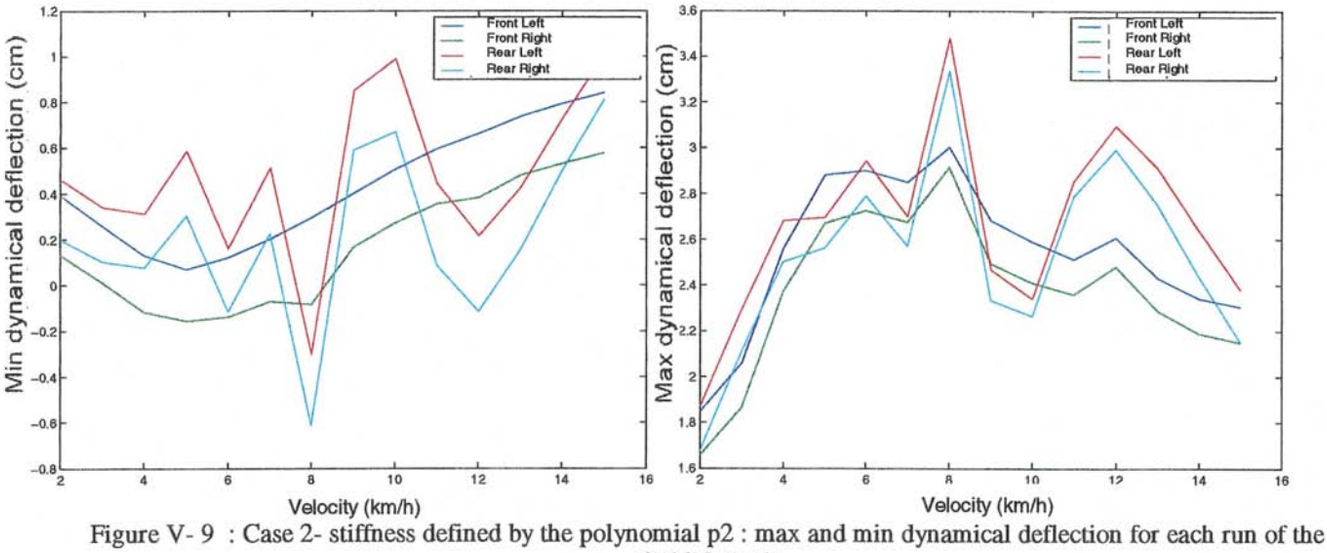

Figure V- 9 : Case 2- stiffness defined by the polynomial p2 : max and min dynamical deflection for each run of the forklift truck

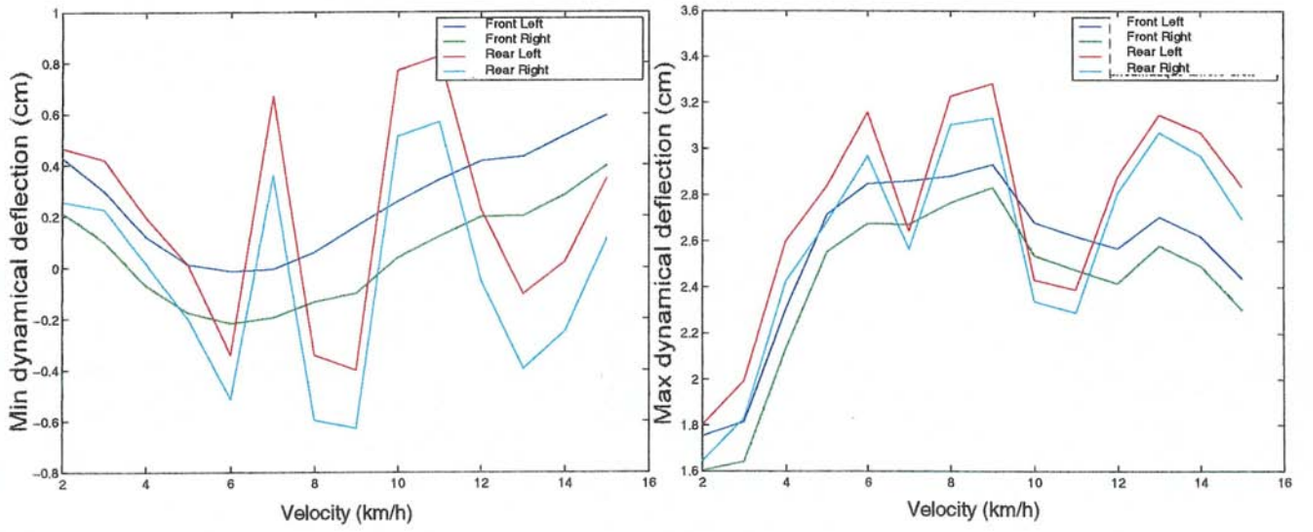

Figure V- 10 : Case 3 - stiffness defined by the polynomial p3 : max and min dynamical deflection for each run of the forklift truck

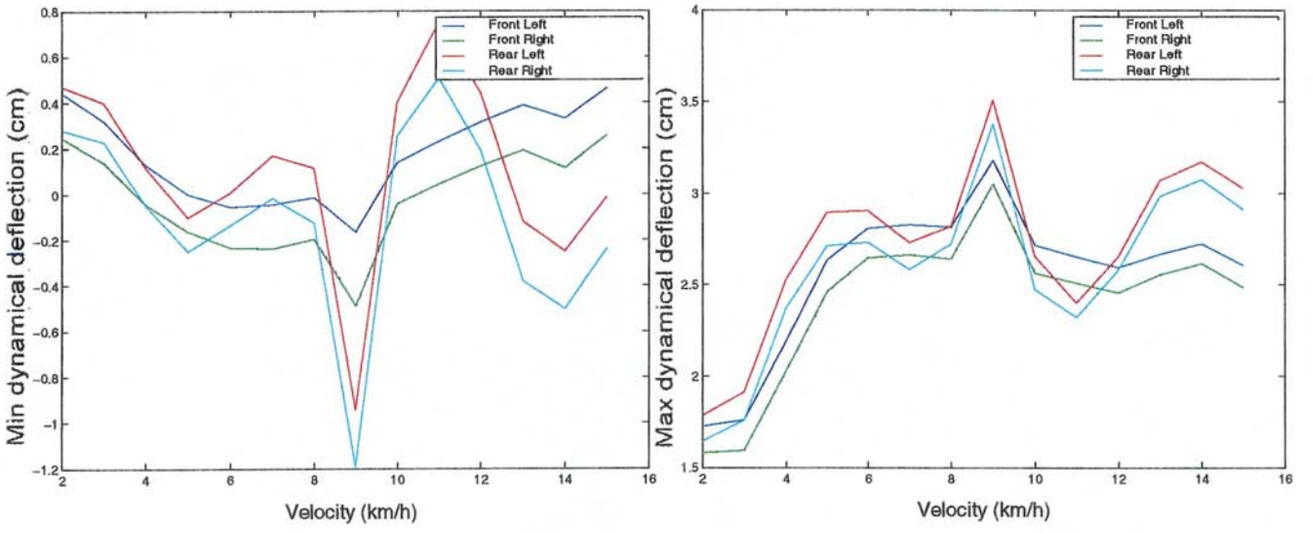

Figure V- 11 : Case 4 - stiffness defined by the polynomial p4 : max and min dynamical deflection for each run of the forklift truck

V-1-3-2 constant stiffness around the static equilibrium position

The constant parameters were the initial static force of 8500 N, and the stiffness around the static equilibrium position 6000 N/cm. Unlike the previous study, the static deflection was varied : 1.1 ; 1.3 ; 1.7 ; 1.9 cm.

The chosen load/deflection curves were defined by the coefficients:

(1,1 cm) q1 = $-1570\ z^2 + 9454\ z$, (1,3 cm) q2 = $-414\ z^2 + 7077\ z$, (decreasing stiffness),
(1,7 cm) q3 = $586\ z^2 + 4000\ z$, (1,9 cm) q4 = $803\ z^2 + 2947\ z$, (increasing stiffness).

Figure V- 12 shows the shape of these polynomials.

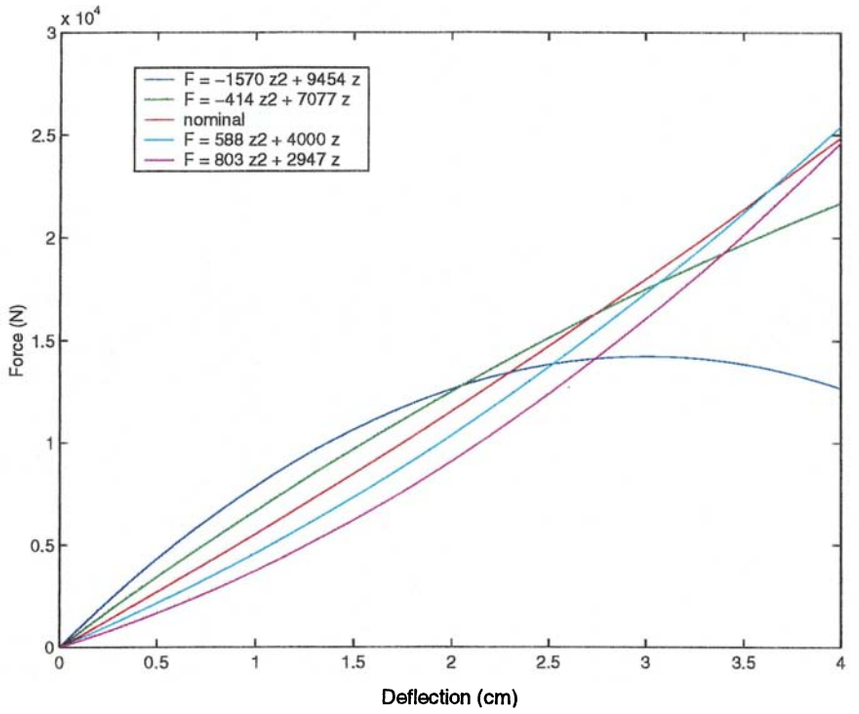

Figure V- 12 : Load/deflection curves with constant stiffness for a given force of 8500 N.

Figure V- 13 shows the calculation results. The values corresponding to the nominal case (initial deflection of 1.5 cm for all the tires) are also presented as a reference. In the case of 1.1 cm of initial deflection, the stiffness value is 0 at around 3 cm and becomes negative for higher deflection which is a non-sense from a mechanical point of view.

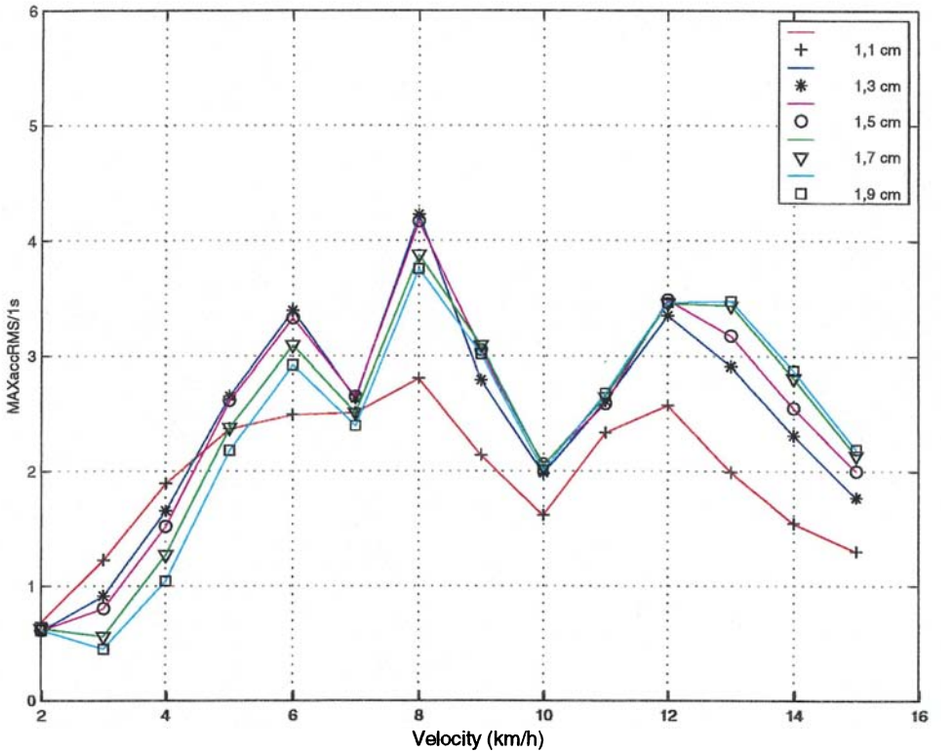

Figure V- 13 : Influence of the tire stiffness on the forklift truck vibration emission.

Non-linear stiffness – same stiffness at static equilibrium.

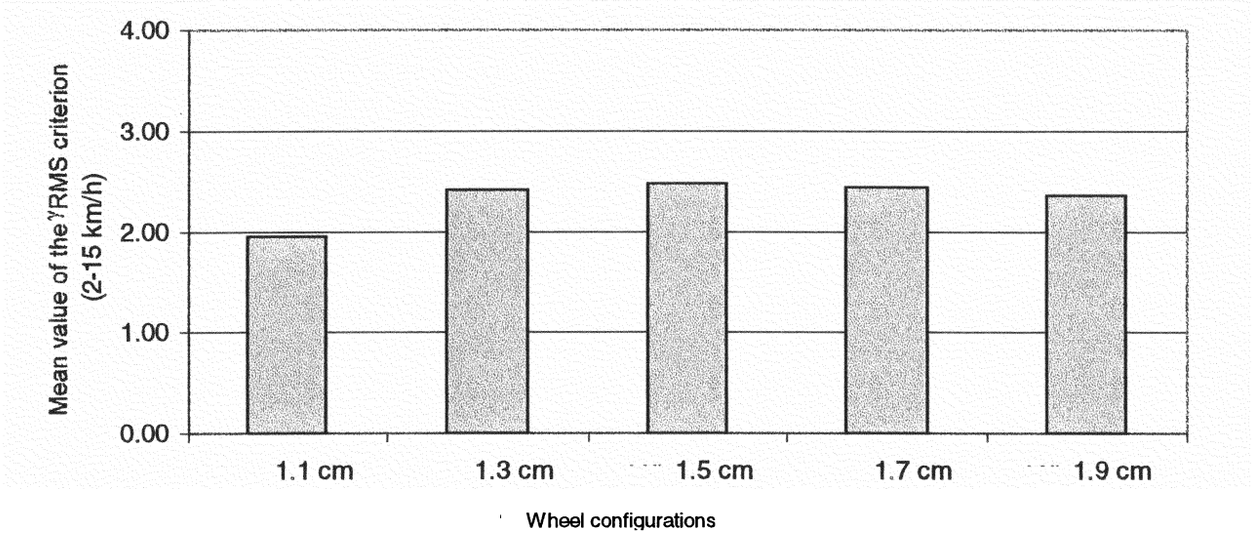

Figure V- 14 : Evolution of the mean value of the γ_{RMS} criterion versus the tire stiffness configurations.

Non-linear stiffness – same stiffness at static equilibrium.

This parameter has no real influence on the vibration emission, especially around 10 km/h, except the case of polynomial « q1 ». In this case, the stiffness is a decreasing function of the deflection like in the previous configuration defined by the polynomial « p1 » and illustrated by Figure V- 6.

Figure V- 15 shows the max and min dynamical deflection for all the calculated runs. It was verified that in any case the wheel moved in the range of negative stiffness (deflection higher than 3 cm, see Figure V- 12).

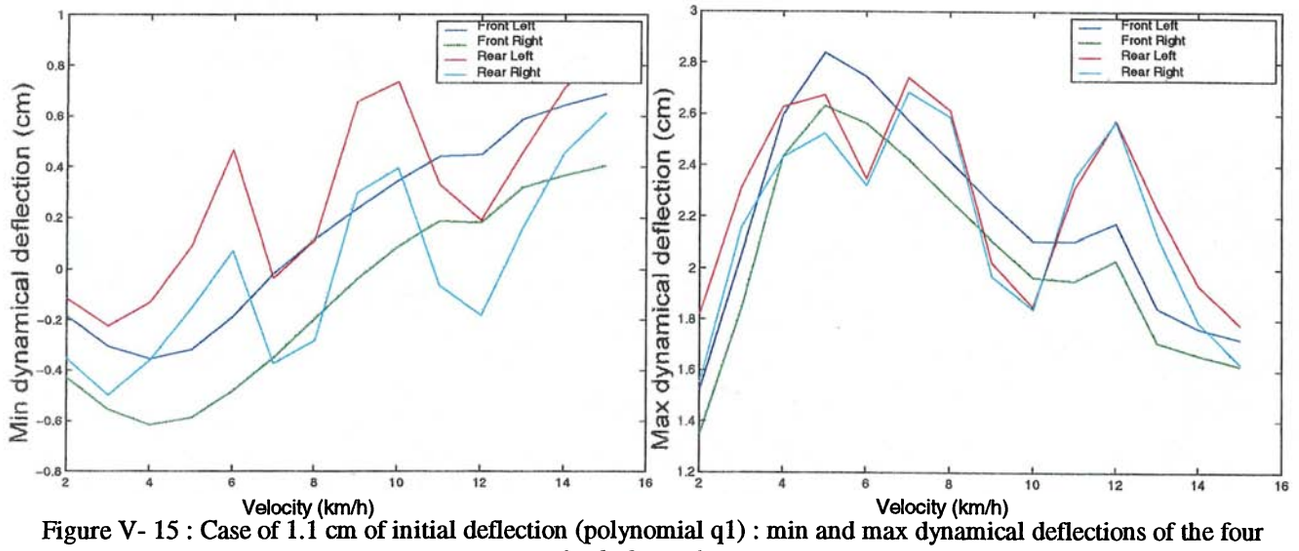

Figure V- 15 : Case of 1.1 cm of initial deflection (polynomial q1) : min and max dynamical deflections of the four wheels for each run.

The tire stiffness may looks attractive to reduce vibration. But we must keep in mind that stiffness is also essential to control the stability. Decreasing the stiffness may reduce the vibration emission but on the opposite, it could have important consequences on the forklift truck stability.

V-2 Influence of the tire damping

Three damping values were successively tested.
They were respectively 1000, 3000 and 5000 Ns/m, the nominal value being 1600 Ns/m.

The calculation results are presented in Figure V- 16.

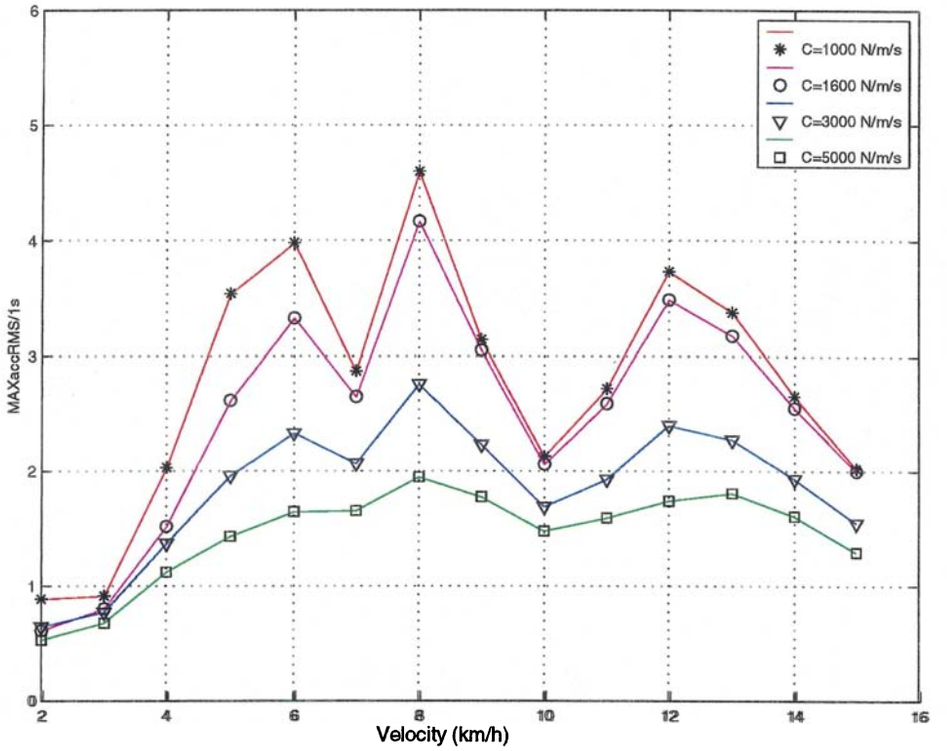

Figure V- 16 : Influence of the tire damping on the forklift truck vibration emission.

Viscous damping

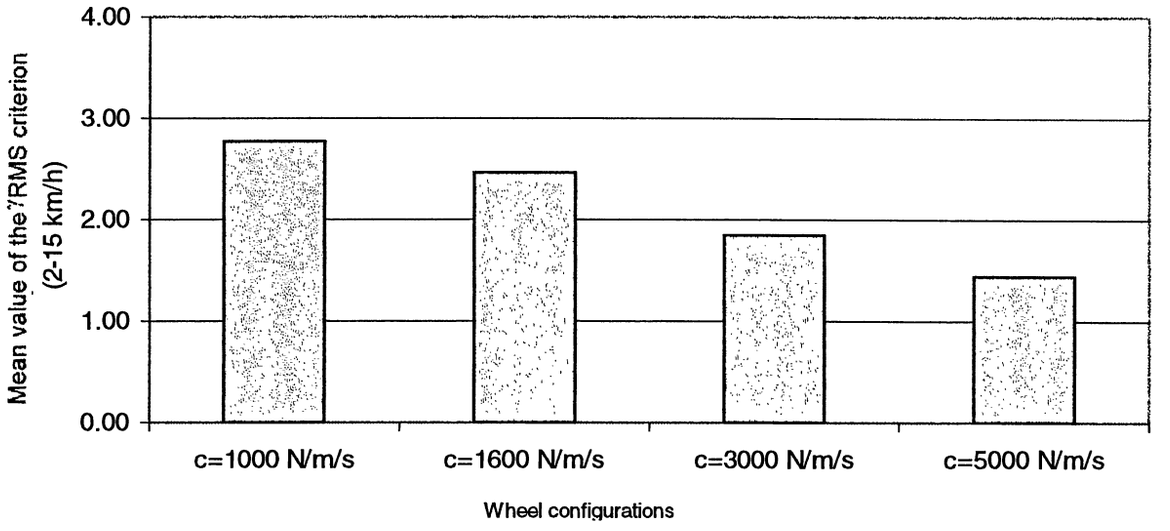

Figure V- 17 : Evolution of the mean value of the γ_{RMS} criterion in function of the damping values.

This parameter has a real effect on the vibration reduction for each value of the velocity. But it is not easy to set up material with such high levels of damping (> 2000 Ns/m). For example, the value of 5000 N/m/s does not seem to be realistic for conventional tires.

V-3 Influence of tire properties at 10 km/h

The European test code stipulates that the trucks shall be tested at 10 km/h.

Figure V- 3 and Figure V- 12 show that at this velocity, the γ_{RMS} criterion (as defined in the introduction of chapter 5) may vary from a factor 2, depending on the type of tires used.

The criterion recommended by the European test code was also calculated [2] as a weighted RMS value (according to the ISO standard 2631 [3]), calculated over the whole acceleration signal emitted by the forklift truck when running over the two obstacles. Our model was used again to predict the values for different configurations of tires.

The calculation results are shown in Figure V- 18 and Figure V- 19.

Figure V- 18 corresponds to the same stiffness for front and rear tires,
(Index 7575 means that the stiffness is 7500 N/cm both for front and rear tires) ;

Figure V- 19 corresponds to different stiffness for front and rear tires,
(Index 7550 means that the stiffness is 7500 N/cm for the front tires and 5000 N/cm for the rear tires) ;

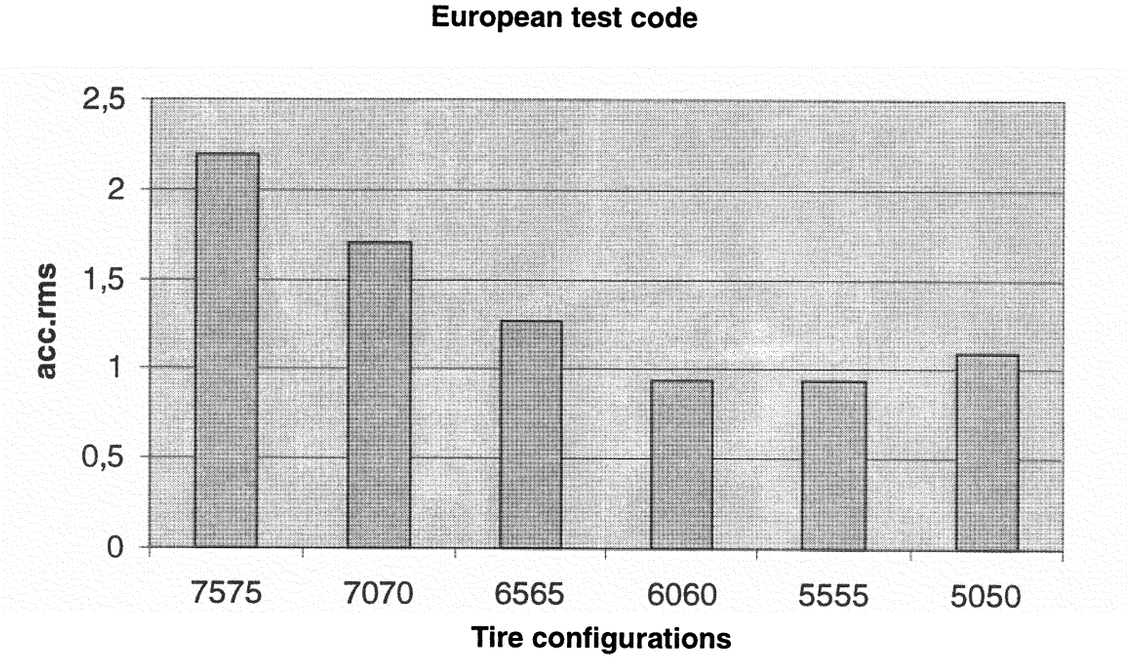

Figure V- 18 : Influence of the tire configuration on the acceleration value measured according to the European test code.

Calculation made with the same characteristics for front and rear tires

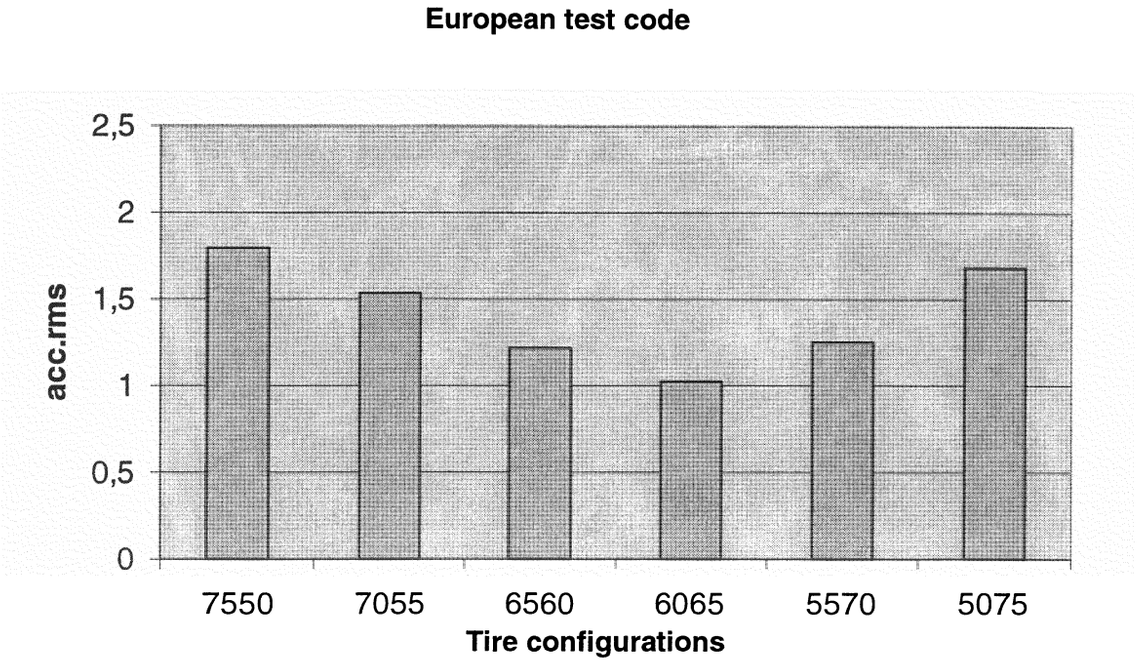

Figure V- 19 : Influence of the tire configuration on the acceleration value measured according to the European test code.

Calculation made with different characteristics for front and rear tires

Although this criterion differs from the previous criterion (γ_{RMS}) it can be seen that it may vary from a factor 2, depending on the type of tire configuration used. The configuration giving the best performance with the γ_{RMS} criterion (configuration 5050) does not give the best result with the procedure of the European test code. The reason is that the European procedure does not take into account the shift of the curves in function of the stiffness changes V-1-1 because only one velocity is considered.

6. References

[1] Lemerle, P. and Mistrot, P. "A New Tire Model to Predict Vibration Emission of Counterbalance Trucks", Tire Science and Technology, TSTCA, Vol. 28. No. 2, April-June 2000, pp. 119-137.

[2] European committee for standardisation, "Safety of Industrial Trucks – Test Methods for Measuring Vibration," European Standard pr EN 13059 prepared by CEN/Tc150/WG8 :1997.

[3] International Standard Organization (ISO), "Mechanical Vibration and Shock – Evaluation of Human Exposure to Whole Body Vibration," – General Requirements – ISO 2631-1, 7 july 1997.

[4] SDS : kinematical and mechanical multi-body modelling software is designed and edited by the company Solid Dynamics :
http://www.solid-dynamics.fr

APPENDIX 1

Calculation of the height of the center of mass

Momentum law applied in point O :

$$\boxed{Mg\ y_h \cos\alpha = F_{d\alpha} d} \qquad (1)$$

Rear view of the FD20

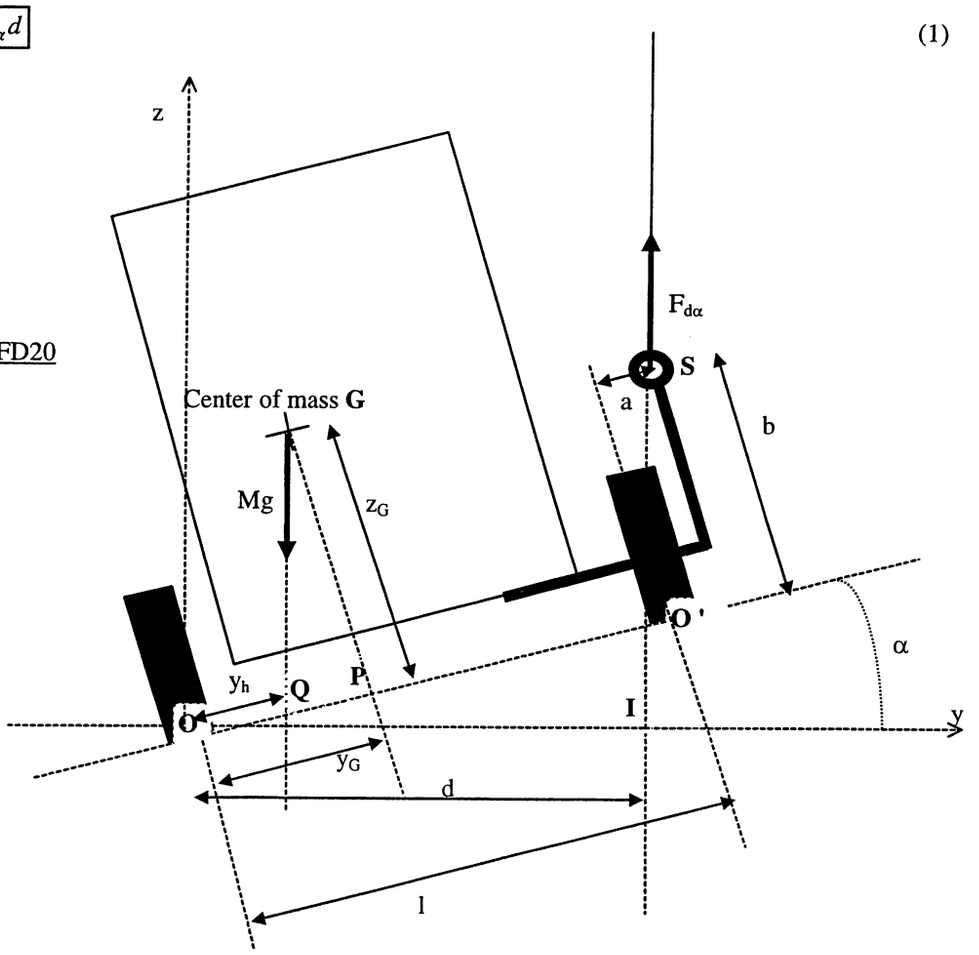

Calculation of d:

relations between angles :

$$(OI,OS) = (OI,OO') + (OO',OS) = \alpha + (OO',OS) \qquad (2)$$

$$(OO',OS) = Arctg\left(\frac{b}{l+a}\right) \qquad (3)$$

Orthogonal projection of S on (Ox) :

$$OI = OS\cos(OI,OS) = OS\cos\left(\alpha + arctg\left(\frac{b}{l+a}\right)\right) \qquad (4)$$

Pythagoras's theorem :

$$OS = \sqrt{b^2 + (l+a)^2} \tag{5}$$

Then d is deduced :

$$\boxed{d = OI = \sqrt{b^2 + (l+a)^2}\ cos\left(\alpha + arctg\left(\frac{b}{l+a}\right)\right)} \tag{6}$$

the momentum law applied in O gives :

$$\boxed{Mg\ y_h \cos\alpha = F_{d\alpha}\sqrt{b^2 + (l+a)^2}\ cos\left(\alpha + arctg\left(\frac{b}{l+a}\right)\right)} \tag{7}$$

Calculation of z_G:

$$\boxed{z_G = GP = QP\ cot\ g\alpha = \left(y_G\ cot\ g\alpha - y_h\ cot\ g\alpha\right)} \tag{8}$$

Reporting the expression of $y_h cos\alpha$ from the equation (7) in equation (8), it gives the expression of z_G in function of y_G, $F_{d\alpha}$ and α :

$$\boxed{z_G = y_G\ cot\ g\alpha - \left(\frac{F_{d\alpha}\ cos\left(Arctg\left(\frac{b}{l+a}\right) + \alpha\right)\sqrt{(l+a)^2 + b^2}}{Mg\ sin\alpha}\right)} \tag{9}$$

truck placed on a section :

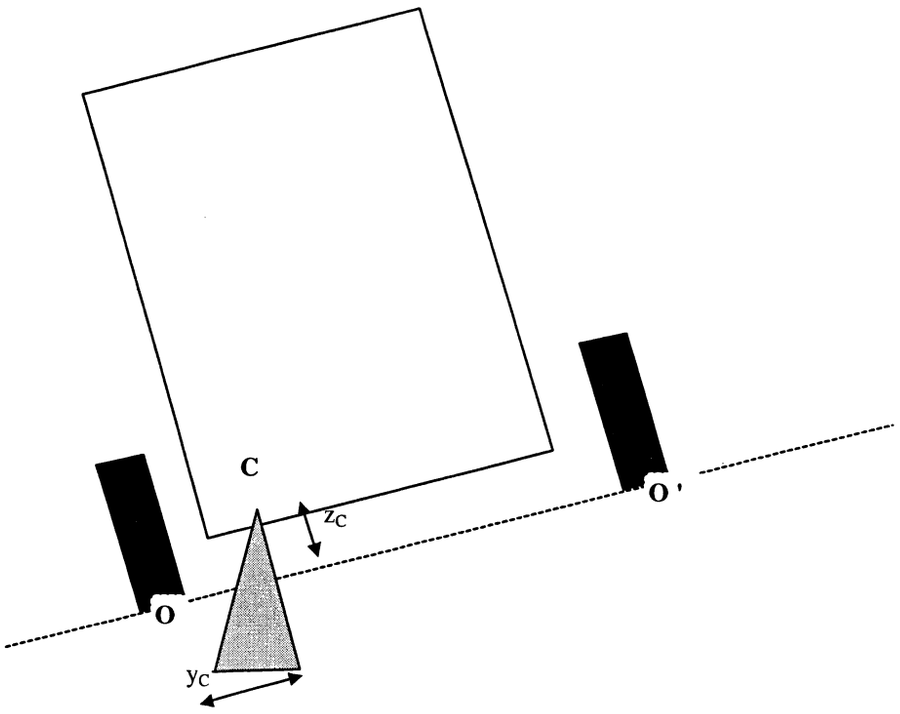

The reasoning is the same changing the origin :

$$\begin{cases} y_G \rightarrow y_G + y_C \\ z_G \rightarrow z_G - z_C \\ l \rightarrow l - y_C \\ b \rightarrow b - z_C \end{cases} \tag{10}$$

the result is :

$$z_G = z_G + (y_G + y_C)\cot g\alpha - \left(\frac{F_{d\alpha} \cos\left(Arctg\left(\frac{b - z_C}{l - y_C + a} \right) + \alpha \right) \sqrt{(l - y_C + a)^2 + (b - z_C)^2}}{Mg \sin\alpha} \right) \tag{11}$$

APPENDIX 2

Spring characteristics

1 manufacturer data :

STRAIN CALCULATION GIVING THE MINIMAL DIAMETER FOR A GIVEN SUPPORTING EFFORT

Known data	
P MAX daN	300
∅ mean mm	52
Max ratio daN/mm	70

Strain calculation	
D wire mm	8.28

TRACTION CALCULATION FOR A LOAD PROPORTIONAL TO THE DEFLECTION

G Shear Modulus daN/mm^2
G steel=8000

KNOWN DATA	
N coils	40
G shear modulus	8000
Deflection mm	
Load daN under deflection	
∅ mean mm	52
Initial tension daN	51

CALCULATION OF N IF UNKNOWN

if d>8 step = Dm*0.35 (modified formula)

L0 body mm	328
n	40
n chosen	40
d calculated	
d chosen	8

FINAL CHARACTERISTICS OF THE TRACTION SPRING

material	steel
D fil mm	8
∅ ext mm	60
L0 body mm	328
N coils	40
step mm	8.20
stiffness daN/mm	0.73
ratio 5<Dm/d<12	6.5
Verif step <0.35*Dm	0.16
L mm if A english	432
L max mm	832
max length mm	400
Initial tension daN	51

2 Verification of the spring characteristics

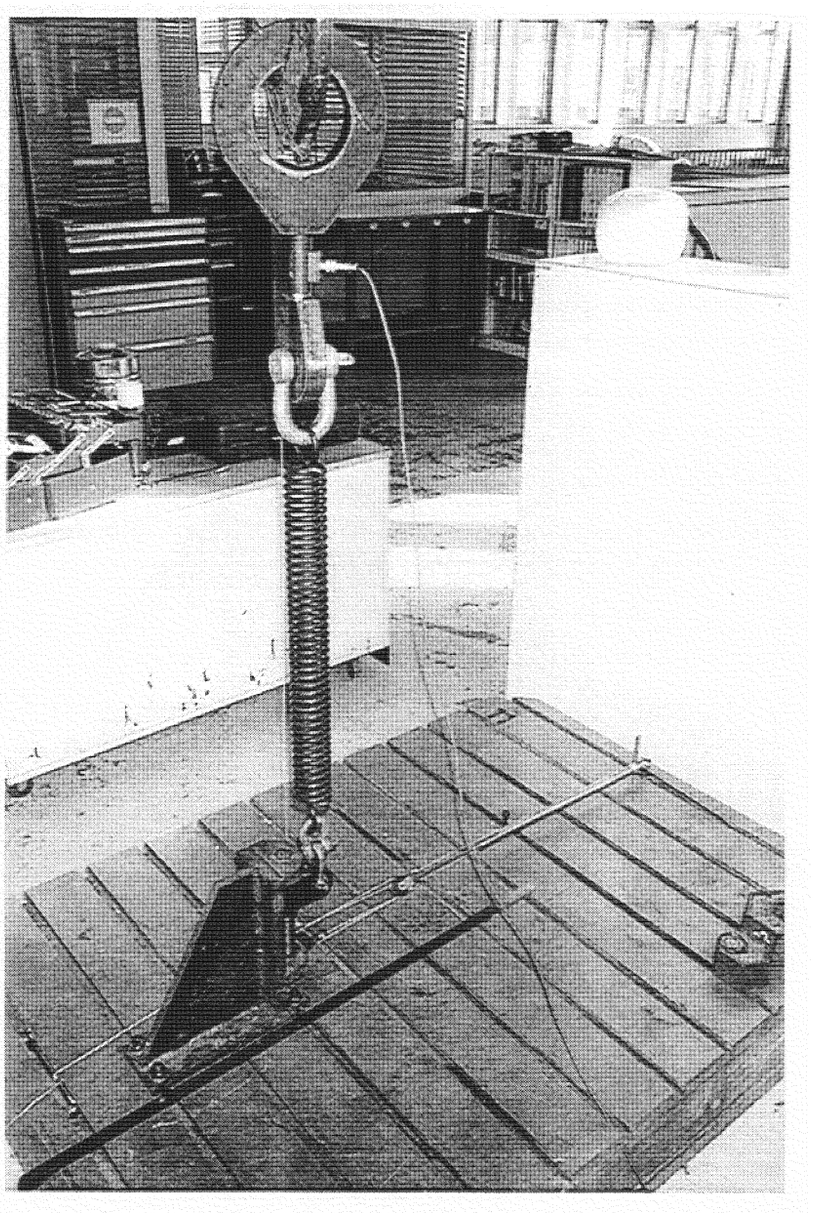

View of the system used to measure the stiffness

One of the 10 springs was tested. It was fixed to the ground on one of its extremities and pulled by a cranage on the other extremity. A system made of pulleys was used to reduce the travel of the spring by a constant factor and to measure it with a LVDT sensor. The results of the traction test are shown in the following figure.

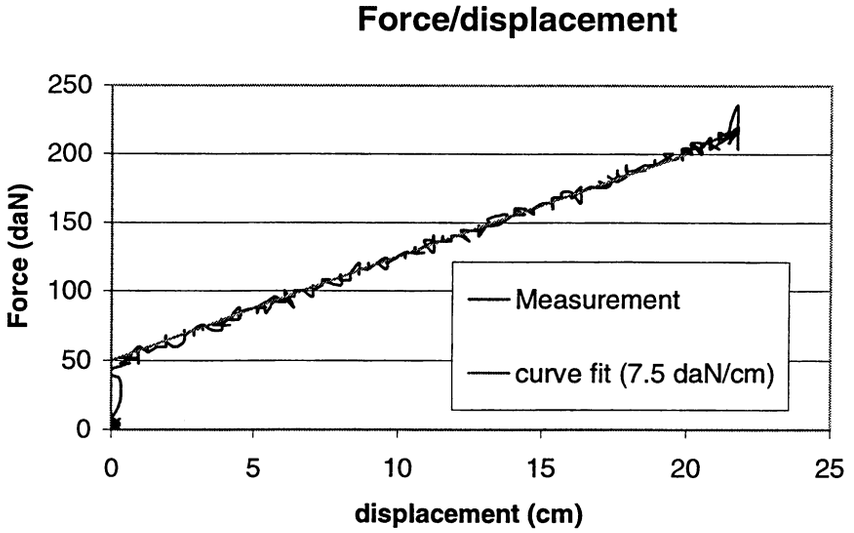

The characteristics given by the manufacturer were confirmed with this test : stiffness of 0.75 daN/mm instead of 0.73 daN/mm and a preload of 50 daN instead of 51 daN.

APPENDIX 3

Calculation of the oscillation period of the suspended forklift truck

Theorem of the angular momentum applied in O :

We called J the angular momentum of the forklift truck around the longitudinal axis in the point 0.

$$J\frac{d^2\alpha}{dt^2} = -MgOO_1 + F_{d\alpha}OO_2 \qquad (1)$$

Rear view of the FD20

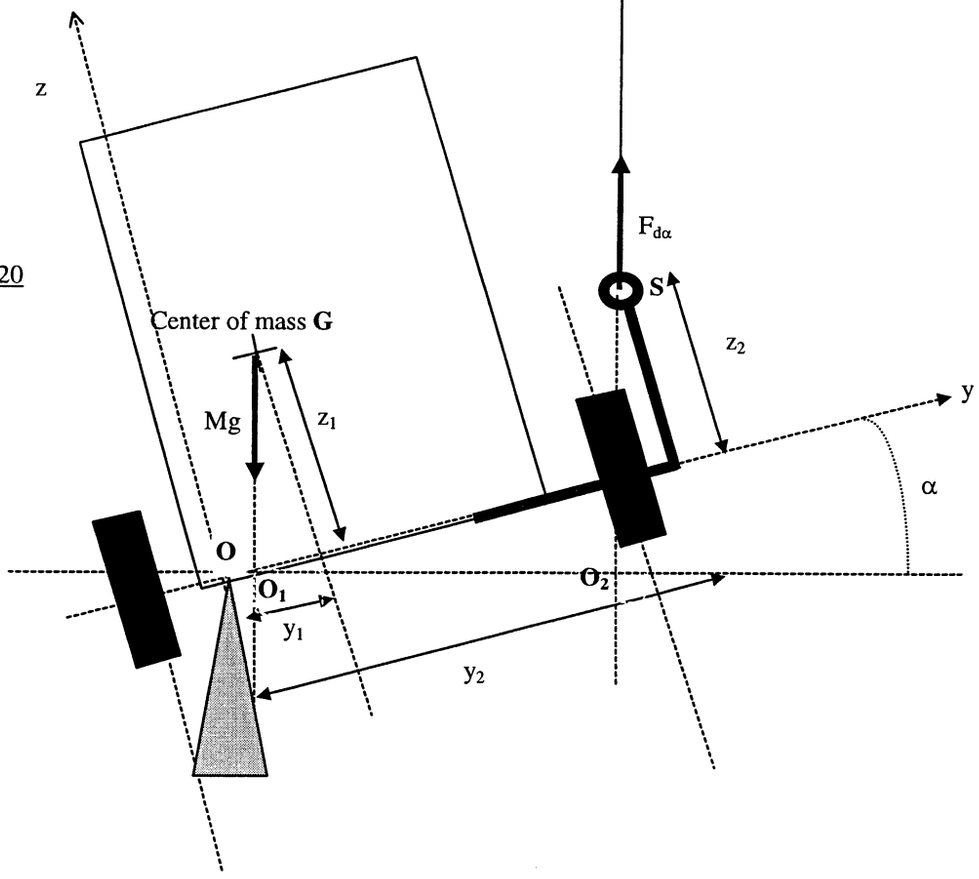

Calculation of OO_1 :

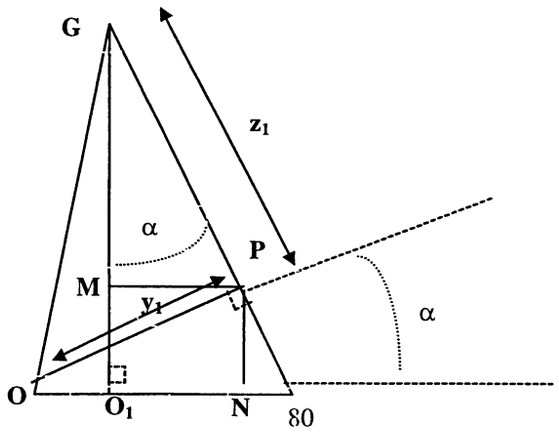

$$OO_1 = ON - O_1N = OP\cos\alpha - MP = OP\cos\alpha - GP\sin\alpha = y_1\cos\alpha - z_1\sin\alpha \tag{2}$$

Calculation of OO_2 :

Again, we have :

$$OO_2 = y_2\cos\alpha - z_2\sin\alpha \tag{3}$$

the equation of motion is now :

$$\boxed{J\frac{d^2\alpha}{dt^2} = -Mg(y_1\cos\alpha - z_1\sin\alpha) + F_{d\alpha}(y_2\cos\alpha - z_2\sin\alpha)} \tag{4}$$

Assumption 1 : z_2 small compared to y_2 and α small

Calculation of $F_{d\alpha}$:

Assuming small rotations, the strain of the springs is due to the change of height of S :

$$F_{d\alpha} = F_{d\alpha 0} - k(z_2\cos\alpha + y_2\sin\alpha) \tag{5}$$

the equation of motion becomes now:

$$\boxed{J\frac{d^2\alpha}{dt^2} = -Mg(y_1\cos\alpha - z_1\sin\alpha) + (F_{d\alpha 0} - k(z_2\cos\alpha + y_2\sin\alpha))(y_2\cos\alpha - z_2\sin\alpha)} \tag{6}$$

Assuming small rotations, we have :

$$\begin{cases}\cos\alpha \approx 1\\ \sin\alpha \approx \alpha\end{cases} \tag{7}$$

In this case, equation (6) becomes :

$$J\frac{d^2\alpha}{dt^2} \approx (-Mgy_1 + F_{d\alpha 0}y_2 - ky_2z_2) + \alpha(Mgz_1 - F_{d\alpha 0}z_2 - ky_2^2 + kz_2^2) \tag{8}$$

At equilibrium the constant coefficients are 0. So can we determine $F_{d\alpha 0}$:

$$F_{d\alpha 0} = \frac{Mgy_1 + ky_2z_2}{y_2} \tag{9}$$

Equation (8) becomes now :

$$J\frac{d^2\alpha}{dt^2} \approx \alpha\left(Mgz_1 - \left(\frac{Mgy_1 + ky_2z_2}{y_2}\right)z_2 - ky_2^2 + kz_2^2\right) \tag{10}$$

The Huygens theorem leads to :

$$J = I_{xx} + M\,OG^2 \tag{11}$$

From equation (10) the oscillation period T of the forklift truck may be deduced. It can be expressed with equation (11) in function of I_{xx} :

$$T = 2\pi\sqrt{\frac{I_{xx} + M\,OG^2}{-Mgz_1 + ky_2^2 - kz_2^2 + \left(\frac{Mgy_1 + ky_2z_2}{y_2}\right)z_2}} \tag{12}$$

Then I_{xx} can be expressed in function of T :

$$I_{xx} = \frac{T^2}{4\pi^2}\left(-Mgz_1 + ky_2^2 - kz_2^2 + \left(\frac{Mgy_1 + ky_2z_2}{y_2}\right)z_2\right) - M\,OG^2 \tag{13}$$

Assumption 2 : α small

Calculation of $F_{d\alpha}$:

The elongation of the springs is characterized by the difference between the lengths:

$$\Delta L = XS - XS' = L - XS' \tag{14}$$

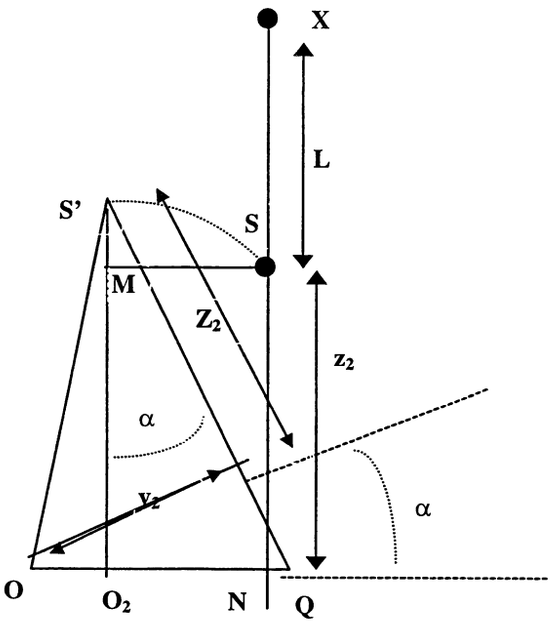

$$XS' = \sqrt{(XS - S'M)^2 + SM^2} = \sqrt{(L - (S'O_2 - MO_2))^2 + (ON - OO_2)^2}$$
$$= \sqrt{(L - (z_2 \cos\alpha + y_2 \sin\alpha - z_2))^2 + (y_2 - (y_2 \cos\alpha - z_2 \sin\alpha))^2} \quad (15)$$

ΔL is obtained from equation (15) :

$$\Delta L = \sqrt{(L - (z_2(\cos\alpha - 1) + y_2 \sin\alpha))^2 + (y_2(1 - \cos\alpha) + z_2 \sin\alpha)^2} - L \quad (16)$$

Assuming small rotations, ΔL becomes then :

$$\Delta L \approx \sqrt{(L - y_2\alpha)^2 + (z_2\alpha)^2} - L = L\left(\sqrt{1 - \frac{2y_2\alpha}{L}} - 1\right) = y_2\alpha \quad (17)$$

this giving $F_{d\alpha}$:

$$F_{d\alpha} = (F_{d\alpha 0} - ky_2\alpha) \quad (18)$$

The equation of motion is now :

$$\boxed{J\frac{d^2\alpha}{dt^2} = -Mg(y_1 - z_1\alpha) + (F_{d\alpha 0} - ky_2\alpha)OT'} \quad (19)$$

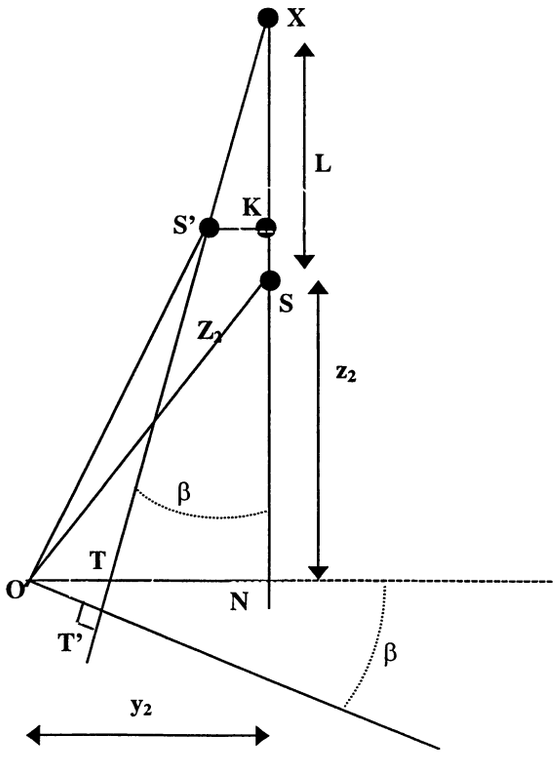

Calculation of the lever arm OT' :

$$OT' = OT\cos\beta \approx OT \tag{20}$$

$$\begin{aligned} OT &= ON - NT = y_2 - S'K\frac{XN}{XK} \\ &= y_2 - \left(y_2(1-\cos\alpha) + z_2\sin\alpha\right)\frac{(L+z_2)}{\left(L+z_2(1-\cos\alpha) - y_2\sin\alpha\right)} \\ &\approx y_2 - z_2\frac{(L+z_2)}{(L-y_2\alpha)} \approx y_2 - z_2\frac{(L+z_2)}{L} \end{aligned} \tag{21}$$

The equation of motion (19) is then :

$$\boxed{\begin{aligned} J\frac{d^2\alpha}{dt^2} &= -Mg(y_1 - z_1\alpha) + (F_{d\alpha 0} - ky_2\alpha)\left(y_2 - z_2\alpha\frac{(L+z_2)}{L}\right) \\ &= \left(F_{d\alpha 0}y_2 - Mgy_1\right) + \left(Mgz_1 - ky_2^2 - F_{d\alpha 0}z_2\frac{(L+z_2)}{L}\right)\alpha \end{aligned}} \tag{22}$$

At equilibrium the constant coefficients are 0. So can we determine $F_{d\alpha 0}$:

$$F_{d\alpha 0} = \frac{Mgy_1}{y_2} \tag{23}$$

Equation (22) becomes then :

$$\boxed{J\frac{d^2\alpha}{dt^2} = \left(Mgz_1 - ky_2^2 - \frac{Mgy_1}{y_2}z_2\frac{(L+z_2)}{L}\right)\alpha} \tag{24}$$

Then the free oscillation period of the forklift truck is deduced:

$$\boxed{T = 2\pi\sqrt{\frac{I_{xx} + M\,OG^2}{-Mgz_1 + ky_2^2 + \left(\frac{Mgy_1z_2}{y_2}\right)\left(\frac{L+z_2}{L}\right)}}} \tag{25}$$

Then I_{xx} may be expressed in function of T :

$$\boxed{I_{xx} = \frac{T^2}{4\pi^2}\left(-Mgz_1 + ky_2^2 + \left(\frac{Mgy_1z_2}{y_2}\right)\left(\frac{L+z_2}{L}\right)\right) - M\,OG^2} \tag{26}$$

APPENDIX 4

Tire numerical model : analytical expression of the tire prints

L_0^{obst} : length of the theoretical tire print calculated with an infinite plane surface at height h_{obst} (considering the tire print as a line segment defined by the intersection between the circle representing the tire and the line representing the plane surface).

$$L_0^{obst} = 2\sqrt{R^2 - (z - h_{obst})^2}$$

z height of the wheel axle, R wheel radius

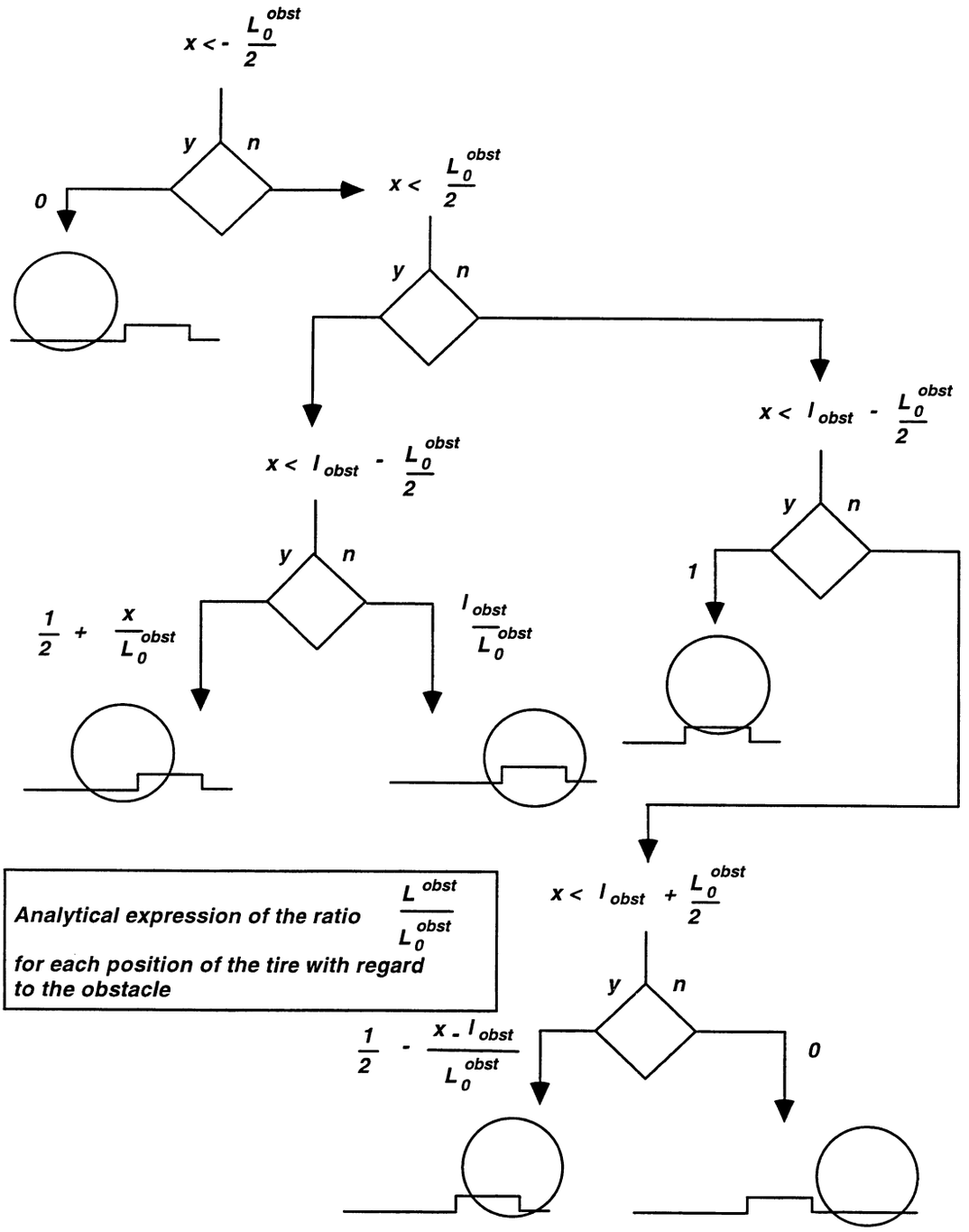

L_0^{ground} : length of the theoretical tire print on the ground (considering the tire print as a line segment defined by the intersection between the circle representing the tire and the line representing the ground).

$L_0^{ground} = 2\sqrt{R^2 - z^2}$ z height of the wheel axle, R wheel radius

Δ : shock advance, shift defining the position of the virtual edge of the obstacle. This shift is in fact a geometrical model of the shear of the tire on the edge of the obstacle (in the area near the edge, the tire is lifted up).

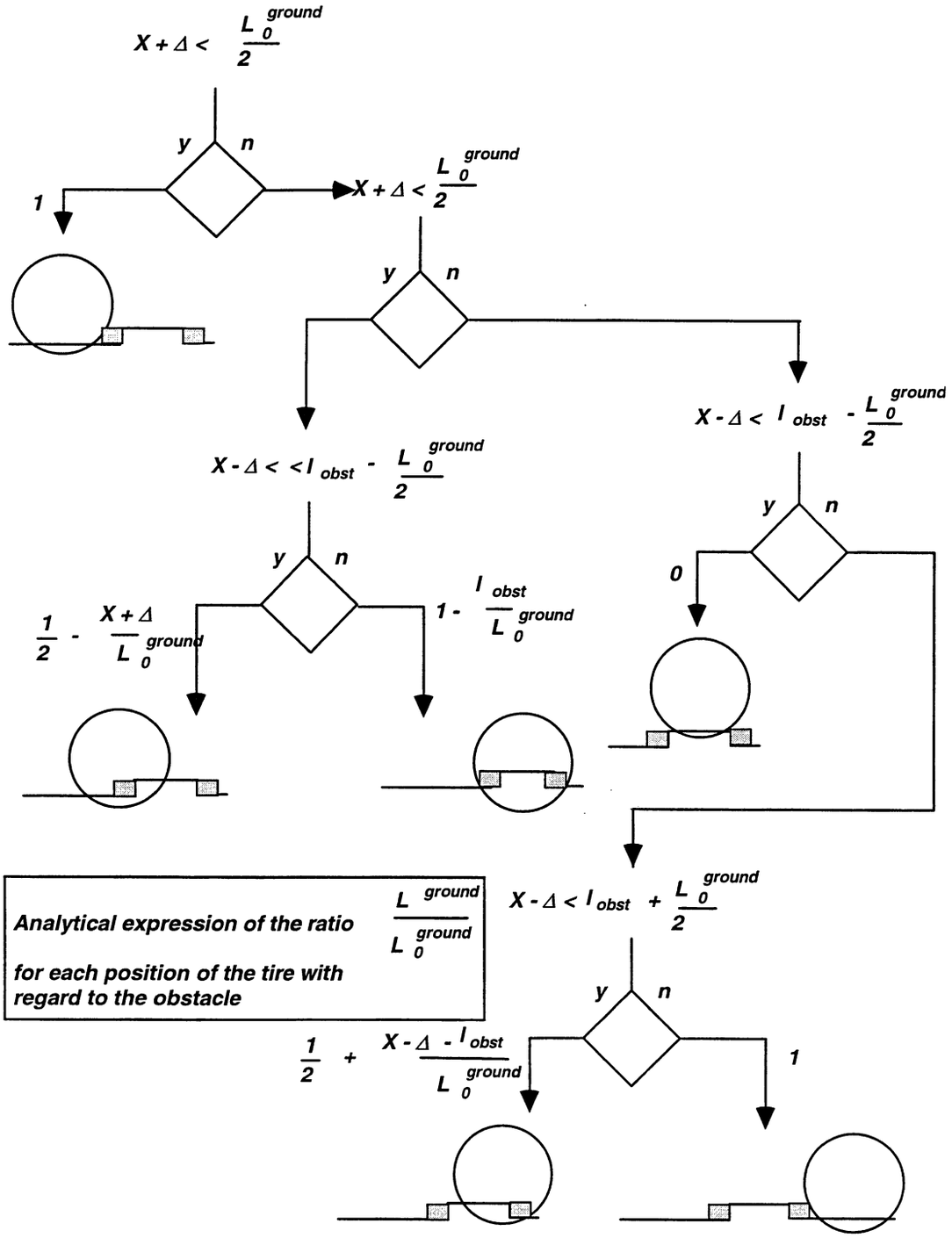

APPENDIX 5

Tire test bench

A tire test bench was designed by INRS to measure the input data for the tire model, e.g. the load/deflection curves and the shape factors. This test bench was also designed to test the tires in dynamical conditions especially with obstacles.
Figures below show a view and a diagram of the tire test bench. The test bench is composed of 4 parts :

1. a support (1) with ball-bearing rollers to guide the ring as it is rotating. The bottom of the support includes the force measurement system (a platform with four load cells) and is firmly attached to the floor.
2. a ring (2) inside of which the wheel being tested can rotate. The ring is 2 cm thick, 28 cm wide and has an inside diameter of 146 cm. The linear speed of the hoop, limited to 20 km/h, is measured by means of an optical encoder. If necessary, obstacles made of PVC material may be stuck inside the ring
3. a body (3) which guides the motorized wheel inside the hoop. This articulated framework includes a 6 kW variable speed motor and can receive additional masses (of up to 2.3 t) in order to load the wheel properly. The height of the joint with respect to the support may be set to ensure that the part of the body supporting the additional masses is horizontal. Both the displacement between the wheel axis and the ring and the acceleration of the wheel axis are measured.
4. an electro-hydraulic actuator (4) which has a 250 mm stroke and allows a force of up to 25 kN to be generated.

For the quasi-static tests, like load/deflection measurements and shape factor identification, this was connected to the body and secured to the floor by means of two spherical joints. Safety systems limit the maximum values of acceleration and force transmitted to the body.

For the dynamic tests including rotating the wheel over the obstacle stuck inside the ring, the electro-hydraulic actuator was disconnected from the body. By so doing, the wheel could behave as an unconstrained system of one degree of freedom.

The limitations imposed by this test bench are due to the curvature of the hoop. For example, for load/deflection measurements, the forces induced by the contact on a curved surface are higher than those on a flat surface. Consequently, when the wheel is moving over an obstacle stuck inside the ring it does not behave as if it were moving over a flat obstacle placed on the ground. In order to measure the characteristics of the tire on a flat surface, an interface system was developed. It is placed on the support above the ring and is illustrated next page.

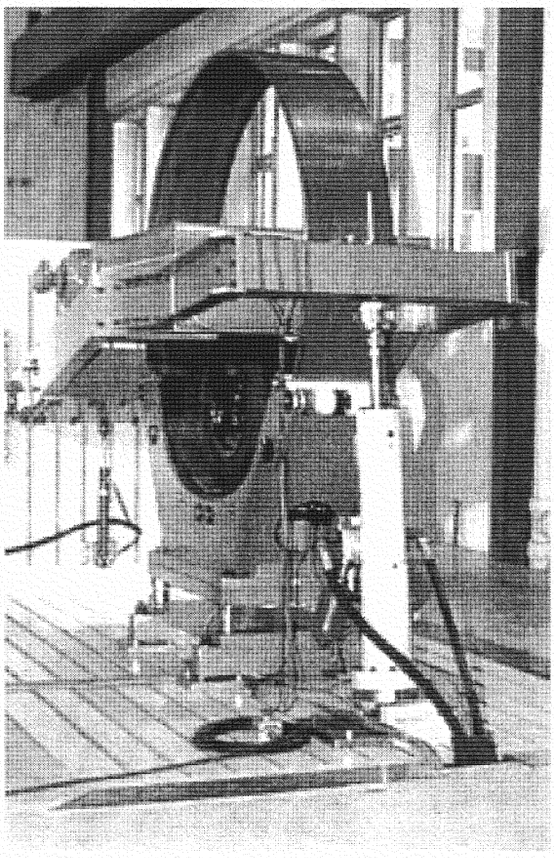

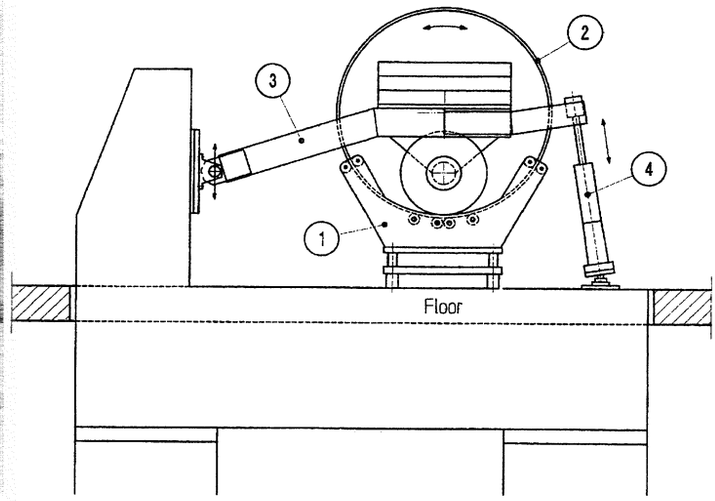

The system comprised a rigid plate covered with a "Teflon" sheet on to which a thin, sliding PVC band was fitted. Obstacles of the same material could be stuck on the band. The motorized wheel induced the movement of the band which was guided on the rigid plate.

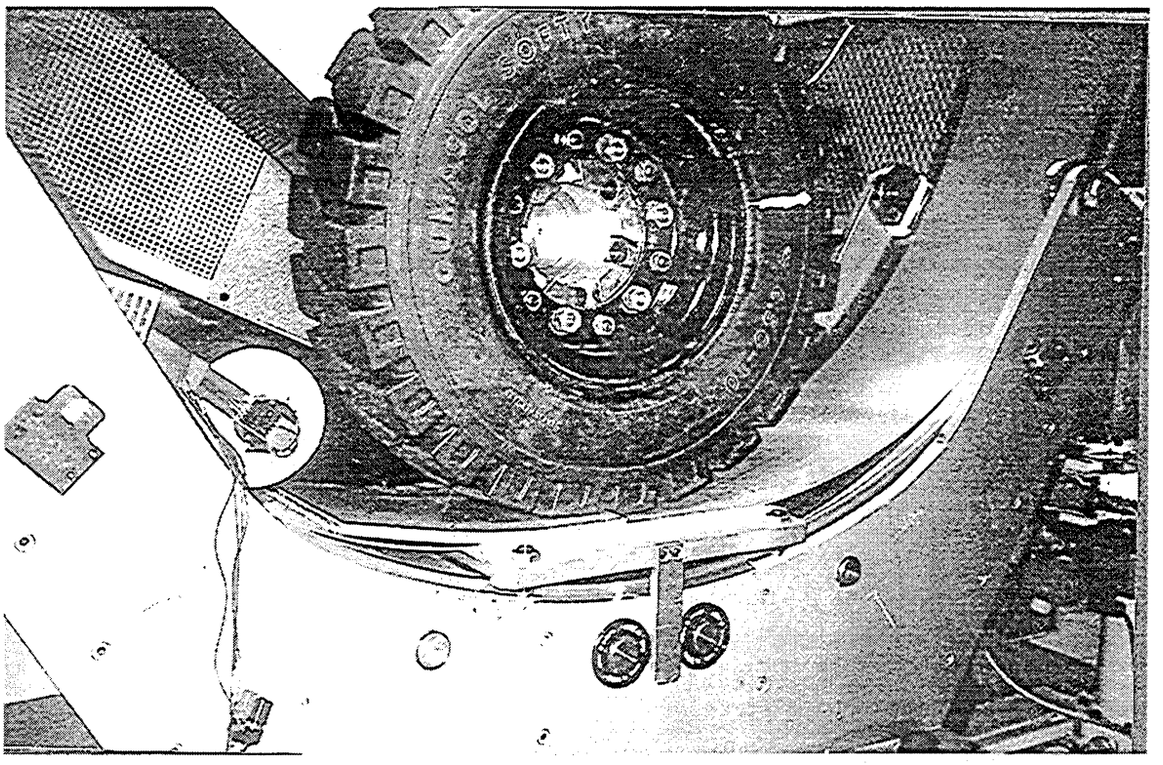

APPENDIX 6

KOMATSU FD20 model : SDS program source

```
DECL
REAL pp tempo accelero resu resu2 z amortissement_ar0 amortissement_av0
REAL int rampe der_rampe h l
REAL vit rot_av der_rot_av  rot_ar der_rot_ar elan
REAL entraxe empatt_av empatt_ar
REAL rayon_av avance_av amortissement_av charge1_av charge2_av charge3_av
REAL polyh1_av polyh2_av polyh3_av polyh4_av polyh5_av polyh6_av
REAL polyb1_av polyb2_av polyb3_av polyb4_av polyb5_av polyb6_av
REAL rayon_ar avance_ar amortissement_ar charge1_ar charge2_ar charge3_ar
REAL polyh1_ar polyh2_ar polyh3_ar polyh4_ar polyh5_ar polyh6_ar
REAL polyb1_ar polyb2_ar polyb3_ar polyb4_ar polyb5_ar polyb6_ar
REAL Lobst_avg0 Lground_avg0
REAL x_avg z_avg ratioh_avg ratiob_avg Fb_avg Fh_avg formb_avg formh_avg
REAL Lobst_avd0 Lground_avd0
REAL x_avd z_avd ratioh_avd ratiob_avd Fb_avd Fh_avd formb_avd formh_avd
REAL Lobst_arg0 Lground_arg0
REAL x_arg z_arg ratioh_arg ratiob_arg Fb_arg Fh_arg formb_arg formh_arg
REAL Lobst_ard0 Lground_ard0
REAL x_ard z_ard ratioh_ard ratiob_ard Fb_ard Fh_ard formb_ard formh_ard
REAL body_idx obj_idx x_cdg y_cdg z_cdg Ixx Iyy masse
VEC3 dir_avg dir_avd dir_arg dir_ard  dir_cdg cdg
VEC3 vecsiège
MAT33 inertie
TAB 9 7 tt
REAL r choix vit0 calcul

OUT

//all
accelero

INTERACTION

CONSTRUCTOR
entraxe=1.675
empatt_av=0.965
empatt_ar=0.94
elan=1
x_cdg=.87
y_cdg=0.0325
z_cdg=0.66
cdg[X]=-y_cdg
cdg[Y]=0.8-x_cdg
cdg[Z]=z_cdg-1.1
masse=3420
Ixx=1450
Iyy=3100
inertie[X][X]=Iyy
inertie[Y][Y]=Ixx
inertie[X][Y]=0
inertie[X][Z]=0
inertie[Y][Z]=0
inertie[Z][Z]=Ixx
body_idx=get_obj_idx("body5")
set_mass(body_idx,masse,cdg,inertie)

INITIALIZATION
tempo=2
//vit=11/3.6
dir_avg[X]=0
dir_avg[Y]=0
dir_avg[Z]=0
dir_avd[X]=0
dir_avd[Y]=0
dir_avd[Z]=0
dir_arg[X]=0
dir_arg[Y]=0
dir_arg[Z]=0
```

```
dir_ard[X]=0
dir_ard[Y]=0
dir_ard[Z]=0
l=0.15
h=0.01
rayon_av=0.34
rayon_ar=0.27


if choix==2
//-------------------------------------------------------------------------
//PLEINS
//-------------------------------------------------------------------------
avance_av=0.050000
avance_ar=0.045000
charge3_av=176
charge2_av=5188
charge1_av=3655
polyh6_av= -0.991967
polyh5_av= 4.617628
polyh4_av= -8.840850
polyh3_av= 6.517820
polyh2_av= -0.300187
polyh1_av= -0.003721
polyb6_av= 0.988859
polyb5_av= 3.579162
polyb4_av= -13.137664
polyb3_av= 10.727185
polyb2_av= -1.156796
polyb1_av= -0.001228
charge3_ar=398
charge2_ar=865
charge1_ar=6600
polyh6_ar= -0.238756
polyh5_ar= 3.524886
polyh4_ar= -8.613286
polyh3_ar= 6.510233
polyh2_ar= -0.183172
polyh1_ar= -0.000091
polyb6_ar= -1.446549
polyb5_ar= 9.090475
polyb4_ar= -18.260364
polyb3_ar= 13.736148
polyb2_ar= -2.117782
polyb1_ar= -0.007583
charge3_ar=charge3_ar*1000000
charge2_ar=charge2_ar*10000
charge1_ar=charge1_ar*100
charge3_av=charge3_av*1000000
charge2_av=charge2_av*10000
charge1_av=charge1_av*100
amortissement_av0=2500
amortissement_ar0=2500
endif

if choix==1
//-------------------------------------------------------------------------
//GONFLES
//-------------------------------------------------------------------------
avance_av=0.070000
avance_ar=0.050000
charge3_av=86
charge2_av=1024
charge1_av=5788
polyh6_av= -3.739172
polyh5_av= 14.265972
polyh4_av= -19.527659
polyh3_av= 10.159708
polyh2_av= -0.158293
polyh1_av= -0.001062
polyb6_av= 12.504640
polyb5_av= -28.061820
polyb4_av= 17.352577
polyb3_av= -0.920485
polyb2_av= 0.100238
```

```
polyb1_av= 0.020459
charge3_ar=0
charge2_ar=474
charge1_ar=5719
polyh6_ar= -2.798085
polyh5_ar= 10.893064
polyh4_ar= -15.842308
polyh3_ar= 9.030262
polyh2_ar= -0.281056
polyh1_ar= -0.003185
polyb6_ar= 6.368179
polyb5_ar= -10.706915
polyb4_ar= -0.226016
polyb3_ar= 6.528285
polyb2_ar= -0.923795
polyb1_ar= -0.042564
charge3_ar=charge3_ar*1000000
charge2_ar=charge2_ar*10000
charge1_ar=charge1_ar*100
charge3_av=charge3_av*1000000
charge2_av=charge2_av*10000
charge1_av=charge1_av*100
amortissement_av0=1600
amortissement_ar0=1600
endif

if choix==3
//-------------------------------------------------------------------------------
//HYBRIDES
//-------------------------------------------------------------------------------
avance_av=0.055000
avance_ar=0.045000
charge3_av=630
charge2_av=503
charge1_av=7144
polyh6_av= -0.588420
polyh5_av= 4.717954
polyh4_av= -10.064918
polyh3_av= 7.231672
polyh2_av= -0.296328
polyh1_av= -0.000439
polyb6_av= 3.915364
polyb5_av= -5.162269
polyb4_av= -4.054526
polyb3_av= 7.093846
polyb2_av= -0.792396
polyb1_av= 0.000099
charge3_ar=810
charge2_ar=-1231
charge1_ar=6775
polyh6_ar= -1.628748
polyh5_ar= 6.749230
polyh4_ar= -10.740428
polyh3_ar= 6.591950
polyh2_ar= 0.031157
polyh1_ar= -0.003541
polyb6_ar= 7.507269
polyb5_ar= -15.656030
polyb4_ar= 6.376905
polyb3_ar= 3.268253
polyb2_ar= -0.501015
polyb1_ar= -0.017393
charge3_ar=charge3_ar*1000000
charge2_ar=charge2_ar*10000
charge1_ar=charge1_ar*100
charge3_av=charge3_av*1000000
charge2_av=charge2_av*10000
charge1_av=charge1_av*100
amortissement_av0=3000
amortissement_ar0=3000
endif

//-------------------------------------------------------------------------------
BATCH
tt[1][1] = "type de pneumatiques"
```

```
tt[1][2] = 0
tt[2][1] = "GONFLES "
tt[2][2] = 1
tt[3][1] = "PLEINS "
tt[3][2] = 1
tt[4][1] = "HYBRIDES "
tt[4][2] = 1
tt[5][1] = "type de calcul"
tt[5][2] = 0
tt[6][1] = "Batch (14 calculs en chaîne (vitesse variant de 2 à 15 km/h)"
tt[6][2] = 1
tt[7][1] = "calcul à vitesse donnée"
tt[7][2] = 1
tt[8][1] = "vitesse (km/h)"
tt[8][2] = 12
tt[8][3] = 1
tt[8][5] = 20
{tt[9][1] = "vue du modèle"
tt[9][2] = 1
tt[9][7] = "truck.bmp"}
r = dialog_box(tt)
if r == 0                    // gestion de l'arrêt
       stop_simulation()
endif
if tt[2][4] == 1
       choix =1
else
if tt[3][4] == 1
choix=2
else
choix=3
endif
endif
if tt[6][4] == 1
calcul=1
else
calcul=2
endif
vit0= tt[8][4]/3.6

if calcul==1
vit = 2/3.6
resu="res1.txt"
resu2="tres1.txt"
pp = run_process(1)
vit = 3/3.6
resu="res2.txt"
resu2="tres2.txt"
pp = run_process(2)
vit = 4/3.6
resu="res3.txt"
resu2="tres3.txt"
pp = run_process(3)
vit = 5/3.6
resu="res4.txt"
resu2="tres4.txt"
pp = run_process(4)
vit = 6/3.6
resu="res5.txt"
resu2="tres5.txt"
pp = run_process(5)
vit = 7/3.6
resu="res6.txt"
resu2="tres6.txt"
pp = run_process(6)
vit = 8/3.6
resu="res7.txt"
resu2="tres7.txt"
pp = run_process(7)
vit = 9/3.6
resu="res8.txt"
resu2="tres8.txt"
pp = run_process(8)
vit = 10/3.6
resu="res9.txt"
```

```
resu2="tres9.txt"
pp = run_process(9)
vit = 11/3.6
resu="res10.txt"
resu2="tres10.txt"
pp = run_process(10)
vit = 12/3.6
resu="res11.txt"
resu2="tres11.txt"
pp = run_process(11)
vit = 13/3.6
resu="res12.txt"
resu2="tres12.txt"
pp = run_process(12)
vit = 14/3.6
resu="res13.txt"
resu2="tres13.txt"
pp = run_process(13)
vit = 15/3.6
resu="res14.txt"
resu2="tres14.txt"
pp = run_process(14)
else
if calcul==2
vit = vit0
resu="res.txt"
resu2="tres.txt"
pp = run_process(1)
endif
endif

//-------------------------------------------------------------------------------

CODE
if time < tempo
amortissement_av=5000
amortissement_ar=5000
rampe=0
der_rampe=0
else
amortissement_av=amortissement_av0
amortissement_ar=amortissement_ar0
rampe=vit*(time-tempo)
der_rampe=vit
endif
rot_ar=rampe/rayon_ar
der_rot_ar=der_rampe/rayon_ar
rot_av=rampe/rayon_av
der_rot_av=der_rampe/rayon_av

kin(1.5,rampe,der_rampe,0)
kin(2.5,rampe,der_rampe,0)
kin(1.3,rot_av,der_rot_av,0)
kin(2.3,rot_av,der_rot_av,0)
kin(3.3,rot_ar,der_rot_ar,0)
kin(4.3,rot_ar,der_rot_ar,0)

kinproc()

acceleration_0(5.9,vecsiège)
accelero=vecsiège[Z]

z=write_data(resu,accelero)
z=write_data(resu2,time)


x_avg=q[1.5]-elan
z_avg=q[1.6]+rayon_av
x_avd=q[2.5]-elan
z_avd=q[2.6]+rayon_av
x_arg=q[3.5]-elan-entraxe
z_arg=q[3.6]+rayon_ar
x_ard=q[4.5]-elan-entraxe
z_ard=q[4.6]+rayon_ar
```

```
if z_avg<rayon_av
Lground_avg0=2*sqrt(sqr(rayon_av)-sqr(z_avg))
else
Lground_avg0=0
endif
if z_avg-h<rayon_av
Lobst_avg0=2*sqrt(sqr(rayon_av)-sqr(z_avg-h))
else
Lobst_avg0=0
endif

if z_avd<rayon_av
Lground_avd0=2*sqrt(sqr(rayon_av)-sqr(z_avd))
else
Lground_avd0=0
endif
if z_avd-h<rayon_av
Lobst_avd0=2*sqrt(sqr(rayon_av)-sqr(z_avd-h))
else
Lobst_avd0=0
endif

if z_arg<rayon_ar
Lground_arg0=2*sqrt(sqr(rayon_ar)-sqr(z_arg))
else
Lground_arg0=0
endif
if z_arg-h<rayon_ar
Lobst_arg0=2*sqrt(sqr(rayon_ar)-sqr(z_arg-h))
else
Lobst_arg0=0
endif

if z_ard<rayon_ar
Lground_ard0=2*sqrt(sqr(rayon_ar)-sqr(z_ard))
else
Lground_ard0=0
endif
if z_ard-h<rayon_ar
Lobst_ard0=2*sqrt(sqr(rayon_ar)-sqr(z_ard-h))
else
Lobst_ard0=0
endif

// calcul des 4 forces de contact verticales-----------------------------------------------------
if rayon_av-z_avg+h>0
Fh_avg=charge1_av*(rayon_av-z_avg+h)+charge2_av*sqr(rayon_av-z_avg+h)+charge3_av*sqr(rayon_av-
z_avg+h)*(rayon_av-z_avg+h)
else
Fh_avg=0
endif
if rayon_av-z_avg>0
Fb_avg=charge1_av*(rayon_av-z_avg)+charge2_av*sqr(rayon_av-z_avg)+charge3_av*sqr(rayon_av-z_avg)*(rayon_av-
z_avg)
else
Fb_avg=0
endif
if rayon_av-z_avd+h>0
Fh_avd=charge1_av*(rayon_av-z_avd+h)+charge2_av*sqr(rayon_av-z_avd+h)+charge3_av*sqr(rayon_av-
z_avd+h)*(rayon_av-z_avd+h)
else
Fh_avd=0
endif
if rayon_av-z_avd>0
Fb_avd=charge1_av*(rayon_av-z_avd)+charge2_av*sqr(rayon_av-z_avd)+charge3_av*sqr(rayon_av-z_avd)*(rayon_av-
z_avd)
else
Fb_avd=0
endif
if rayon_av-z_arg+h>0
Fh_arg=charge1_ar*(rayon_ar-z_arg+h)+charge2_ar*sqr(rayon_ar-z_arg+h)+charge3_ar*sqr(rayon_ar-
z_arg+h)*(rayon_ar-z_arg+h)
else
Fh_arg=0
endif
```

```
if rayon_av-z_arg>0
Fb_arg=charge1_ar*(rayon_ar-z_arg)+charge2_ar*sqr(rayon_ar-z_arg)+charge3_ar*sqr(rayon_ar-z_arg)*(rayon_ar-
z_arg)
else
Fb_arg=0
endif
if rayon_av-z_ard+h>0
Fh_ard=charge1_ar*(rayon_ar-z_ard+h)+charge2_ar*sqr(rayon_ar-z_ard+h)+charge3_ar*sqr(rayon_ar-
z_ard+h)*(rayon_ar-z_ard+h)
else
Fh_ard=0
endif
if rayon_av-z_ard>0
Fb_ard=charge1_ar*(rayon_ar-z_ard)+charge2_ar*sqr(rayon_ar-z_ard)+charge3_ar*sqr(rayon_ar-z_ard)*(rayon_ar-
z_ard)
else
Fb_ard=0
endif

// avg-------------------------------------------------------------------------
if x_avg <-Lobst_avg0/2
        ratioh_avg=0
else
        if x_avg < Lobst_avg0/2
                if x_avg < 1 - Lobst_avg0/2
                        ratioh_avg=0.5+x_avg/Lobst_avg0
                else
                        ratioh_avg=1/Lobst_avg0
                endif
        else
                if x_avg< 1 - Lobst_avg0/2
                        ratioh_avg=1
                else
                        if x_avg< 1 + Lobst_avg0/2
                                ratioh_avg=0.5-(x_avg-1)/Lobst_avg0
                        else
                                ratioh_avg=0
                        endif
                endif
        endif
endif

if x_avg+avance_av <-Lground_avg0/2
        ratiob_avg=1
else
        if x_avg+avance_av < Lground_avg0/2
                if x_avg-avance_av < 1 - Lground_avg0/2
                        ratiob_avg=0.5-(x_avg+avance_av)/Lground_avg0
                else
                        ratiob_avg=1-1/Lground_avg0
                endif
        else
                if x_avg-avance_av < 1 - Lground_avg0/2
                        ratiob_avg=0
                else
                        if x_avg-avance_av < 1 + Lground_avg0/2
                                ratiob_avg=0.5+(x_avg-1-avance_av)/Lground_avg0
                        else
                                ratiob_avg=1
                        endif
                endif
        endif
endif

// avd-------------------------------------------------------------------------
if x_avd <-Lobst_avd0/2
        ratioh_avd=0
else
        if x_avd < Lobst_avd0/2
                if x_avd < 1 - Lobst_avd0/2
                        ratioh_avd=0.5+x_avd/Lobst_avd0
                else
                        ratioh_avd=1/Lobst_avd0
                endif
        else
```

```
                if x_avd< l - Lobst_avd0/2
                        ratioh_avd=1
                else
                        if x_avd< l + Lobst_avd0/2
                                ratioh_avd=0.5-(x_avd-l)/Lobst_avd0
                        else
                                ratioh_avd=0
                        endif
                endif
        endif
endif

if x_avd+avance_av <-Lground_avd0/2
        ratiob_avd=1
else
        if x_avd+avance_av < Lground_avd0/2
                if x_avd-avance_av < l - Lground_avd0/2
                        ratiob_avd=0.5-(x_avd+avance_av)/Lground_avd0
                else
                        ratiob_avd=1-l/Lground_avd0
                endif
        else
                if x_avd-avance_av < l - Lground_avd0/2
                        ratiob_avd=0
                else
                        if x_avd-avance_av < l + Lground_avd0/2
                                ratiob_avd=0.5+(x_avd-l-avance_av)/Lground_avd0
                        else
                                ratiob_avd=1
                        endif
                endif
        endif
endif

// arg-------------------------------------------------------------------------
if x_arg <-Lobst_arg0/2
        ratioh_arg=0
else
        if x_arg < Lobst_arg0/2
                if x_arg < l - Lobst_arg0/2
                        ratioh_arg=0.5+x_arg/Lobst_arg0
                else
                        ratioh_arg=l/Lobst_arg0
                endif
        else
                if x_arg< l - Lobst_arg0/2
                        ratioh_arg=1
                else
                        if x_arg< l + Lobst_arg0/2
                                ratioh_arg=0.5-(x_arg-l)/Lobst_arg0
                        else
                                ratioh_arg=0
                        endif
                endif
        endif
endif

if x_arg+avance_ar <-Lground_arg0/2
        ratiob_arg=1
else
        if x_arg+avance_ar < Lground_arg0/2
                if x_arg-avance_ar < l - Lground_arg0/2
                        ratiob_arg=0.5-(x_arg+avance_ar)/Lground_arg0
                else
                        ratiob_arg=l-l/Lground_arg0
                endif
        else
                if x_arg-avance_ar < l - Lground_arg0/2
                        ratiob_arg=0
                else
                        if x_arg-avance_ar < l + Lground_arg0/2
                                ratiob_arg=0.5+(x_arg-l-avance_ar)/Lground_arg0
                        else
                                ratiob_arg=1
                        endif
```

```
            endif
        endif
endif

// ard---------------------------------------------------------------------------
if x_ard <-Lobst_ard0/2
        ratioh_ard=0
else
        if x_ard < Lobst_ard0/2
                if x_ard < 1 - Lobst_ard0/2
                        ratioh_ard=0.5+x_ard/Lobst_ard0
                else
                        ratioh_ard=1/Lobst_ard0
                endif
        else
                if x_ard< 1 - Lobst_ard0/2
                        ratioh_ard=1
                else
                        if x_ard< 1 + Lobst_ard0/2
                                ratioh_ard=0.5-(x_ard-1)/Lobst_ard0
                        else
                                ratioh_ard=0
                        endif
                endif
        endif
endif

if x_ard+avance_ar <-Lground_ard0/2
        ratiob_ard=1
else
        if x_ard+avance_ar < Lground_ard0/2
                if x_ard-avance_ar < 1 - Lground_ard0/2
                        ratiob_ard=0.5-(x_ard+avance_ar)/Lground_ard0
                else
                        ratiob_ard=1-1/Lground_ard0
                endif
        else
                if x_ard-avance_ar < 1 - Lground_ard0/2
                        ratiob_ard=0
                else
                        if x_ard-avance_ar < 1 + Lground_ard0/2
                                ratiob_ard=0.5+(x_ard-1-avance_ar)/Lground_ard0
                        else
                                ratiob_ard=1
                        endif
                endif
        endif
endif

formb_avg=polyb1_av+polyb2_av*ratiob_avg+polyb3_av*sqr(ratiob_avg)+polyb4_av*sqr(ratiob_avg)*ratiob_avg+polyb
5_av*sqr(ratiob_avg)*sqr(ratiob_avg)+polyb6_av*sqr(ratiob_avg)*sqr(ratiob_avg)*ratiob_avg
formh_avg=polyh1_av+polyh2_av*ratioh_avg+polyh3_av*sqr(ratioh_avg)+polyh4_av*sqr(ratioh_avg)*ratioh_avg+polyh
5_av*sqr(ratioh_avg)*sqr(ratioh_avg)+polyh6_av*sqr(ratioh_avg)*sqr(ratioh_avg)*ratioh_avg
formb_avd=polyb1_av+polyb2_av*ratiob_avd+polyb3_av*sqr(ratiob_avd)+polyb4_av*sqr(ratiob_avd)*ratiob_avd+polyb
5_av*sqr(ratiob_avd)*sqr(ratiob_avd)+polyb6_av*sqr(ratiob_avd)*sqr(ratiob_avd)*ratiob_avd
formh_avd=polyh1_av+polyh2_av*ratioh_avd+polyh3_av*sqr(ratioh_avd)+polyh4_av*sqr(ratioh_avd)*ratioh_avd+polyh
5_av*sqr(ratioh_avd)*sqr(ratioh_avd)+polyh6_av*sqr(ratioh_avd)*sqr(ratioh_avd)*ratioh_avd
formb_arg=polyb1_ar+polyb2_ar*ratiob_arg+polyb3_ar*sqr(ratiob_arg)+polyb4_ar*sqr(ratiob_arg)*ratiob_arg+polyb
5_ar*sqr(ratiob_arg)*sqr(ratiob_arg)+polyb6_ar*sqr(ratiob_arg)*sqr(ratiob_arg)*ratiob_arg
formh_arg=polyh1_ar+polyh2_ar*ratioh_arg+polyh3_ar*sqr(ratioh_arg)+polyh4_ar*sqr(ratioh_arg)*ratioh_arg+polyh
5_ar*sqr(ratioh_arg)*sqr(ratioh_arg)+polyh6_ar*sqr(ratioh_arg)*sqr(ratioh_arg)*ratioh_arg
formb_ard=polyb1_ar+polyb2_ar*ratiob_ard+polyb3_ar*sqr(ratiob_ard)+polyb4_ar*sqr(ratiob_ard)*ratiob_ard+polyb
5_ar*sqr(ratiob_ard)*sqr(ratiob_ard)+polyb6_ar*sqr(ratiob_ard)*sqr(ratiob_ard)*ratiob_ard
formh_ard=polyh1_ar+polyh2_ar*ratioh_ard+polyh3_ar*sqr(ratioh_ard)+polyh4_ar*sqr(ratioh_ard)*ratioh_ard+polyh
5_ar*sqr(ratioh_ard)*sqr(ratioh_ard)+polyh6_ar*sqr(ratioh_ard)*sqr(ratioh_ard)*ratioh_ard

if formb_avg <0
        formb_avg=0
endif
if formb_avg>1
        formb_avg=1
endif
if formh_avg <0
        formh_avg=0
endif
```

```
if formh_avg>1
        formh_avg=1
endif

if formb_avd <0
        formb_avd=0
endif
if formb_avd>1
        formb_avd=1
endif
if formh_avd <0
        formh_avd=0
endif
if formh_avd>1
        formh_avd=1
endif

if formb_arg <0
        formb_arg=0
endif
if formb_arg>1
        formb_arg=1
endif
if formh_arg <0
        formh_arg=0
endif
if formh_arg>1
        formh_arg=1
endif

if formb_ard <0
        formb_ard=0
endif
if formb_ard>1
        formb_ard=1
endif
if formh_ard <0
        formh_ard=0
endif
if formh_ard>1
        formh_ard=1
endif

dir_avg[Z]=formb_avg*Fb_avg+formh_avg*Fh_avg-amortissement_av*dq[1.6]
dir_avd[Z]=formb_avd*Fb_avd+formh_avd*Fh_avd-amortissement_av*dq[2.6]
dir_arg[Z]=formb_arg*Fb_arg+formh_arg*Fh_arg-amortissement_ar*dq[3.6]
dir_ard[Z]=formb_ard*Fb_ard+formh_ard*Fh_ard-amortissement_ar*dq[4.6]

forcem_0(1.1,dir_avg)
forcem_0(2.1,dir_avd)
forcem_0(3.1,dir_arg)
forcem_0(4.1,dir_ard)
```